UNIVERSITE D'ABOMEY - CALAVI (UAC)

INSTITUT NATIONAL DE L'EAU

Federal Ministry of Education and Research

WASCAL
West African Science Service Center on Climate Change and Adapted Land Use

A DISSERTATION

Submitted

In partial fulfillment of the requirements for the degree of

DOCTOR of Philosophy (PhD) of the University of Abomey-Calavi (Benin Republic)

In the framework of the

Graduate Research Program on Climate Change and Water Resources (GRP-CCWR)

By

Adama Touré

Public defense on: 03/08/2017

======

IMPACTS OF CLIMATE CHANGE AND POPULATION GROWTH ON GROUNDWATER RESSOURCES: CASE OF THE KLELA BASIN IN MALI, WEST AFRICA

======

Supervisors:

Abel Afouda, Full Professor, University of Abomey-Calavi, Benin
Bernd Diekkrüger, Full Professor, University of Bonn, Germany
Adama Mariko, Full Professor, University of Bamako, Mali

======

Reviewers

Julien G. Adounkpe, Associate Professor, University of Abomey-Calavi, Benin
Boureima Ousmane, Full Professor, University of Abdou Moumouni, Niger
Bernd Diekkrüger, Full Professor, University of Bonn, Germany

======

JURY

Moussa Boukari	Full Professor, University of Abomey-Calavi, Benin	President
Julien G. Adounkpe	Associate Professor University of Abomey-Calavi, Benin	Reviewer
Boureima Ousmane	Full Professor, University of Abdou Moumouni, Niger	Reviewer
Bernd Diekkrüger	Full Professor, University of Bonn, Germany	Reviewer
Sounmaila Moumouni	Associate Professor, University of Parakou, Benin	Examiner
Abel Afouda,	Full Professor, University of Abomey-Calavi, Benin	Director

To my family, my parents Abdoulaye Touré and Mariam Touré, my wife Halimata Camara and all my siblings.

ACKNOWLEDGEMENTS

At the end of my thesis, I would like to thank all those people who made this thesis possible and an unforgettable experience for me.

First of all, I will start to express my sincere gratitude to Prof. Dr. Bernd Diekkrüger at Department of Geography, University of Bonn, who offered his continuous advice and encouragement throughout the course of this thesis. His guidance and support accompanied me during the time of PhD research and writing the dissertation. He gave me the opportunity to spend six months as a trainee at University of Bonn, Germany. Without him, I can imagine how this study could be done. I am grateful to him. I would like to thank also Prof. Adama Mariko at Department of Geology, National Engineering School, Bamako. He helped me in the field data collection and data analysis.

Let me thank all the members of the department of Graduation Research Program on Water Resources and Climate Change in Benin especially Prof. Abel Afouda and Doctor Julien Adounkpe who accepted me in this PhD program and advised me throughout this thesis.

I am grateful to Prof. Wolfgang Kinzelbach, Institute of Environment Engineering, ETH Zürich and Doctor Lamine Baba Sy at the Sahara and Sahel Observatory (OSS), Tunisia, for their encouragement and guidance in learning PMWIN. Prof. Stephen Silliman, at Gonzaga University, advised and helped me to be oriented throughout this study, I am grateful to him. I thank all the members (students and assistants of Prof. Diekkrüger) of the team of the Department of Geography at University of Bonn, for fruitful exchange each other during my stay in Germany.

I cannot end this without address my sincere thanks to the personals of Regional Hydraulic Direction of Sikasso, particularly to Mr. Pierre Kassogue and Mr. Nouhoum Traore who facilitated me the field data collection. My sincere gratitude goes to Dr. Ibrahima Daou and Mr. Damassa Bouare for their helping in learning GIS software and PMWIN model, respectively.

ABSTRACT

Due to the effects of climate change and population growth, global water resources are threatened in terms of quantity and quality. As groundwater is more resilient to climate variability, to date, many studies are addressing the simulation of groundwater dynamics for adaptation purpose. Groundwater on the Klela basin in Mali, a subbasin of the Bani's basin (one of the main tributaries of the Niger River), is very important for the population because it is required for domestic use, irrigation and livestock. Surface water is limited to seasonal rainfall and runs dry a few months after the rainy season. Therefore, investigations of groundwater resources to understand aquifer system behavior are vital to the inhabitants of the Klela basin. Actually, groundwater resources are sufficiently enough and available to cover the current water demand, but in the face of climate variability and change, growing population and high urbanization rates, this vital resource is being threatened. Therefore, water assessment tools were used to understand the aquifer behavior of the basin. The focus of this study is on estimating the amount of rainwater that replenishes the aquifer, understanding the hydraulic interactions between surface-water and groundwater, and quantifying and evaluating groundwater dynamics in the context of climate change and population growth, using different scenarios. Different approaches such as the water table fluctuation (WTF), chloride mass balance (CMB), simulations using the EARTH model and the Thornthwaite model for recharge estimation, MODFLOW for groundwater modeling, and the WEAP model for evaluating groundwater resources are applied to achieve the study objectives. Climatological, hydrological, geological, hydrogeological, hydraulic and demographic data are collected and used as models input data. The sandstone aquifer in the study area was simulated under steady and transient conditions, and the groundwater budget was computed. Recharge was estimated to be approximatively 635 Mm^3/a or 13.9% of the mean annual rainfall for the period 2012-2013. The amount of water discharging the aquifer into the streams was estimated to be approximatively 618 Mm^3/a, representing 97% of recharge amount. Currently, the reduction of groundwater storage of about 39 Mm^3/a (10.6 mm/a) is mainly due to groundwater extraction by population. Scenarios of climate change, population growth and socio-economic development were developed to assess future groundwater resources. The results reveal that the impacts of climate change on groundwater are greater than that of the socio-economic development. However, the climate scenario RCP8.5 appeared to be the worst for groundwater availability. The overall conclusion of this study is that groundwater recharge, groundwater level and storage are decreasing over time, especially in the 2030s, where the simulated drought events are expected. The greatest impacts on groundwater resources are due to climate change and population growth.

Keywords: Klela basin, groundwater resources, climate change, scenarios, Mali

SYNTHESE

Cette étude était basée sur le présent et le futur comportement des ressources en eau souterraine dans le bassin versant de Klela. En fait, les ressources en eau souterraine dans le bassin versant de Klela au Mali, un sous bassin du bassin versant du Bani (l'un des principaux affluents du fleuve Niger), sont très importantes pour la population de cette localité, car cette ressource est utilisée à des fins domestiques, dans l'irrigation, l'industrie et aussi pour le besoin des bétails. Les ressources en eau de surface sont insuffisantes et limitées aux précipitations saisonnières qui s'assèchent quelques mois après la saison pluvieuse. Les ressources en eau souterraine sont les seules ressources permanentes d'eau dans la zone et une grande partie de la population exploite seulement les eaux provenant des puits traditionnels qui tarissent quelques mois après la période de recharge. Il faut noter également que le bassin versant de Klela est une zone agricole et que une grande quantité de pomme de terre consommée au Mali provient de cette zone, et la culture de la pomme de terre exploite surtout les ressources en eau souterraine pour sa production. Cependant, des investigations sur les ressources en eau souterraine pour essayer de comprendre le comportement du système de l'aquifère sont vitales pour les habitants du bassin versant de Klela en particulier et ceux de l'ensemble du Mali en général. Actuellement, les ressources en eau souterraine existantes sont nettement suffisantes et disponibles pour couvrir la présente demande en eau, mais face à la variabilité et au changement climatique, aux taux élevés de la croissance démographique et de l'urbanisation, cette ressource vitale se trouve menacée dans le futur.

Le grand problème est que sur l'ensemble du territoire du Mali très peu d'études ont abordé des sujets de modélisation des ressources en eau souterraine et le bassin de Klela n'en fait pas exception. Aucune étude n'a été dirigée sur le bassin versant de Klela concernant l'estimation de l'infiltration (la recharge) des nappes et encore moins la simulation de la dynamique des ressources en eau souterraine. Alors, face à toutes ces réalités mentionnées ci-dessus, les outils d'évaluation des ressources en eau ont été utilisés pour comprendre le comportement de l'aquifère du bassin. Cette étude était focalisée (a) sur l'estimation de la quantité du volume d'eau de pluie qui approvisionne l'aquifère, (b) sur la compréhension des interactions hydrauliques entre les eaux de surface et les eaux souterraines, et (c) sur la quantification et l'évaluation des dynamiques des eaux souterraines dans le contexte du changement climatique et de la croissance démographique en utilisant des différents scenarios.

Pour atteindre ces objectifs, des données nécessaires ont été collectées et des méthodes appropriées ont été utilisées. Les données (climatologiques, hydrologiques, géologiques, hydrogéologiques, démographiques, satellitaires, etc.) collectées sur le terrain et ailleurs ont été utilisées d'abord pour estimer la quantité d'eau de pluie qui s'infiltre dans le sous-sol et qui représente le paramètre le plus important dans la modélisation des ressources en eau souterraine. Quatre outils (méthode de fluctuation du niveau d'eau des nappes, WTF, méthode du bilan de masse de chlorure, CMB, modèle EARTH et modèle Thornthwaite) ont été utilisés pour l'estimation de cet important paramètre. Tout d'abord, les trois premiers ont été utilisés pour l'estimation actuelle de la recharge des nappes du bassin de Klela et ensuite, le quatrième a été utilisé pour la prédiction de l'infiltration des eaux de pluies dans les aquifères du bassin. L'objectif principal de l'utilisation de plusieurs techniques dans l'estimation de la recharge est d'obtenir un résultat optimal par comparaison, car les méthodes généralement utilisées pour l'estimation de l'infiltration contiennent beaucoup de contraintes, de limites et aussi des

incertitudes. Cependant, il est recommandé d'appliquer éventuellement plusieurs méthodes d'estimation de recharge dans une zone donnée afin de choisir le meilleur résultat basé sur des comparaisons statistiques. La recharge optimale obtenue à partir du modèle EARTH était utilisée comme paramètre d'entrée dans des modèles (MODFLOW et WEAP) appliqués pour la détermination de la dynamique et l'évaluation des impacts du changement climatique et de la croissance démographique sur les ressources en eau souterraine dans le bassin de Klela respectivement. L'organigramme explicite de la méthodologie se trouve dans la Figure 1 ci-dessous.
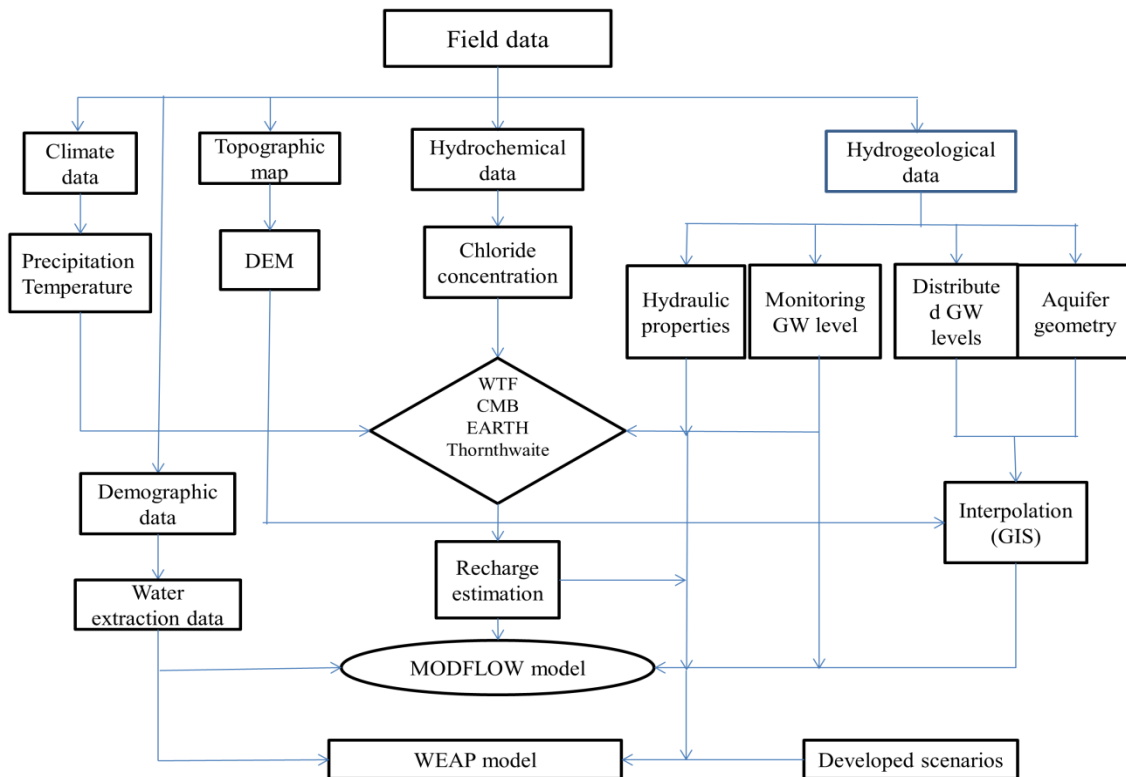

Figure 1. L'organigramme de la méthodologie utilisée dans cette étude

L'aquifère du grès de la zone d'étude a été simulé dans des conditions stables et transitoires, le bilan des eaux souterraines a été établi, et les ressources en eau souterraine ont été évaluées dans le contexte du changement climatique et de la croissance démographique. La recharge calculée par le modèle EARTH a été estimée à approximativement 635 Mm^3/an, soit 13.9% de la moyenne annuelle des pluies pour la période 2012-2013. La prévision sur la recharge montre qu'elle décroit dans le futur notamment plus rapidement à partir des années 2030 pour les scenarios RCP4.5 et RCP8.5 et continue de décroitre jusqu'en 2048 pour le deuxième scenario (Figure 2). MODFLOW avait permis de calculer la quantité du volume d'eau libérée par l'aquifère pour alimenter les cours d'eau du bassin et était estimée approximativement à 618 Mm^3/an, représentant 97% de la quantité de la recharge. La réduction actuelle du stockage des eaux souterraines est principalement due à l'extraction de l'eau par la population soit environ 39 Mm^3/an (voir le tableau 1).
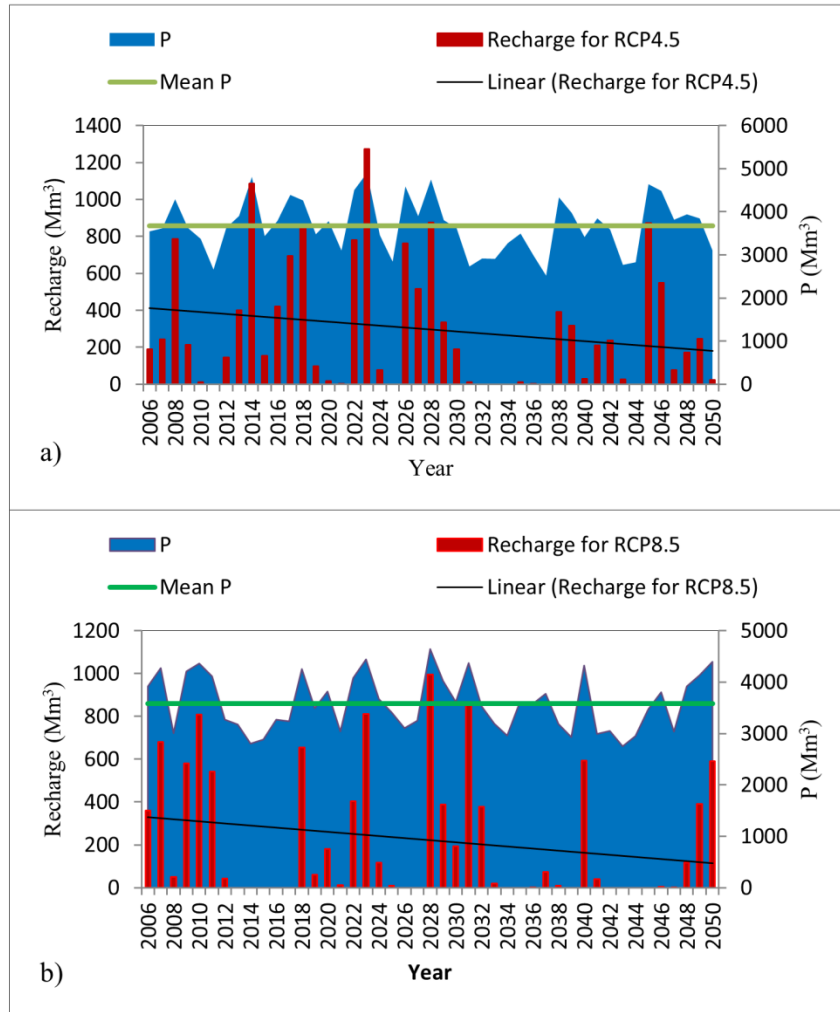
Figure 2. Recharge estimée et la précipitation annuelle (Mm^3) pour les scenarios (a) RCP4.5 et (b) RCP8.5 dans le bassin versant de Klela de 2006-2050

Tableau 1. La moyenne annuelle du bilan de l'eau souterraine en m^3/an dans le bassin versant de Klela pour la période Novembre 2010-Novembre 2014

Ecoulement	Afflux (m^3/an)	Sortie (m^3/an)
Stockage	485,869,302	446,718,545
Recharge	635,293,979	0
Puits	0	57,287,607
Fuite du flux	947,401	618,122,906
Total	1,122,110,683	1,122,129,060

Les scenarios du changement climatique, de la croissance démographique et du développement socio-économique ont été développés pour évaluer les ressources en eau souterraine dans le futur. Les résultats révèlent que les impacts du changement climatique sur les ressources en eau

vii

souterraine sont plus significatifs que ceux du développement socio-économique. Par exemple, la Figure 3 illustre que le stockage des eaux souterraines est menacé et réduit dans le temps. Cette diminution du stockage des nappes d'eau souterraines affecte tous les secteurs d'usage d'eau et est plus importante à partir des années 2030 pour les deux scenarios RCP4.5 et RACP8.5. Malgré que la plupart des modèles climatiques globaux aient prévu des évènements de sécheresse dans le futur, ce résultat montre que les années 2019 et 2023 seraient une période humide pour le scenario RCP4.5. Cependant, le scenario RCP8.5 semble être le pire concernant la disponibilité de l'eau souterraine dans le futur.
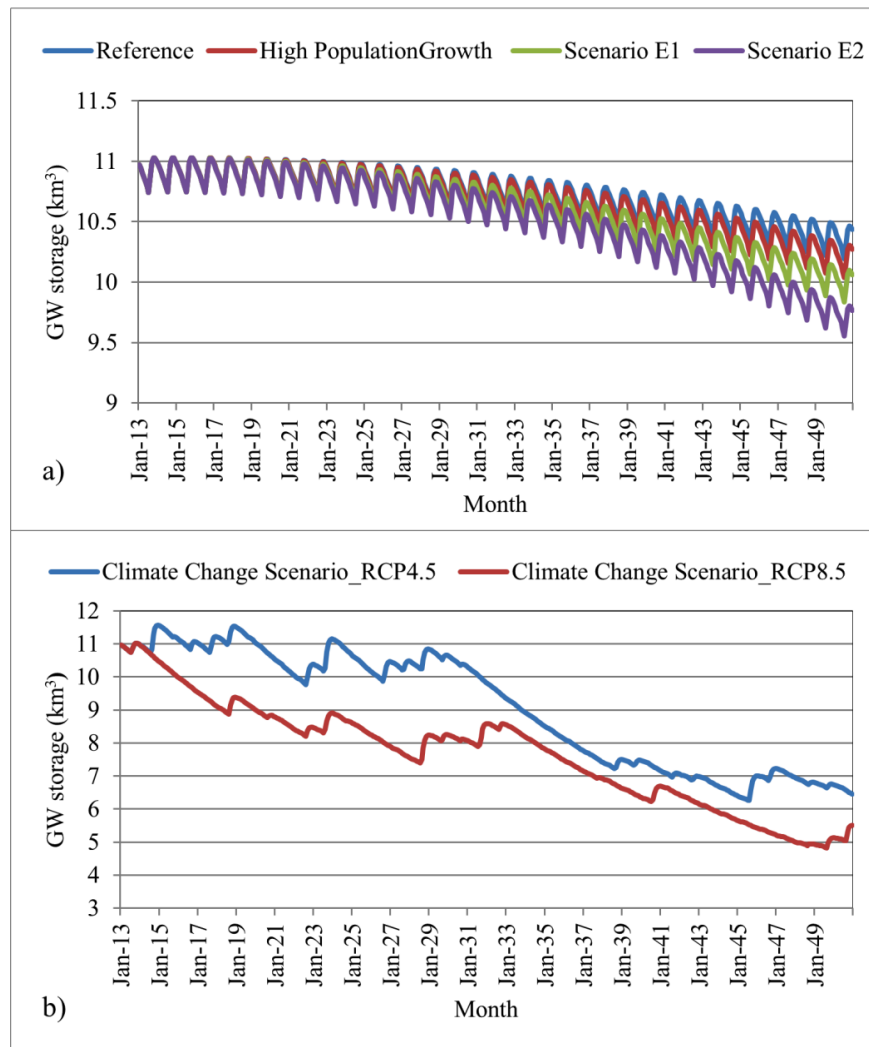

Figure 3. Le stockage des eaux souterraines en kilomètre cube pour les différents scenarios (a) référence, croissance démographique, socio-économique E1 et E2, et (b) changement climatique RCP4.5 et RCP8.5

La conclusion générale de cette étude est que l'infiltration des eaux dans le sous-sol, le niveau de l'eau dans les nappes et le stockage des eaux souterraines sont en train d'être réduits dans le temps, spécialement dans les années 2030 où les évènements de sècheresse sont prévus. Les impacts importants sur les ressources en eau sont le changement climatique et la croissance démographique.

Il faut ajouter à cela que la disponibilité des données est un problème majeur pour tout le Mali en général et le bassin de Klela en particulier. Alors, des actions réelles doivent être entreprises pour atténuer voire éviter les dommages qui peuvent être causés suite au manque d'eau dans le futur. Pour cela, les décideurs doivent penser à l'implantation spatiale des piézomètres dans le bassin versant de Klela et au suivi temporaire des mesures du niveau piézomètre afin de bien maitriser la fluctuation des nappes qui est un élément capital dans la modélisation et la gestion des ressources en eau souterraine. Les outils utilisés dans cette étude, Processing MODFLOW for Windows (PMWIN 5.3) et Water Evaluation Planning system (WEAP), sont bien adaptés aux conditions climatiques et géologiques de la zone d'étude, par conséquent peuvent être appliqués pour la gestion des ressources en eau du bassin de Klela.

Mots-clés : Bassin versant de Klela, les ressources en eau souterraine, la modélisation, la recharge, les scenarios, Mali

Table of Contents

List of figures

List of tables

xviii

List of abbreviations

AOGCM   Atmospheric-Ocean General Circulation Model

CMB   Chloride Mass Balance

CMDT   Malian Company of Textile Development (Compagnie Malienne de Développent des Textiles)

CORDEX   Coordinated Regional Climate Downscaling Experiment

DEM   Digital Elevation Model

DNM   National Meteorology Direction (Direction Nationale de la Météorologie)

DRGR   Rural Engineering of Regional Direction (Direction Régionale du Génie Rural)

DRH   Regional Hydraulic Direction (Direction Régionale de l'Hydraulique)

EARTH   Extended model for Aquifer Recharge and soil moisture Transport through the unsaturated Hardrock

ECHAM   European Centre Hamburg Model

FAO   Food and Agriculture Organization

GCM   General Circulation Model

GIS   Geographic Information System

HydroSHEDS   Hydrology of data and map based on SHuttle Elevation Derivatives at multiple Scales

IER   Rural Economic Institute (Institut d'Economie Rural)

IPCC   Intergovernmental Panel on Climate Change

ITCZ   Inter Tropical Convergence Zone

ITF   InterTropical Front

LC   Land Cover

lpcpd   Liter per capital per day

mamsl   Meters above mean sea level

mbgl   Meters below ground level

PCDA   Project of Agricultural Competitivity and Diversion (Projet pour la

	Compétitivité et Diversion Agricole)
PMWIN	Processing MODFLOW for Windows
RCP	Representative Concentration Pathway
RGPH	General Census of Human Population (Recensement General de la Population Humaine)
SEI	Stockholm Environment Institute
SMHI	Swedish Meteorological and Hydrological Institute
SOMAGEP	Malian Society of Potable Water Management (Société Malienne de la Gestion de l'Eau Potable)
SPI	Standard Precipitation Index
SRTM	Shuttle Radar Topography Mission
UN	United Nations
UNEP	United Nations Environmental Program
UNESCO	United Nations Educational, Scientific and Cultural Organization
UNFCCC	United Nations Framework Convention on Climate Change
USAID	United States Agency for International Development
USGS	United States Geological Services
WCRP	World Climate Research Program
WEAP	Water Evaluation And Planning System
WHO	World Health Organization
WTF	Water Table Fluctuation
WWAP	World Water Assessment Program
WWF	World Wildlife Fund

CHAPTER 1: GENERAL INTRODUCTION

1.1.   General overview

Life depends entirely on water. All human activities such as agriculture, irrigation, industry, fishery, household, hydropower generation, transportation, and ecosystems are related to water availability. Water resources can be divided into two parts: blue water ("the visible liquid water flow moving above and below the ground") and green water ("the invisible flow of vapor to the atmosphere") (FAO, 1995, 1997; Falkenmark and Rockström, 2004). The blue water is the most important for human water needs and contains about 2.5% of freshwater (Falkenmark and Rockström, 2004). This last resource must be protected in terms of quantity and quality in order to maintain the sustainability of this life. Freshwater play an important role in the global economic sector (Ackerman and Stanton, 2011), especially in developing countries where their daily activities depend on it. Unfortunately, nowadays, many studies (UN, 2007; Bates *et al.,* 2008) have already discussed the stress, scarcity and vulnerability of freshwater worldwide. Bates *et al.* (2008) have argued that the variability of precipitation is very likely to be increased, which can lead to the anticipation of drought and flood events throughout the world. According to UNEP (2002), more than half of the world's population might face serious problems related to the increase in water-stressed areas by 2032. In addition, approximatively 1.1 billion people still suffer from safe drinking water availability and the improvement of the sanitation is very poor that reaches 2.4 billion people over the world especially in developing countries (UNEP 2002).

This vital resource is facing to several challenges. Climate change, one of these challenges, is defined by (IPCC, 2001) as "any change in climate over time, whether due to natural variability or as a result of human activity". Another definition is given by UNFCCC (1992) as "a change of climate which is attributed directly or indirectly to human activity that alters the composition of the global atmosphere and which is in addition to natural climate variability observed over comparable time periods". Land use and land cover changes and the increased of fossil fuel combustion could be the most

responsible for raising the atmospheric concentrations of greenhouse gases and that would tend to warm the atmosphere (Rosenberg *et al.,* 1999, Woldeamlak *et al.,* 2007). This warming could change the temperature and rainfall patterns. Therefore, climate variability and change, and global warming as a result of human activities may temporally and spatially affect the availability and quality of numerous components in the global hydrologic cycle (Loaiciga *et al.,* 1996; Sherif and Singh, 1999; Milly *et al.,* 2005; Holman, 2006; IPCC, 2007; Green *et al.,* 2011). All the "components of the surface hydrologic cycle may be affected by climate change including atmospheric water vapor content, precipitation, and evapotranspiration patterns, snow cover and melting of ice and glaciers, soil temperature and moisture, and surface runoff and streamflow (Bates *et al.,* 2008), which will likely result in changes to the subsurface hydrologic cycle within the soil, unsaturated zone, and saturated zone, and may affect recharge, discharge, and groundwater storage of many aquifers worldwide" (Timothy R. Green, 2009, cited in Gurdak *et al.,* 2009). Groundwater is one of the most significant freshwater resources over the world (Gurdak *et al.,* 2009). For example, in the United States, many Nations are using groundwater in domestic water supply, which supports agricultural and industrial economies, and contributes flowing to the surface water bodies (lakes, rivers, wetlands) (Gurdak *et al.,* 2009). However, the potential impacts of climate change on groundwater resources are poorly understood (Jyrkama and Sykes, 2007; Clifton *et al.,* 2010; Calow *et al.,* 2011; Kumar, 2012) because the relationship between climate and groundwater is more complicated than that of surface water (Holman, 2006; IPCC, 2007; Green *et al.,* 2011). This complication is mainly related to its non-visibility and difficult accessibility; though, some studies (Calow *et al.,* 2011; Kumar, 2012, Toure *et al.* 2016) have shown that groundwater is affected in the context of climate variability and change. Change in precipitation may bring to large changes in recharge especially in arid and semi-arid regions (Woldeamlak *et al.,* 2007; Barron *et al.,* 2012; Crosbie *et al.,* 2012; Thomas *et al.,* 2016) because precipitation affects directly groundwater recharge. Sandstorm (1995) argued that a 15% reduction in precipitation, with constant temperature, might occasion in a 40-50% decrease in recharge. In addition to climate change, population growth, which is projected to reach 9.6 billion by 2050 (UN, 2013), also increases water stresses. It has been projected that between 1 and 2.7 billion of people will experience an increase

in water stress by 2050s (Arnell 2004, Alavian *et al.,* 2009). World population growth will lead to an increase of the surface areas of agriculture in order to assure food security. Agriculture alone exceeds more than 70% of the world's total water use (UN, 2007). Even if the precipitation amount remains unchanged, the increase of temperatures and rainfall variability could lead to increase irrigation water demand. Therefore, the water demand for agriculture will be increased in many regions of the world including Africa where most of their economic income depends on crop production. In a region where the population density is high, the freshwater availability is low.

Freshwater availability and quality is and will be one of the big challenges for African continent because of climate variability and change effects, rapid population increase, urbanization development, intensification of land cultivation area, *etc.* In fact, as mentioned in Taylor *et al.* (2009), currently, Africa's population is about one billion people, and it is predicted to reach 1.5 billion by 2050, with the highest growth rate of 1.6-3.6% per year in the world (UN, 2007; Carter and Parker, 2009). Increasing of the urban population will require a significant increase of the food production in both rural and peri-urban areas, which depend on sufficient availability of water resources in a continent where groundwater quantity (51%) is higher than surface water (Döll and Fiedler, 2008). For this reason, about 50% of the Africa's population rely on shallow or deep groundwater for their daily domestic water supply (Calow and MacDonald, 2009; Carter and Parker, 2009). Although groundwater resources are important in Africa, its accessibility remains a real problem due to its cost. Several authors (Al-Gamal *et al.,* 2009; Goulden *et al.,* 2009; Nyenje and Batelaan, 2009; Odada, 2013; Taylor *et al.,* 2009) have already discussed groundwater and climate in Africa. Most of them have shown that there is a high uncertainty in groundwater recharge, but it has been clarified that groundwater recharge is linked to the local precipitation. The mean annual precipitation is expected to change (decrease or increase) depending on the region in the context of climate variability and change. However, Carter and Parker (2009) have demonstrated that it is likely that mean annual rainfall decreases in the northern Sahara, whereas in the eastern Africa it should increase. Cavé *et al.* (2003) supported the idea on which the precipitation reduction leads to decrease groundwater recharge. In their study, they found that reduction of mean annual rainfall from 500 to 400 mm could result in an 80%

reduction in annual recharge. Mali including the Klela basin is concerned by all water stresses cited before.

1.2. Background of the study

Klela basin, situated in southern Mali at Sikasso region, is shared by two countries (Mali and Burkina Faso). It is a subbasin of the Bani basin, which is one of the main tributary rivers of the Niger River. The Niger River is the principal river of western Africa with the longest reach (1,700 km) extending through southern Mali (Olivry *et al.*, 2005). It is the main surface water resources for the entire region in Mali where it crosses. The Bani basin is mostly localized in Mali from South to Center and is created by the confluence of the Bagoé and the Baoulé of which their upstreams are located within Côte d'Ivoire (Olivry *et al.*, 2005). The course of the Bani is nearly entirely located in southern Mali. The only principal permanent surface water that drains the Sikasso region (includes the study area) is the confluence of the Lotio-Banifing, of which the length of the whole Banifing is about 2,000 km (Diall, 2001). Sikasso region is the most cultivated area in Mali after the Office du Niger at Segou region. Almost, all the various crops in Mali are practiced in Sikasso region such as cereals (*e.g.,* rice, maize, sorghum, millet, corn, *etc.*), cotton and horticulture (*e.g.,* potato, yam, tomato, onion, manioc, *etc.*). For example, the annual production of potatoes in Sikasso region reaches about 88% of national production (Maiga, 2004). This production is very important for the local economy because it is exported to the surrounding countries (*e.g.,* Côte d'Ivoire) for trade purpose. Although the basin is an important area for agriculture, the index of poverty is the highest compared to other regions in Mali (Rapport, 2005).

Two principal water sources (surface water and groundwater, both related to the seasonal rainfall) are used by the basin's population for their diverse crops. Especially, groundwater is the most important resource not only for irrigation but also for domestic water need. Sikasso commune is the only town in the basin, which derives its domestic water supply from deep groundwater, distributed by the Malian Society of Potable Water Management (SOMAGEP). As the commune is enlarging due to rapid urbanization, the need for water is increasing too. Most of the remainder of the rural population is using "water from traditional wells that are recharged by rainfall and dry out a few months after

the recharge period" (Toure *et al*. 2016). The cultivated area is expected to increase in the future due to a rapid population increase of which the growth rate was about 3.6% in 2009 (SDRFPTE, 2010). This vital resource must be protected for the well-being of the basin's population. To date, many topics have talked about the threat that the Niger River and its tributaries are facing mainly due to climate variability and change. Taylor *et al.* (2002); Funk *et al.* (2012) have predicted a decrease in the annual rainfall amount over the whole Mali. According to Mahé (2009), there is a strong correlation between negative rainfall anomalies and a decrease in groundwater table in the Niger River basin. This correlation is also true for the tributaries of the Niger River because the study carried out by Mahé *et al.* (2000) has been concluded that during the periods (1981-1995) of rainfall deficit, the groundwater table at the level of Bani at Douna was reduced. In parallel to these studies, Bricquet *et al.* (1997) showed a decrease in groundwater storage in the Bani basin (which includes Klela basin) due to the decline in rainfall and runoff. Furthermore, a study carried out in the Kolondieba catchment, a subbasin of the Bani basin, by Bokar *et al.* (2012), have demonstrated that groundwater levels decline from 2 to 15 cm per year in the period of 1940-2008. The Klela region was rated by Roudier and Mahé (2010) as threatened region to drought facing to climate change.

1.3. Statement of the problem

The water management authorities in the Klela basin are working in order to satisfy the population water demands. Groundwater resources are used for this purpose; since groundwater is the only water supply system applied in the basin. The area that is assured by water supply system is increasing due to population and urbanization growth. Therefore, water demand is increasing, and no study has been directly focused in the Klela basin to evaluate an eventual present and future impact of climate change and population growth on water resources. The partitioning of rainfall into groundwater (recharge) and the interaction between surface water and groundwater are unknown in the Klela basin. Groundwater dynamics have also not been studied in order to plan the future water supply. Facing these challenges, physical and chemical methods as well as a numerical model were firstly applied to estimate groundwater recharge; after that a numerical groundwater flow model, Processing MODFLOW for Windows (PMWIN 5.3),

was used in this study to simulate groundwater behavior in steady and transient conditions; and finally, the hydrological model WEAP has been applied to evaluate the impacts of climate change on groundwater resources.

1.4.   Research questions

Given the problems mentioned above, it is urgent to find the answer to these following questions

1. What is the quantity of rainfall which is recharging the groundwater table in the Klela basin?
2. What is the hydraulic connection between surface water and groundwater in the study area?
3. To what extent will climate change impact groundwater availability by 2050 in the Klela basin?
4. Will groundwater be sufficiently available in the Klela basin considering population growth by 2050?

1.5.   Research objectives

In order to answer these questions, the general and specific objectives are fixed.

The main objective of this current study is to contribute to the sustainable management of groundwater resources in the study area by modeling groundwater dynamics and evaluating it using scenarios data.

The specific objectives are:

1. To estimate the quantity of groundwater recharge of the study area.
2. To simulate groundwater regime in the study area under steady and transient state conditions in order to establish the hydraulic connection between surface water and groundwater.
3. To evaluate the impact of climate change on groundwater resources in the Klela basin.
4. To assess the impact of population growth on groundwater resources in the study area.

1.6. Hypothesis

This study considered two hypotheses

1. The population growth and urbanization rates are negatively affecting groundwater dynamics in the Klela basin

2. Due to climate change impacts, groundwater storage of the Klela basin is decreasing.

1.7. Novelty

No study has been done in the Klela basin addressing the thematic such as groundwater recharge and dynamics modeling before this study. Therefore, the results from this study should be a guide for the new future studies. For example, the best method for groundwater recharge estimation, which is EARTH model, has been identified.

The projected results from this study should be for the decision makers a help in terms of water resources management.

1.8. Expected results

At the end of this study we expect:

1. The estimation of recharge in the Klela basin with the best appropriated method

2. The estimation of the groundwater quantity in time and space in the Klela basin

3. The assessment of the impact of climate change and population growth on groundwater resources in the Klela basin by 2050.

1.9. Thesis structure or thesis outline

The study is organized into seven main chapters. Chapter 0 discusses the general introduction in which the background of the study is clarified, followed by the problem statement, and the research questions and objectives. Chapter 0 presents the general description of the study area. Chapter 0 treats the topic on data, materials, and methods used in this study. Chapter 0 addresses the results from groundwater recharge estimation by applying different techniques of recharge. The outputs of numerical groundwater flow modeling in the Klela basin is used in this chapter 0. Chapter 0 gives the details on the results of the assessment of the impacts of climate change and population growth on

groundwater resources. The major conclusions and recommendations for the study constitute the last chapter (chapter 0).

The methodology of this study can be seen in Figure 0.1
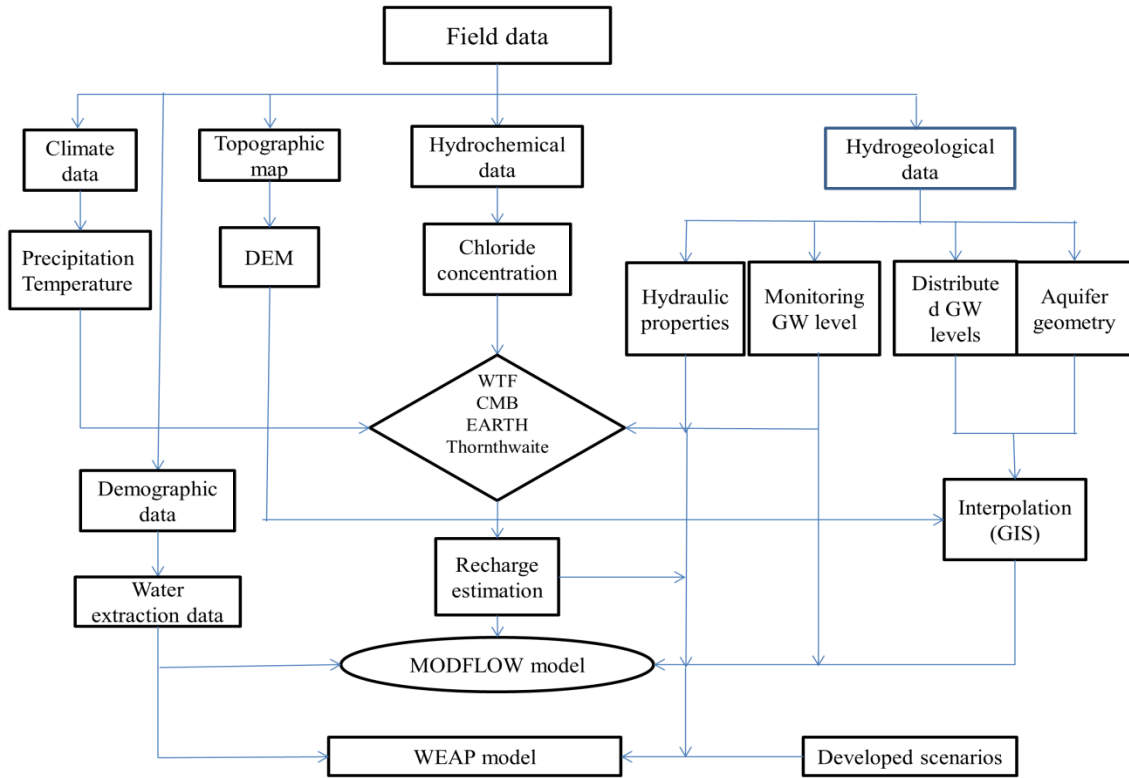
Figure 0.1. Flow chart of the methodology used in this study

CHAPTER 2: THE STUDY AREA

2.1   Location of the study area

The Klela basin is located in West Africa, towards the south of Mali; it is situated between 5° 56' to 5° 17' west longitude and 11° 41' to 10° 60' north latitude (Figure 0.1). The basin is shared by two countries. The major part is in the Sikasso region, southern Mali, representing about 97% of the total area of the basin, while the small remaining portion about 3%, is found in the west of Burkina Faso. The Klela basin covers a total surface area of about 3,680 km^2, is one of the subbasins of the Bani basin. The main river occurring in the basin area is the Lotio, tributary of the Banifing river.
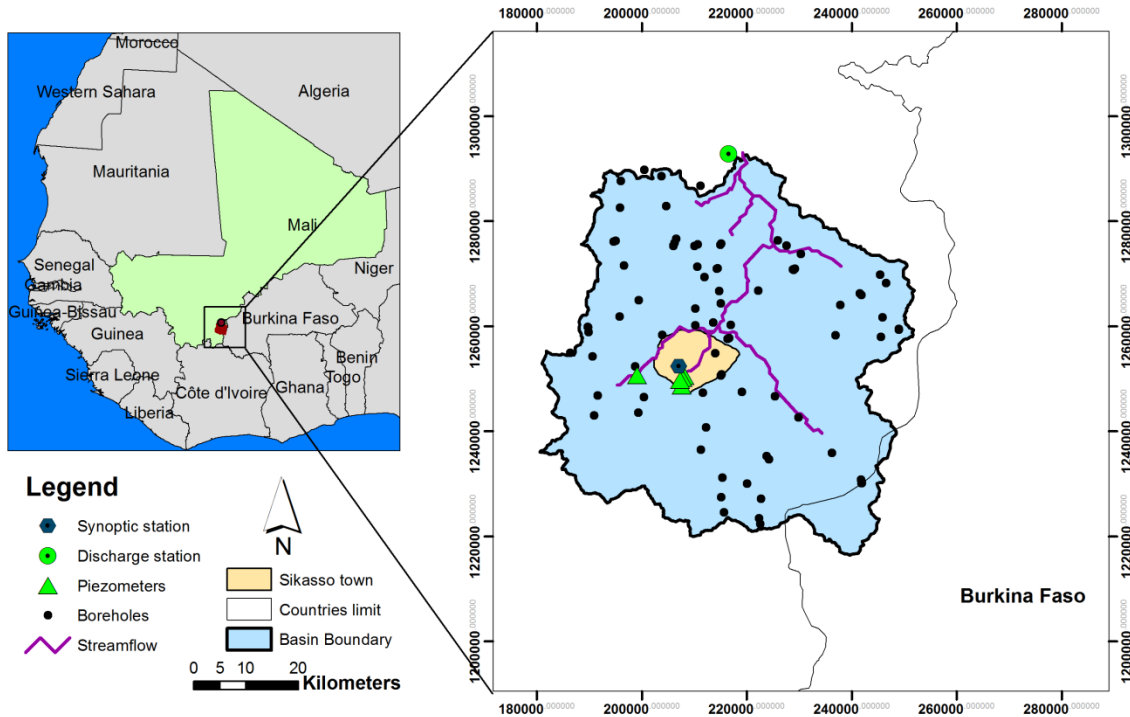
Figure 0.1 Location of the study area (data source from DNH of Mali)

2.2.   Climate

In the West African atmospheric circulation, the movement of two subtropical anticyclones condition the different annual seasons. The anticyclone of Sahara with northeast and southwest direction generates the Harmattan (dry and warm wind)

(Schwanghart and Schütt, 2008), while the monsoon (Nicholson, 2009), which is characterized by lukewarm and humid maritime wind, is produced by the south Atlantic anticyclone known as St. Helena anticyclone with southwest and northeast direction (Figure 0.2). The Intertropical Convergence Zone (ITCZ) is defined by Leroux 1996 cited in Mariko, (2003) as "the dynamic contact between these two air masses (warm and dry) from the north (Harmattan) and humid from the south (monsoon)". The ITCZ is the main responsible of the climate in West Africa region (Obuobie, 2008). Its ground track is called Intertropical Front (ITF), in which its passage causes precipitation (Mariko, 2003). From July to September, the position of ITF is near the north and reaches its extreme south from December to February.
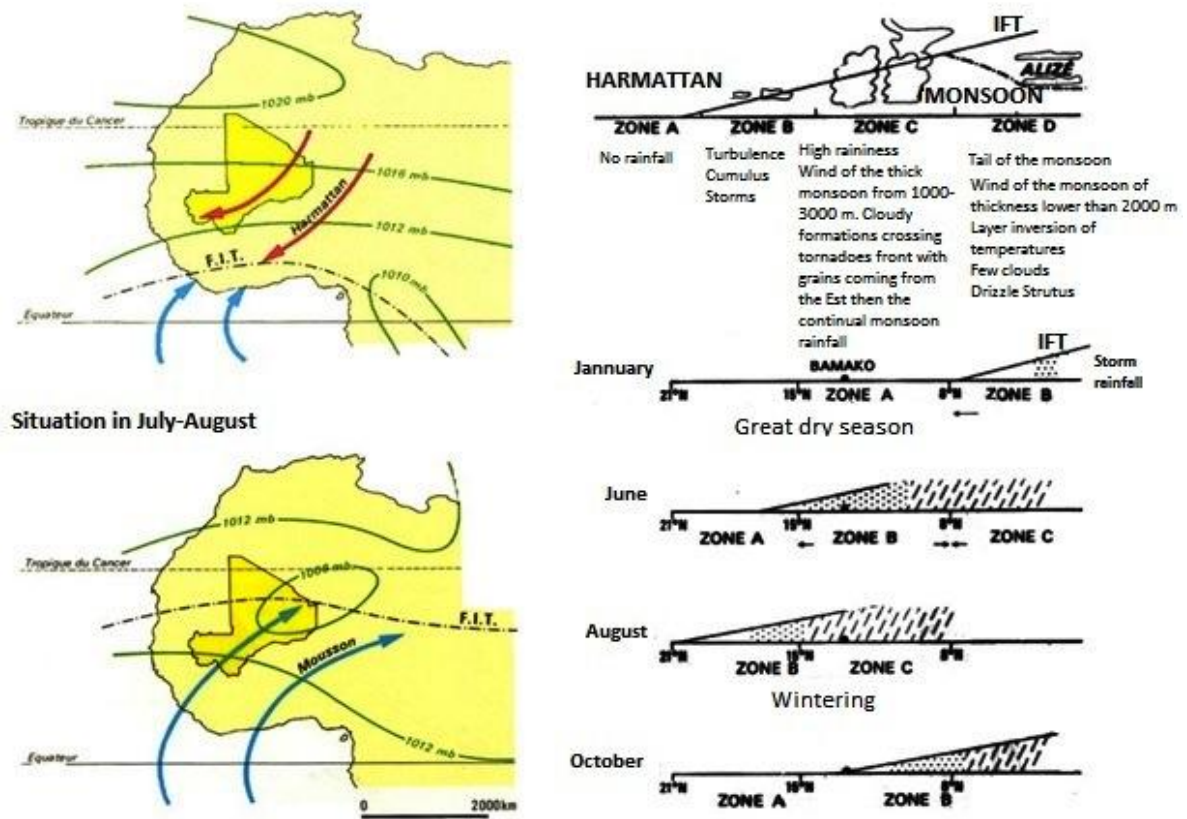
Figure 0.2 Air masses position: At left map, the Harmattan and monsoon winds, and at right, associated time types to the ITF zones and their movement during the year (Figure modified from Kamate 1980 cited in Mariko (2003); Dao (2013))

Mali is entirely situated in the north tropical zone, which is characterized by the dry season alternation from six to nine months from south to north, respectively; and of a humid rainy season or wintering, from May to October in the south and July to September in the north. The rainfall regime in Mali is characterized by a regular decreasing of precipitations and as well as the reduction of rainy days from south to north. The entire territory of Mali can be divided into four climate zones:

- Soudanian zone with a Guinean climate type, located in southern Sikasso region, the annual rainfall may exceed 1,200 mm

- Soudano-Sahelian zone with a tropical climate type, covering Bamako (Capital of Mali) area, the average annual precipitation is comprised between 700 and 1,200 mm

- Sahelian zone covering the western part with Sahelian climate type, the annual precipitation is between 200 and 700 mm

- Sub-Sahelian zone located in the northeast of Mali with subdesert climate type, the annual rainfall is lower than 200 mm.

The Klela basin belongs to Soudano-Sahelian zone with a tropical climate type; it is characterized by an alternating between a dry season, which starts from November to May, controlled by a dry wind from Sahara (Harmattan) and five months of a rainy season, which is from June to October, with wet wind from Guinean Gulf (monsoon) (USAID, 2006; Toure *et al.,* 2016). The study area is chiefly characterized by the unimodal rainfall distribution with the local average annual rainfall varying from 800 to 1,300 mm with 60 to 80 days of the occurrence of precipitation.

2.2.1. **SPI:** Standard Precipitation Index

The historical rainfall data from 1970 to 2013 was used to determine the drought index using Standard Precipitation Index (SPI) tool. The SPI can calculate drought index based on the probability of precipitation for any time scale, which is transformed into an index (World Meteorological Organization, 2012). The SPI was developed by McKee *et al.* (1993) who "calculated the SPI for 3-, 6-,12-, 24- and 48-month time scales". Indeed, the SPI calculation depends on long-term precipitation record for any geographical location (McKee *et al.,* 1993). For example, in the Klela basin, the distribution of precipitation is unimodal from June to October, thus, the SPI calculation for 6 month

timescales is better indicated in that region. The value of SPI may designate the state of the events (drought, wet or normal). The positive SPI value indicates a trend of wet events, while its negative value indicates a trend of drought events. However, McKee *et al.* (1993) have classified the drought events according to the SPI values (Table 0.1) and defined a drought event for any time scale as "a period in which the SPI is continuously negative and the SPI obtains a value of -1 or less". The event ends when the SPI becomes positive.

The usage of SPI presents some advantages; it requires only precipitation as the input parameter, it can be calculated for multiple timescales, provides early warning of drought and helps assess drought severity. It is less complex compared to other index calculations. In contrast, it can only quantify the precipitation deficit; no evapotranspiration cannot be calculated which is an important parameter for drought indicators.

According to the McKee *et al.* (1993) classification (Table 0.1), Figure 0.3 shows that the years of 1971, 1973, 1989 and 2002 were considered as the moderately dry periods, and the year 1983 was the worst and classified as a severely dry year.
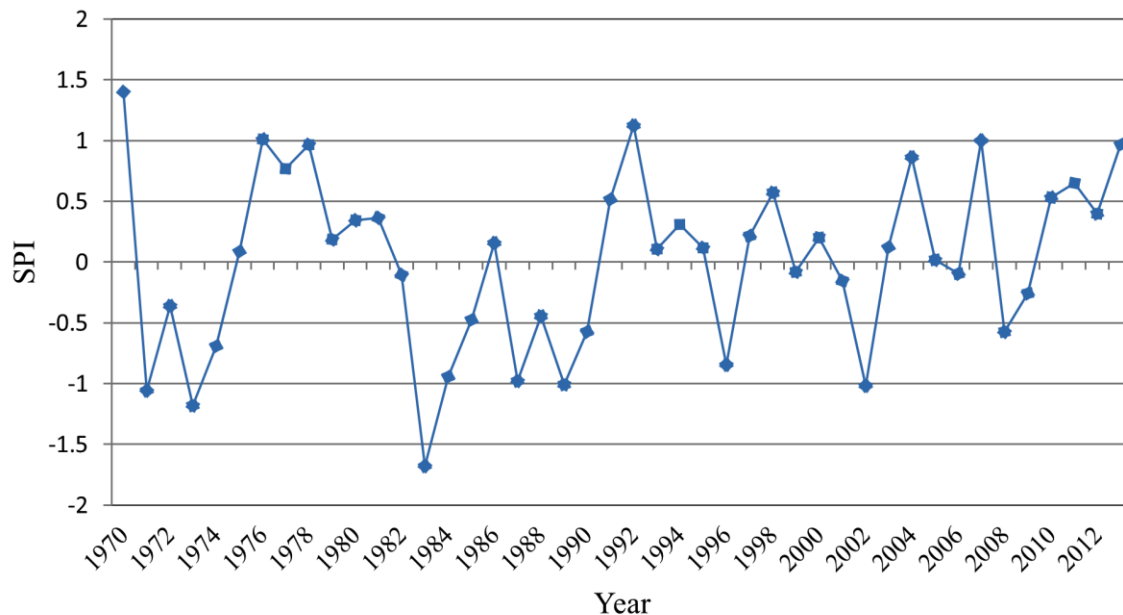
Figure 0.3 Standardized Precipitation Index for the rainy season (June to November) for the period 1970-2013 (data source from DNM of Mali)

Table 0.1 SPI values (McKee *et al.,* 1993)

≥ 2	Extremely wet
1.5 to 1.99	Very wet
1 to 1.49	Moderately wet
-0.99 to 0.99	Near normal
-1 to -1.49	Moderately dry
-1.5 to -1.99	Severely dry
≤-2	Extremely dry

2.2.2. Temperature

The temperatures of the Klela basin are relatively higher. However, the mean monthly values vary during the year. The average monthly temperature recorded for the basin area varies from 31.2 °C in April, the highest period of temperature, to 24.5 °C in December, the lowest period (Figure 0.4). The minimum monthly temperature fluctuates from 12.3°C to 26.8°C and the maximum temperature varies from 28.8°C to 39.9°C.
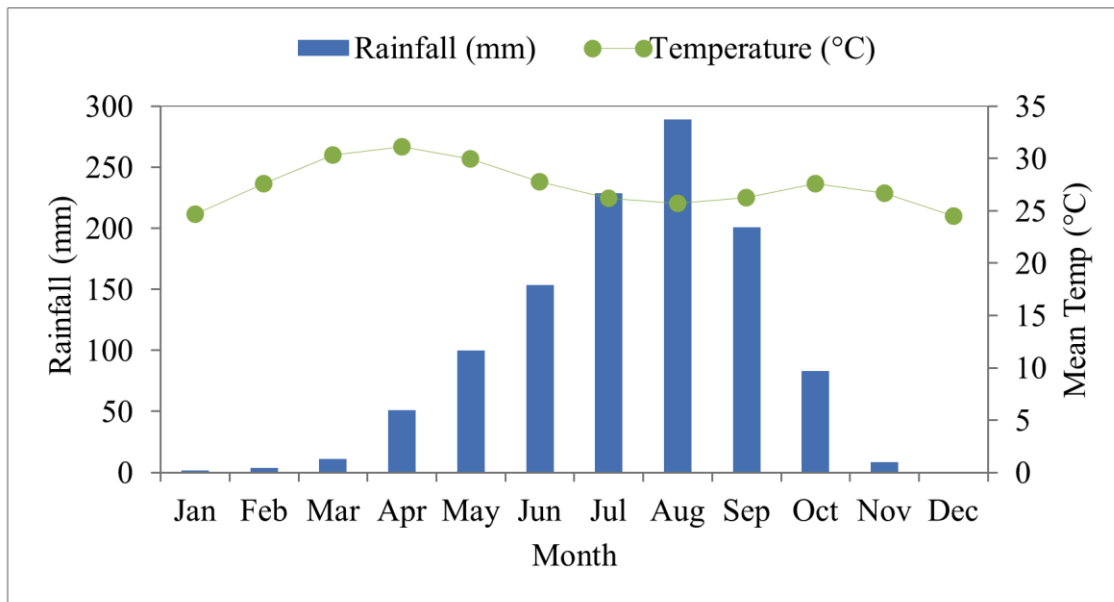
Figure 0.4 Average monthly rainfall (mm) bar graph and line chart for the average monthly temperature (°C) from 1970-2013 (data source from DNM of Mali)

2.2.3. Evapotranspiration

High temperature, low relative humidity, and strong trade winds during the rainy season, may explain the high level of evapotranspiration in the study area. Evapotranspiration is one of the most important parameters in the water budget in all the areas of Mali including the Klela basin, where the mean annual potential evapotranspiration exceeds 2,000 mm. The maximum value of the mean monthly potential evapotranspiration is recorded in May with about 196 mm and the minimum is about 150 mm, obtained in December. During the year, the value of mean potential evapotranspiration exceeds the rainfall, except some months where the intensity of rainfall reaches its maximum (Figure 0.5). Potential evapotranspiration here is calculated based on Blaney and Criddle (1962) method. This method is simple, using only measured data on temperatures, but it provides a rough estimate value (Brouwer and Heibloem, 1986).
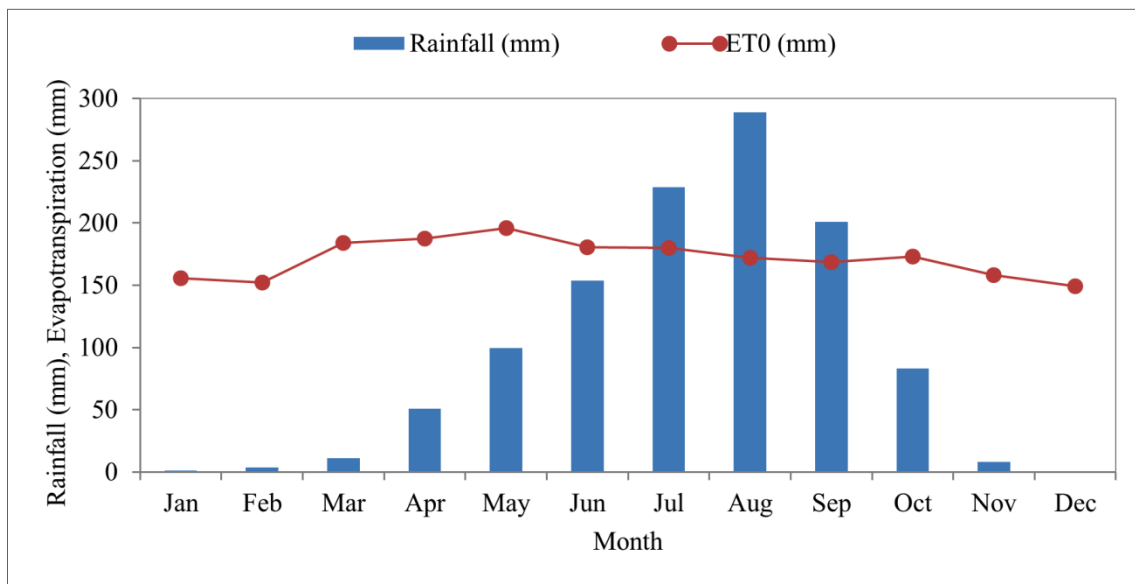
Figure 0.5 Mean monthly rainfall and potential evapotranspiration at Sikasso in the Klela basin, from 1970-2013 (data source from DNM of Mali)

2.3. Topography

The topography of the study area is accentuated by the sandstone plateaus. The elevation of the basin ranged from great "bas-fonds" to sandstone plateaus with values of

land elevation varying from 305 mamsl in the north of the basin at Klela to 750 mamsl in the south towards Burkina Faso west at Koloko. The central and northern parts of the basin are many constituted by the existence of numerous immense "bas-fonds". The information on the topography of the basin is deducted from Digital Elevation Model (DEM) provided by HydroSHEDS described thereafter.

Digital Elevation Model

The HydroSHEDS (Hydrology of data and map based on SHuttle Elevation Derivatives at multiple Scales) data, which is derived from elevation data of Shuttle Radar Topographic Mission (SRTM), was used in this study to extract surface elevation data. It was developed by the Conservation Science Program of World Wildlife Fund (WWF) (Lehner, 2013) and can be downloaded[1] for free of charge. A void-filling technique was applied to the SRTM Digital Elevation Model (DEM) for HydroSHEDS to correct the error due to the existence of no-data. The HydroSHED has a resolution of five-degree by five-degree tiles (or 90 m * 90 m approximatively). Prior to using it in this current study, it was reconverted to 300 m* 300 m, which is the model cell size (see the detail in chapter 0). According to Lehner (2013), the precision of HydroSHED exceeds that of the existing global watershed and the river maps.

The DEM was used to delineate the watershed boundaries of the study area. It has also allowed determination of the number of stream flows (number of streams) that were used in this modeling and flow directions (Figure 0.6).

---

[1]HydroSHED site: http://hydrosheds.cr.usgs.gov
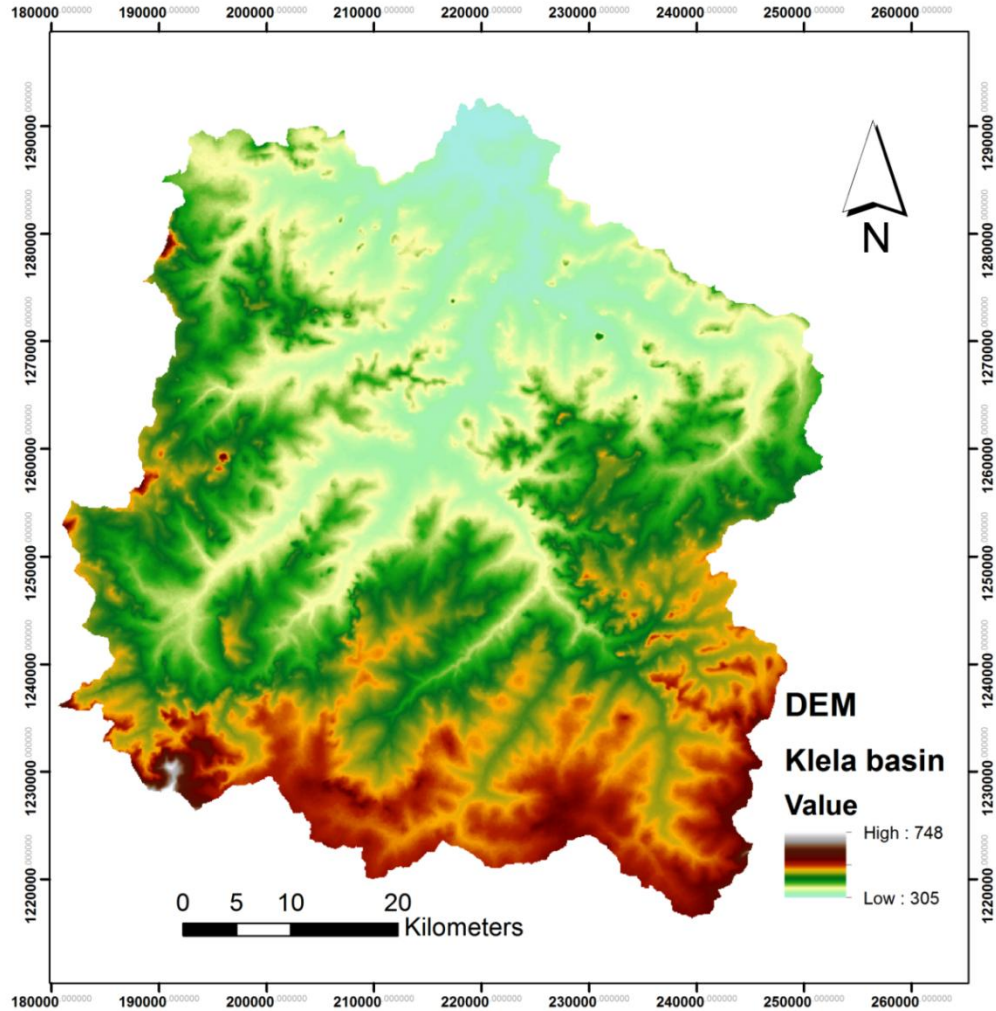
Figure 0.6 Elevation map of the Klela basin (DEM used is from HydroSHED)

Furthermore, all the elevation of water table points was extracted from DEM in order to determine hydraulic head before its interpolation in GIS using Kriging method. The scatter plot between surface elevation vs water table (Figure 0.7) displays that in most boreholes, the water table is between 0 to 20 m below ground level. This may suppose that there is an eventual important interaction between groundwater and streams within the basin.
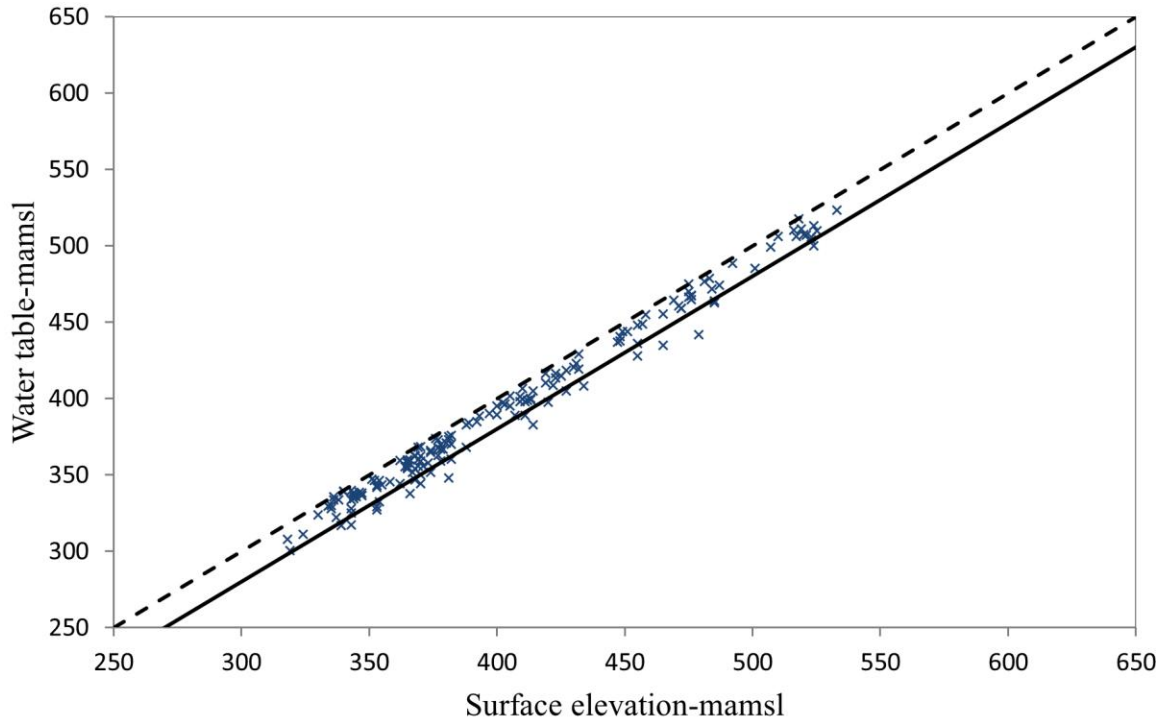
Figure 0.7 Scatter plot between surface elevation and water table, the star points are field data of water table; the discontinuous line represents surface elevation and the black line corresponds to surface elevation minus 20 m (data source from DNH and HydroSHED).

2.4.   Population

Southern Mali including Klela basin is the most populated region in Mali, with 1,782,157 inhabitants in 1998. The population of the Klela basin was estimated to approximately 462,544 in 2009, according to RGPH (2009), with 3.6% of growth rate (N'Djim and Doumbia, 1998). According to the classification of urbanization rate in Mali (WWAP, 2006), which is mainly based on the number of population, most of the area of the basin is a village. In the area where the population is lower than 2,000 people, it is considered as a village (Figure 0.8) and semi-urban or urban when it is greater than 5,000. As most of are villages, therefore it can be concluded that the principal activity in Klela is agriculture and livestock.
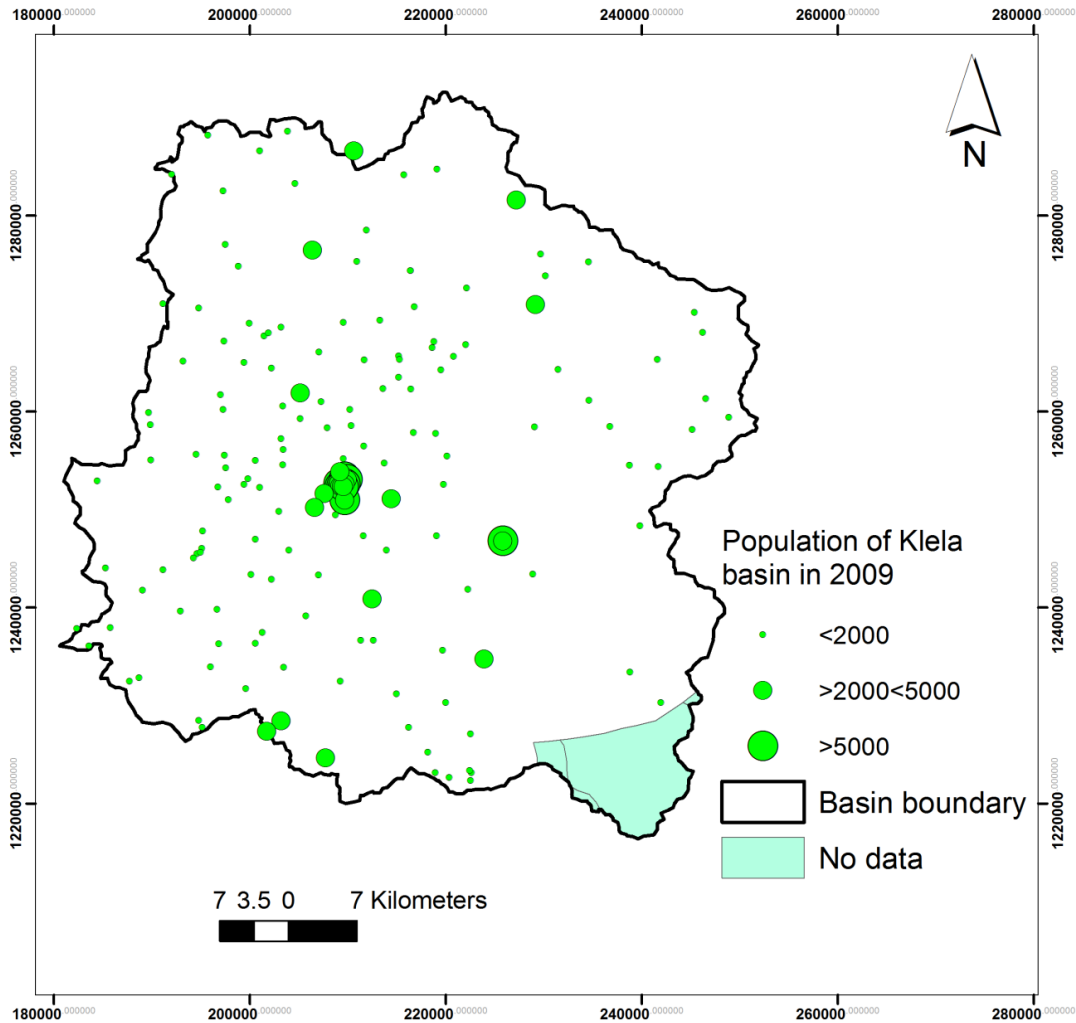
Figure 0.8 Population map of the Klela basin in 2009 (data source from RGPH 2009)

2.5.   Geology

In Mali, the geological formations cover the principal stratigraphic groups defined for the geology of Africa. The Taoudenni sedimentary basin, one of the major structures of the West African geologic formation, is mostly represented in Mali (Synthèse hydrogéologique du Mali, 1990). The lithostratigraphic system in Mali has experienced nine major geological subdivisions. Most of the information on geology and hydrology are from Synthèse hydrogéologique du Mali (1990).

a. The Birimian basement (Precambrian C): it outcrops in the southwest and western part of the country, and northern Taoudenni, emphasizing the northern boundary of

the Taoudenni basin. The Birimian basement is mainly constituted by volcano-sedimentary formations with varied lithology and intrusive granite massif. It is represented by several different facies such as schists, greywackes, conglomerates, quartzite with the intrusion of volcanic rocks, biotite granite, tuffs, quartz diorites, and granodiorites.

b. Infracambrian (Precambrian A): primarily composed of sandstone and schist facies, Infracambrian widely outcrops in the southern half of Mali. The lithological succession and thickness of Infracambrian are variable. Therefore, three domains were considered

   - **Sandstone plateau**, although the complexity of its lithological system due to its rapid variability and high thickness, the following succession has been adopted from down to up: lower sandstone formation, sandstone formation with intercalated dolomitic, schist of Toun, sandstone Sotuba and Bandiangara.

   - **Gourma basin**, defined as a basin filled with a set of folded sedimentary, extending to the northeast of horizontal sandstone and shield of the voltaic north (Reichelt, 1971). It is characterized by the accumulation of Ydouban group formation widely dominated by the shale and clay formation. This basin is considered as a domain of folded and metamorphosed Infracambrian (WWAP, 2006).

   - **Hombori threshold-Douentza**, it is an area that occupies the southwest and west of the Gourma, and presents the following succession from down to up: basement formation of quartzite sandstone, clayey schist of Beli's formation, Irma formation consisting of dolomite and shale, the sandstone and quartzite of Hombori-Douentza formation, the Oualo-Sarniere formation dominated by clayey sandstone and limestone and sandstone of Bandiangara formation.

c. Cambrian: exposed in the northwestern Mali, the Cambrian formation is mainly constituted by schists, shales and argillite with intercalations of sandstone and dolomitic limestone in the middle and upper parts. Probably the upper layers are Ordovician age.

d. Primary of Taoudenni: it outcrops in the extremity northern Mali, the primary formation is constituted by three geologic stages.

- The cambro-silurian, essentially represented by the pelitic facies which turns into sandstone in its upper part
- The Devonian is composed of limestone, marl, clay and gypsum
- The carboniferous, it is represented by the limestone of Visean. Its upper part is characterized by the continental facies with red clay, sandstone stage, and gypsiferous horizon.

e. Dolerite intrusion: principally deposited at Permian and Triassic periods. They are dominated by the series of sandstone and pelitic and gathered a wide variety of volcanic rock constituted particularly of gabbros and basalts.

f. Continental intercalary: largely represented in the north and east as well as the central of Mali, it consists of the continental formations that are accumulated in the sedimentary basins. Its lithology is formed by the quartzite sandstone of the northern Azaouad basin; sand, gravels and siliceous of the trough of Nara. The northwest and southeast of the Adrar des Iforas border are formed by sandstone and conglomerate, and the basement of arkosic sandstone formation, respectively.

g. Upper cretaceous/lower Eocene, they are represented by four geologic stages in the northwest of the Adrar that are: Senonian – Maastrichtian (clayey sandstone), lower Paleocene (sand and marl limestone), terminal Paleocene (limestone and phosphate gravel) and Middle Eocene (schist and gypsum).

h. Continental terminal, it is constituted by the continental formations, which are deposited in Miocene and Pliocene. Its lithostratigraphy is composed of sand, sandstone, clay and laterite cuirass.

i. Overlying formations, there are four types that are: (1) laterite formation is the outcrop of the Birimian and Infracambrian, (2) alluvial deposits consist of clay and sand, (3) lacustrine formation represented by marls and limestones, and (4) dune formations in the desert area of Mali.

2.6.   Geology of the Klela basin

The Klela area, which belongs to the tabular Infracambrian formation, is mainly constituted by consolidated sedimentary rock, namely the sandstone and shale facies (Figure 0.9). It is largely dominated by sandstone basement, which is composed of quartzite sandstone with conglomerate, and the thickness is between 10 to 40 m. The lower sandstone formation is located in the southwestern basin, and it is represented by the epicontinental sandstone with a thickness of 10 to 200 m. The thickness of the lower sandstone is distinguished by the irregular sedimentation and frequent oblique stratification. The second important geologic unit in the Klela basin is the dolerite intrusion, which is localized in the west in high quantity, and in the northwards where the dolerite is lower. This formation has occurred in the Permian and Triassic periods. Dykes are predominant in the sandstone series and formed an important compartmentalization within the sedimentary rock formations. Their thickness can reach some tens of meters. In contrast, the sills are frequent in the pelitic formations. With a considerable thickness exceeding 100 m, they constitute the volcanic complex of laccolite type in some schistose zones of the Cambrian and Infracambrian. In addition, these dolerite intrusions contain a wide variety of volcanic rocks and constitute principally by gabbro and basalt formations. The extreme south of the basin, situated in Burkina Faso west, is composed of sandstone of pebble of quartz, which is higher, following by the Sotuba sandstone, and finally the dolomitic schistose sandstone. In general, the basin is crossed by the faults. The outcrop of the dominated sandstone in the area is shown in the image 2.1.
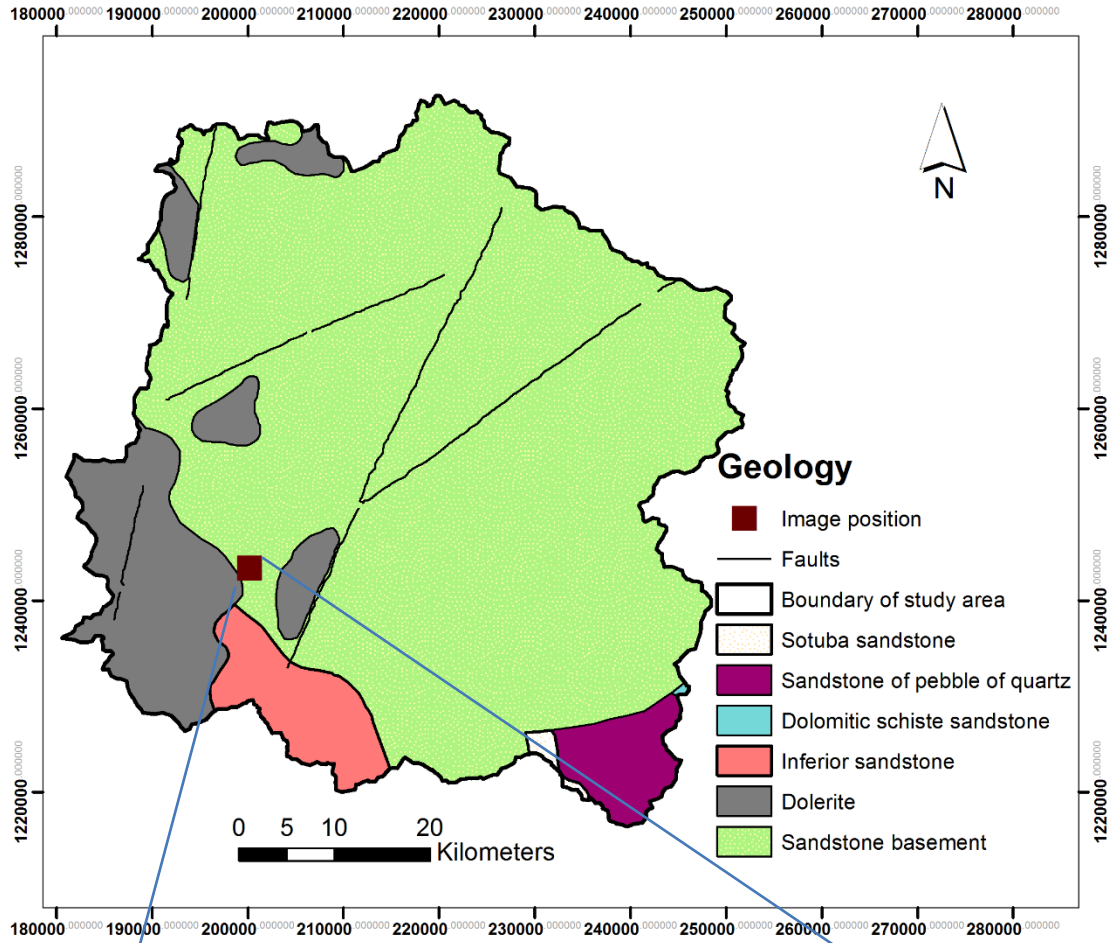
Figure 0.9 Geology of the study area (map source from DNH of Mali)
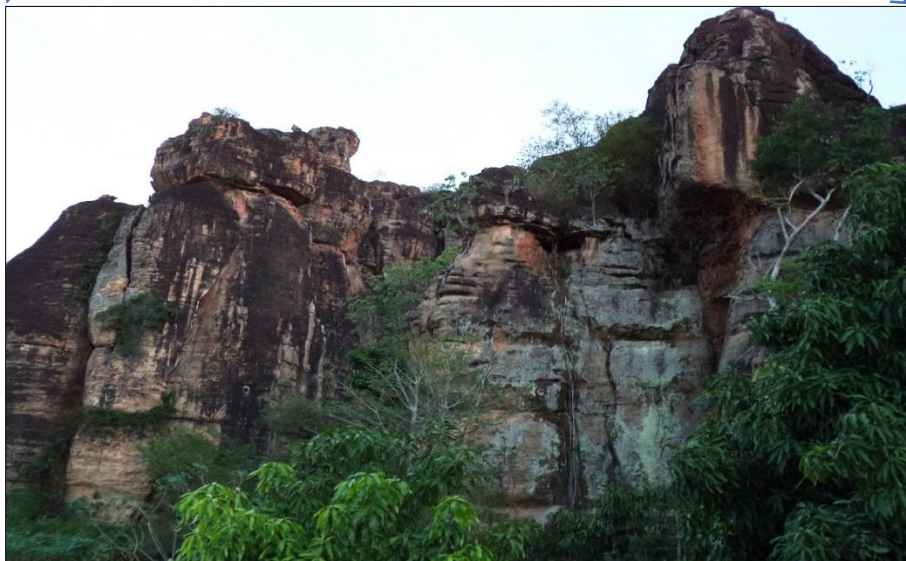
Image 2.1. Outcrop of the sandstone in the Klela basin

2.7. Hydrogeology

2.7.1. General aquifer system

According to the origin of groundwater, there are nine deep aquifers in Mali, which are classified into two categories. Fissured and discontinuous aquifer types, which are represented by crystalline and sedimentary formations from Precambrian and Primary, and the generalized aquifer, which is associated to the few or none consolidated formation, is accumulated in the sedimentary basins from Secondary to Quaternary.

a. Fissured aquifers: characterized by lower permeability, the presence of groundwater is essentially due to, on the one hand, the fissure in the deep part of the formations, and the weathering of the formations in the upper zone, on the other hand. In the fissured aquifer, the water is transferred laterally, while it is accumulated to a certain level in the alterites. The interaction between the overlying formations and the fissured substratum constitute a preferential flowing zone for some aquifers. Mali accounts for five principal fissured aquifer systems.

b. Basement aquifer: in the south toward Sikasso region, the Birimian basement is characterized by shallow aquifer with a thick covering of alterites. The streams are draining the aquifer system that explains the permanent surface water flow upstream the Niger River. In the western part, the thickness of the superficial formations is reduced, and the piezometric level depth increases progressively in the northern part. Unlike the south, the surface runoff contributes to recharging the fissured aquifer in the other parts of Mali. In the Sahelian and desertic zones, in the eastern part, fissured aquifer is discontinuous with depth variable water.

c. Tabular Infracambrian aquifer: it is the largest fractured aquifer exploited in Mali and is characterized by the Secondary permeability. Infracambrian is primarily composed of schistose sandstone formations, which are overlaid by lateritic formations, except the Dogon and Mandingue plateaus, where the sandstone outcrops. The horizontal hydraulic discontinuity occurs in the fissured aquifer during the intercalation between pelitic quartzite and weathered sandstone, and schist that constitute the facies of Infracambrian. On the other side, the dolerite intrusions constitute the vertical discontinuity nearly continuous.

d. Metamorphic folded Infracambrian aquifer: situated in the Sahelian and subdesert zones, its hydrogeological characteristics are very different that distinguishes it to tabular Infracambrian. The aquifers are discontinuous and permeable in the quartzite sandstone, limestone and dolomite formations with a deep water table.

e. Cambrian aquifer: schistose in the Cambrian series and dolerite intrusions formations constitute the principal hydrogeological characteristics for this aquifer, which is discontinuous. The lateritic weathering formations present a thin thickness; therefore, groundwater resources occur essentially in the fissured zones. This aquifer exceeds the northwest of Mali and extends towards the Hodh basin in Mauritania.

f. Taoudenni primary formation aquifers: this aquifer is located in the series of fissured sandstone and limestones, and occurring in northern Taoudenni cuvette. There are also some small shallow aquifers in the alluvium and colluvium of wadi bed, which are provided by surface water runoff.

g. Generalized aquifer: these aquifers are continuous types and characterized by an intergranular permeability. They are localized in the north and east part of Mali and covering the major part of the Sahelian and desert zones. The generalized aquifers are constituted by the detritic formations essentially clayey-sand that occurred from Secondary to Tertiary. They are composed of four aquifer types: Continental Intercalaire (sandstone quartzite, pelitic sandstone of Ordovician-Cambrian, sandy-sandstone), Continental Terminal (clayey-sand, sandstone, laterite), Upper Cretaceous/ Lower Eocene (argillite, schist, clayey sandstone, phosphate limestone) and Continental Intercalaire/Continental Terminal (sandstone schist, sandy clay).

h. Overlying aquifers or superficial aquifers: they cover the most of the Malian land surface, and have a significant hydrogeological role because they constitute the first reservoir that captures the infiltration and runoff from rainwater. These formations are classified into two types: semi-continuous aquifers and discontinuous aquifers.

- Semi-continuous aquifers, in west and south of Mali, they are associated to fissured basement and Infracambrian sandstone aquifers and are characterized by shallow aquifer overlaid by lateritic weathering and alluvium, and colluvium deposits of the bottom of the valley. Hydraulically, the fissured aquifer is connected to the superficial aquifer allowing monitoring the recharge and discharge. The hydraulic characteristics

depend not only on the substratum of the lithology but also the rainfall as well as the geomorphological conditions. One can distinguish two types of overlying in the semi-continuous aquifer:

- overlying on the basement, it is hydrologically characterized by three superposed zones, (i) upper aquifer layer corresponding to lateritic cuirass with a good vertical and horizontal permeability; (ii) constituted by a clayey arena with low permeability; and (iii) lower aquifer layer represented by the arena of variable granulometry and upper fractured, and weathered basement.

- Overlying on Infracambrian sandstone, these formations are similar to the basement formation but differ from the permeability. The overlying formations on sandstone are more permeable than that on the basement.

- Discontinuous aquifers, situated in the Sahelian and desert zones in Mali, it is represented by:

  - overlying on fissured aquifers which form small shallow aquifers in the alluviums in the bottom of the valley. They are essentially replenished by infiltration from surface water runoff, and the most important water is going by evapotranspiration;

  - overlying on generalized aquifers, present the deep aquifers, which are recharged by infiltration from local rainfall and runoff.

2.7.2. Aquifer system in the Klela basin

The Klela basin belongs to the tabular Infracambrian aquifer, essentially constituted by schistose sandstone formation. This aquifer is divided by seven hydrogeological units of which Klela basin is the unit of middle Bani with sector 73b[2] according to the classification of Synthèse hydrogéologique du Mali (1990). Groundwater occurs only in the deep fissured aquifer zone and the upper alteration formation part of the sandstone of the Klela basin because the intrinsic permeability of the sedimentary and metamorphic formations in the Precambrian is very low.

---

[2] The code 73b is explained as: the figure 7 signifies Infracambrian Tabular, the following 3 indicates middle Bani and the last letter b represents the sandstone at Sikasso circle.

The overlying formations, which are generated from the weathering of the sandstone bedrock, are very important in the study area, but less thick varying from 3-70 m with an average of 17 m. Their thickness constitutes the first reservoir that intercepts the infiltration, before arriving the aquifer, from precipitation and easily accessible for the population without spending a lot of means. They are characterized by a horizontal permeability very important due to the presence of the sand fraction, and also a secondary permeability related to the biologic activity developed on the entire height of weathering profiles. This shallow aquifer is mainly exploitable during the recharge period due to the strong evapotranspiration occurring in the study area. They are principally covered by the lateritic alteration and are semi-continuous aquifers. The highest thickness of the overlying aquifer of the Klela basin occurs in the south, while the lowest is observed in the northwards.

Since the overlying shallow aquifers are limited in quantity (in dry season due to strong evapotranspiration) and quality (in the rainy season due to the low depth and important runoff), the traditional wells are replaced by the deep boreholes in the study area. Because of their depth, the boreholes are more protected against evapotranspiration and chemical or bacteriological contamination compared to the tradition wells.

The existing drilling log data from 1985 up to 2013, available from the DRH of Sikasso and DEM were used to draw the elevation of bedrock map (Figure 0.10). This data, from 185 boreholes spatially distributed throughout the basin scale, was interpolated using Kriging method into GIS. The figure generated from this interpolation shows a decreasing trend from the south to the north of the basin.
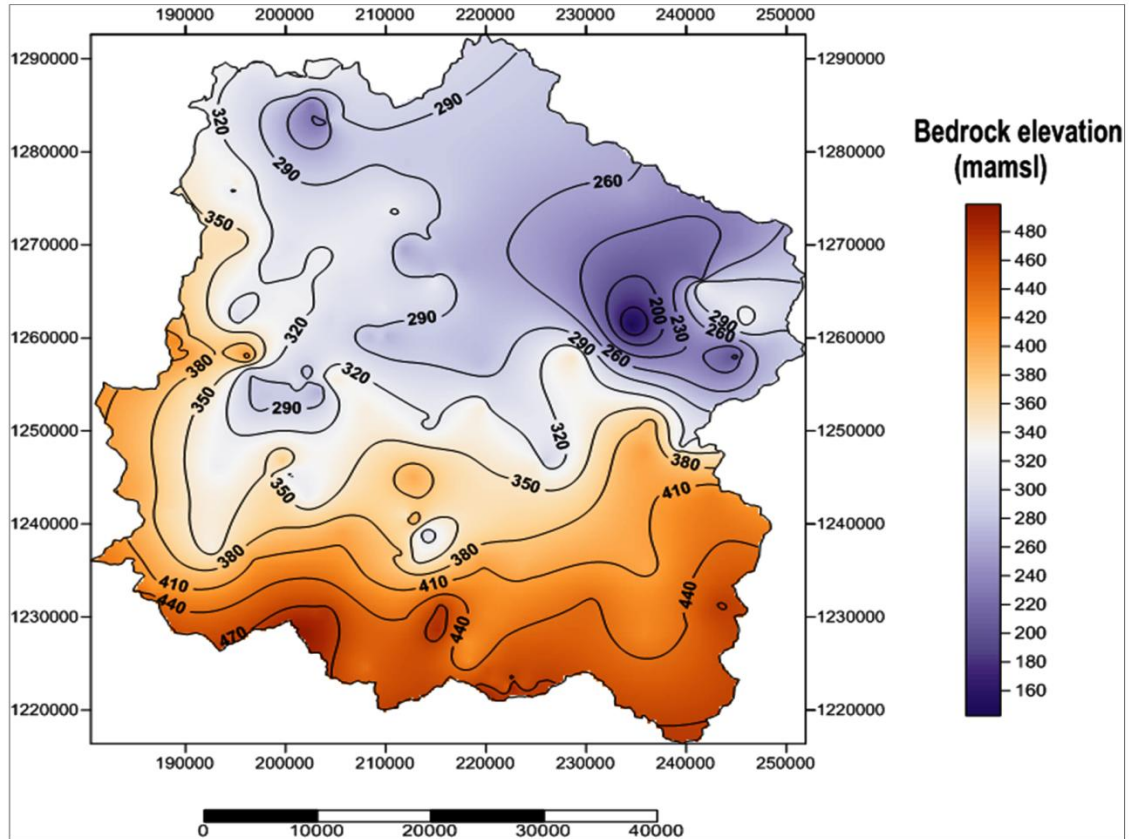
Figure 0.10 Bedrock elevation of the study area (data source from DRH of Sikasso)

Investigations of the measurement of piezometric level are crucial in groundwater monitoring. Groundwater table measurement permits to predict the evolution of groundwater storage. It is an important parameter used for calibrating groundwater model. The data from the same dataset used in aquifer bedrock elevation was used to interpolate, applying Kriging technique. The interpolated groundwater table map (Figure 0.11) reveals that the water is flowing from the south to north.

Furthermore, most of the borehole bedrock elevations fall between 50-80 m below ground level (Figure 0.12a), but some exceed 100 m, and the maximum reaches 248 m. The histogram (Figure 0.12b) shows that most of the static water level is between 5 to 15 m below ground level.
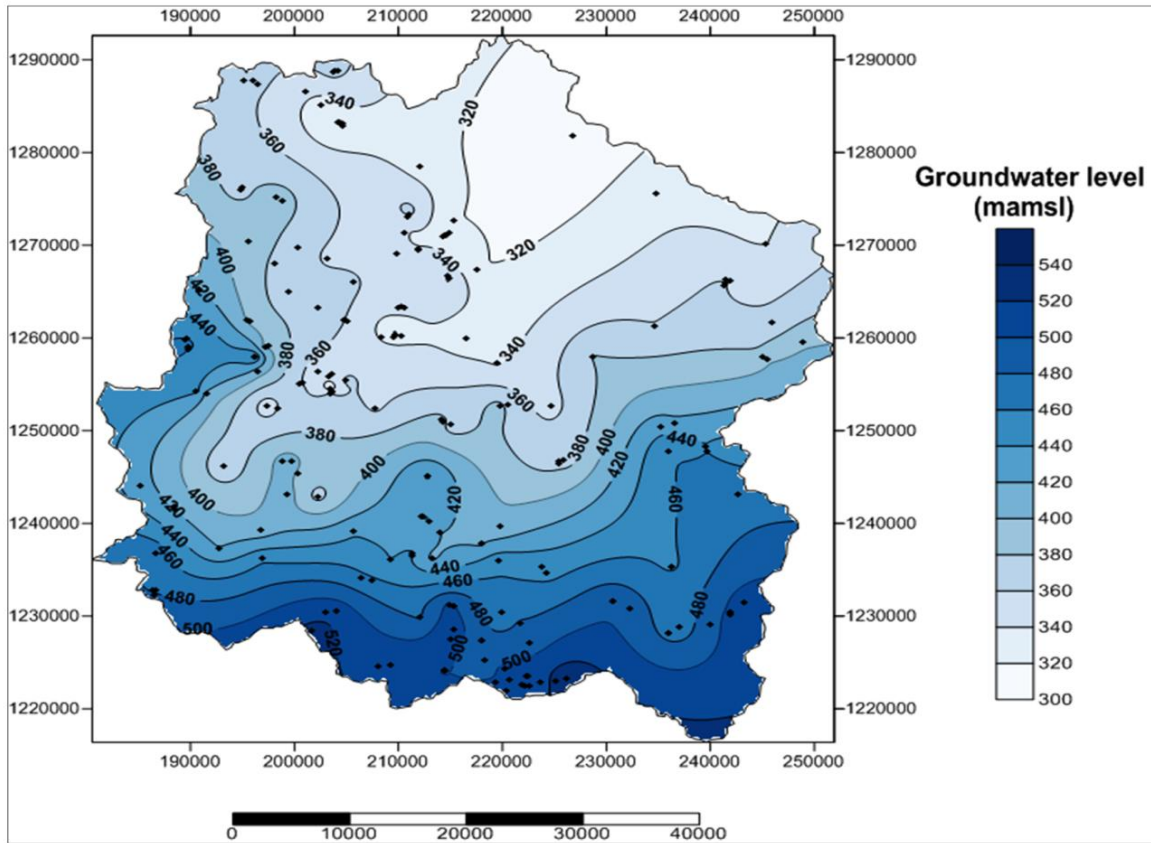
Figure 0.11 Groundwater level and borehole locations in the Klela basin (data source from DRH of Sikasso)
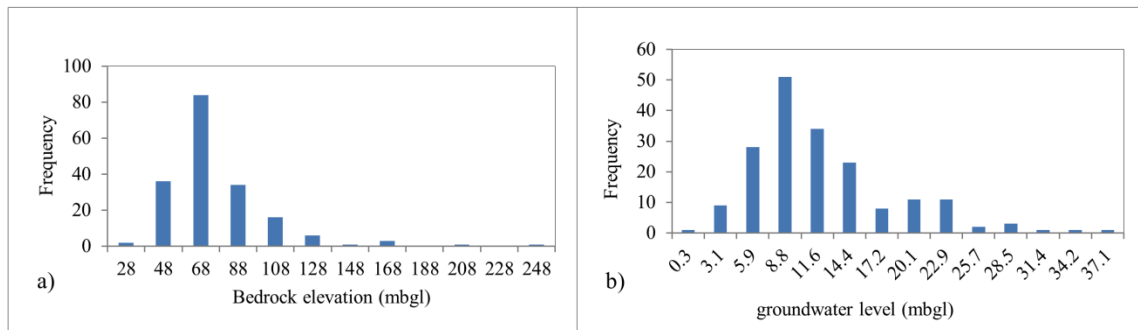
Figure 0.12 Histogram of the frequency (a) of the depth of the borehole in meter below ground level; and (b) groundwater level (mbgl)

2.8. Hydrology

The Klela basin, the principal tributary of the Banifing, is drained by many small streams that are dried out a few months after the rainy season. The principal river is the Lotio, which has its source in the hill of Tiogola village in the rural commune of Kapala. The length of the course of the Lotio River is estimated to 136 km. The main surface water courses are the tributaries of the Lotio, which are the following: Farako, Kobani, Kodialani, Banankoni and Kobleni (Figure 0.13). All these tributaries flow from south to northward into the Banifing River.
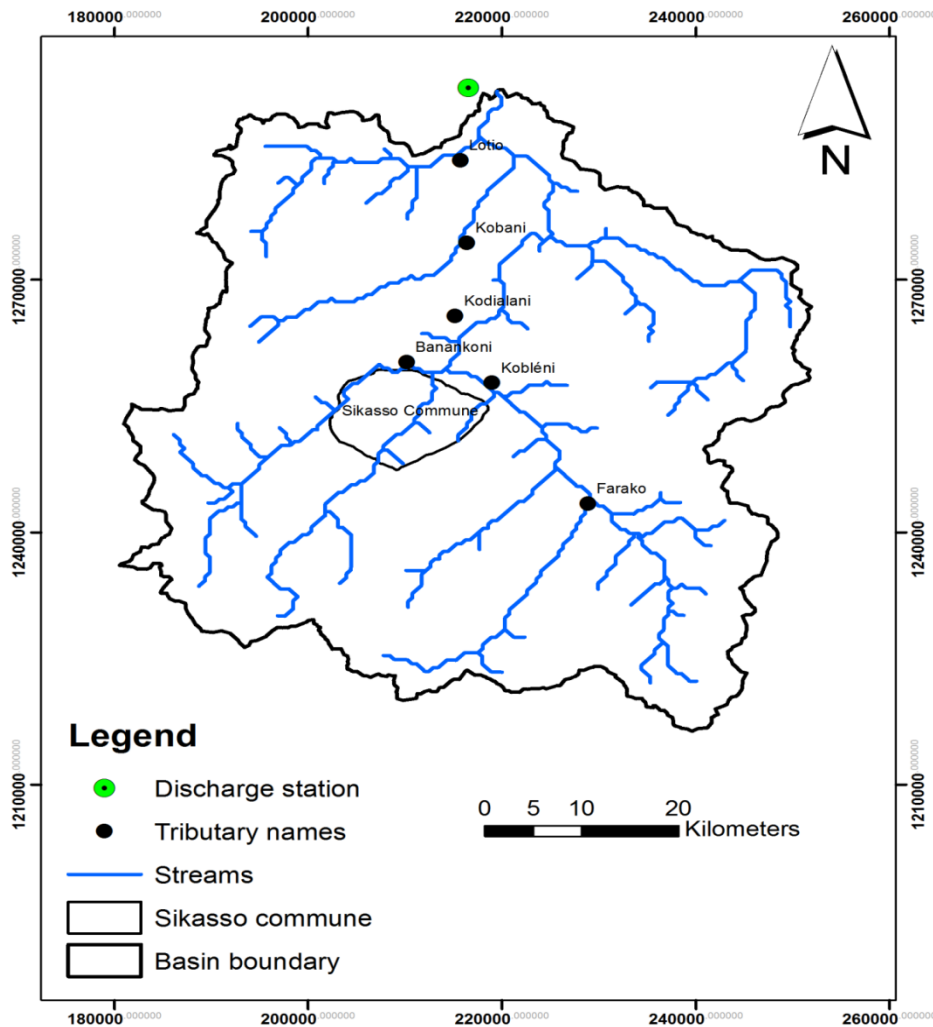
Figure 0.13 The main surface water courses in the Klela basin (data source from DNH of Mali).

In total, three stations are installed to monitor the discharge of the Lotio River: the station at Klela, Sikasso town, and Finkolo. Unfortunately, only the station at Klela, which drains 3,680 km^2 in area, is regularly monitored in the daily time step, and the data available and used in this study is from the DRH of Sikasso from 1980-2014. It is also important to notice that this dataset contains some missing data. Figure 0.14 displays the mean monthly hydrograph at the Klela station. The overall monthly mean hydrograph shows the peak during the rainy season, in September and the low flow in the dry season, in April (Figure 0.14a). Over a period of 35 years, the minimal monthly discharge was about 1.9 mm/month, recorded in April 1990, while the maximal monthly discharge was 52.4 mm/month, recorded in September 2007 (Figure 0.14b). The mean monthly discharge was approximatively 7.9 mm/month. Figure 0.14c exhibits the low flow period from 1982-2000 and the remaining years were considered as a high flow period, except the years 2002, 2008 and 2014. The overall mean annual discharge was approximatively 94.7 mm/a.
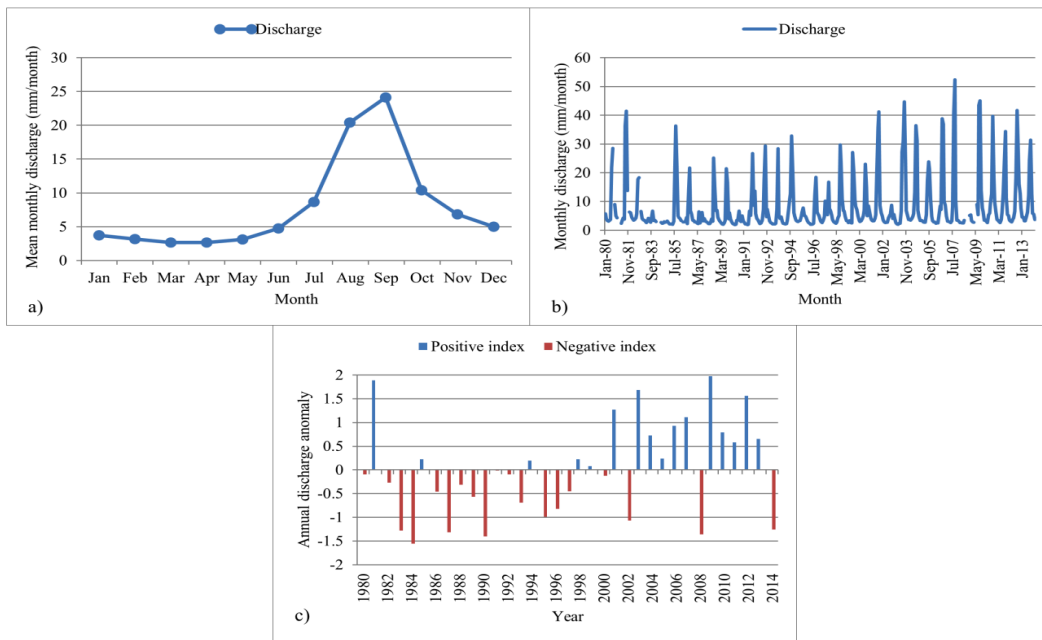
Figure 0.14 (a) and (b) Mean monthly discharge (mm) from 1980-2014, and (c) annual discharge anomalies from 1980-2013, at the Klela station (data source from DNH of Mali)

2.9.   Land cover (LC)

The map (Figure 0.15) of land cover types of the Klela basin is based on the image data from 30-meter Global Land Cover Dataset (GlobeLand30). This image data is developed by the National Geomatics Center of China in 2014. The classification used for these images are mainly constituted by 30 m multispectral images including Landsat TM and ETM+ multispectral images and multispectral images of Chinese Environmental Disaster Alleviation Satellite. According to this global classification, in total, eight (LC) units were identified (Table 0.2). The study area is principally dominated by grassland type that represents 57% of the basin area. For this LC unit, the lands are covered by natural grass. The second most important LC unit is the cultivated land that is mainly used in agriculture including paddy and cotton fields, irrigated and dry farmland, vegetation and fruit gardens, *etc*. It is account for 22% of the total land. Agriculture is essentially based on seasonal rainfall, hoes and plows are manually used as cultivation tools. Most of the land in the basin is still suited for the major cultivated crops such as cotton, rice, potatoes, maize, millet, *etc*. The shrubland characterized by a covering of shrubs including deciduous and evergreen shrubs represents about 12% of the study area. Two main types of forest are presented in Klela: the natural forests constituted by a large variety of trees and the classified forests that are selected. The total percentage of the forest is about 8% distributed throughout the basin and principally concentrated in the east south and western parts. Other types of associated land such as wetland, water bodies (including river, lake, reservoir, *etc*.), artificial surfaces (lands modified by human activities including all kinds of habitation and all development sectors such as mining and industrial areas), and bareland (including bare rocks, sandy fields, *etc.*) are less than 2%.

Irrigation is the main economic activity practiced by the population over the year. Most of the cultivated lands are cultivated with potatoes and paddy fields; however, the cultivation rate of paddy is reducing compare to potatoes.
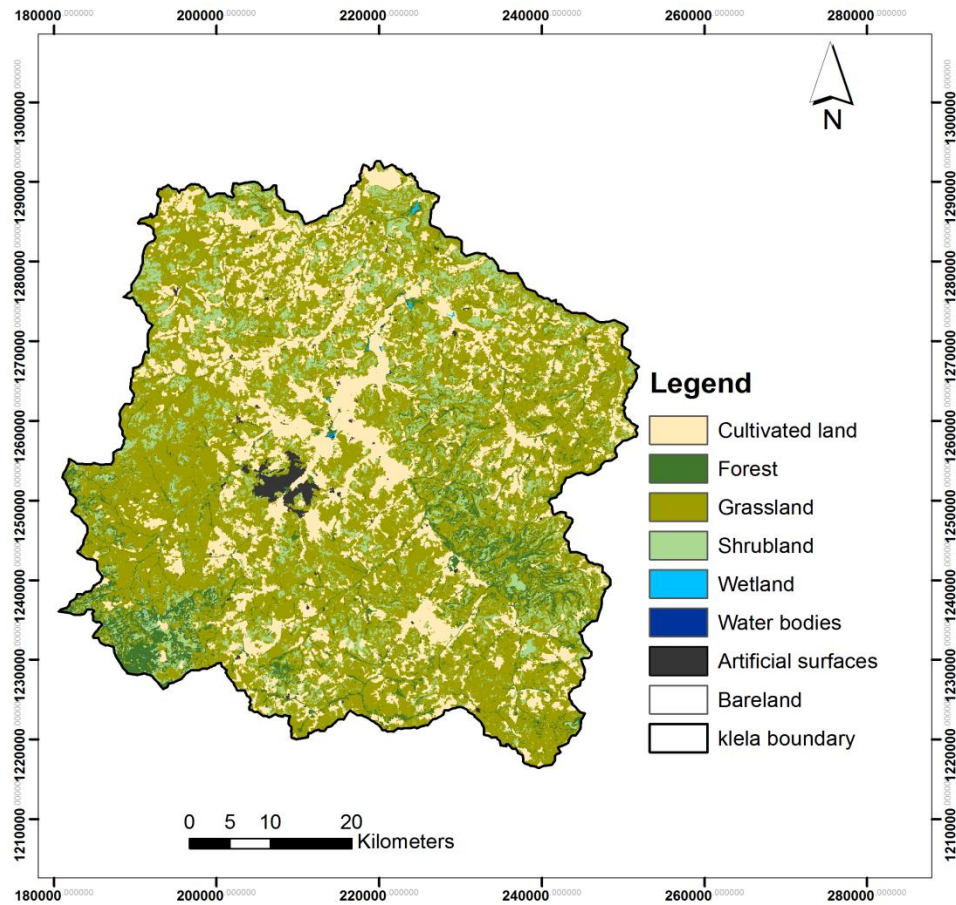
Figure 0.15 Land cover in the study area (map source from National Geomatics Center of China[3])

Table 0.2 Principal types of land cover in the Klela basin (data source from the National Geomatics Center of China)

Land cover	Number of pixels	Area (%)
Cultivated land	901,643	22.05
Forest	316,299	7.74
Grassland	2,337,377	57.16
Shrubland	482,115	11.79
Wetland	1,902	0.05
Water bodies	441	0.01
Artificial surfaces	36,812	0.90
Bareland	12,279	0.30
Total	4,088,868	100

[3]Source of globeland30: http://www.globallandcover.com/GLC30Download/index.aspx

2.10. Soil types

According to the FAO-UNESCO (1974) classification, four major units of soil have been found in the study area. The most important soil type is nitosols, which is localized in the southeastern part of the basin occupying 45% of the total basin area. Nitosols are soils that are "strongly weathered kaolinitic soils having an argillic B horizon" (Juo and Franzluebbers, 2003), with a clay ($\geq$ 20% of its maximum amount within 150 cm of the surface) distribution. This soil unit is characterized by deep, well drained and red tropical soils, and it is by far more productive than most of the red tropical soils (IUSS Working Group WRB, 2015). Nitosols present only a dystric nitosols subclass in the study area, which has a base saturation less than 50% by ammonium acetate (NH_4OAc) in at least a part of the argillic B horizon within 125 cm of the surface (IUSS Working Group WRB, 2015). Luvisols are the second important dominant soil units and are found almost everywhere within the basin, except the central area where nitosols and cambisols dominate (Figure 0.16). They represent about 38% of the total basin area. According to Osman (2013), "Luvisols are soils that have an illuvial argic subsoil horizon with high-activity clays and a high base saturation". Usually, luvisols are fertile soils, appropriate for a large range of agricultural use, and chiefly appear in the young land surface (IUSS Working Group WRB, 2015). Three subclasses occur in the basin area: (i) ferric luvisols, medium textured with lithosols associated and level to gently undulating relief; (ii) gleyic luvisols13 with dystric nitosols associated and dystric regosols inclusions; and (iii) gleyic luvisols5-2a constitute of ferric luvisol and eutric regosol with medium textured and level to gently undulating. Other types of soils are cambisols and gleysols representing 6% and 11% of the study area respectively. Gleysols are formed from unconsolidated materials with recent alluvial deposits and showed hydromorphic properties within 50 cm of the depth (FAO-UNESCO, 1974); they present fine textured and level to gently undulating, while eutric cambisols have a cambic B horizon, an altered clayey horizon, and an ochric A horizon (light-colored). The parent material of these weathered is constituted by diorite, dolerite, gabbro, recent alluvial deposits, Cambrian sandstone and tillite, and minor limestone. Different soil types classified by FAO are mentioned in Table 0.3.

Table 0.3 Different types of soil in the Klela basin based on FAO classification (data source FAO-Unesco, 1974)

FAO Soils	Dominant soils	Texture	Area (%)
Nd1	Dystric Nitosols	sandy loam, clay, silt	44.7
Lg5-2a	Gleyic Luvisols	sandy clay loams, silt loams, silty clay loams	26.6
G2-3a	Gleysols	silty clay, sandy clay, clay loams	11.1
Be26	Eutric Cambisols	sandy loam, clay	6.0
Lf41-2a	Ferric Luvisols	sandy clay loams, silt loams, silty clay loams	5.5
Lg13	Gleyic Luvisols	sandy clay loams, silt loams, silty clay loams	4.7
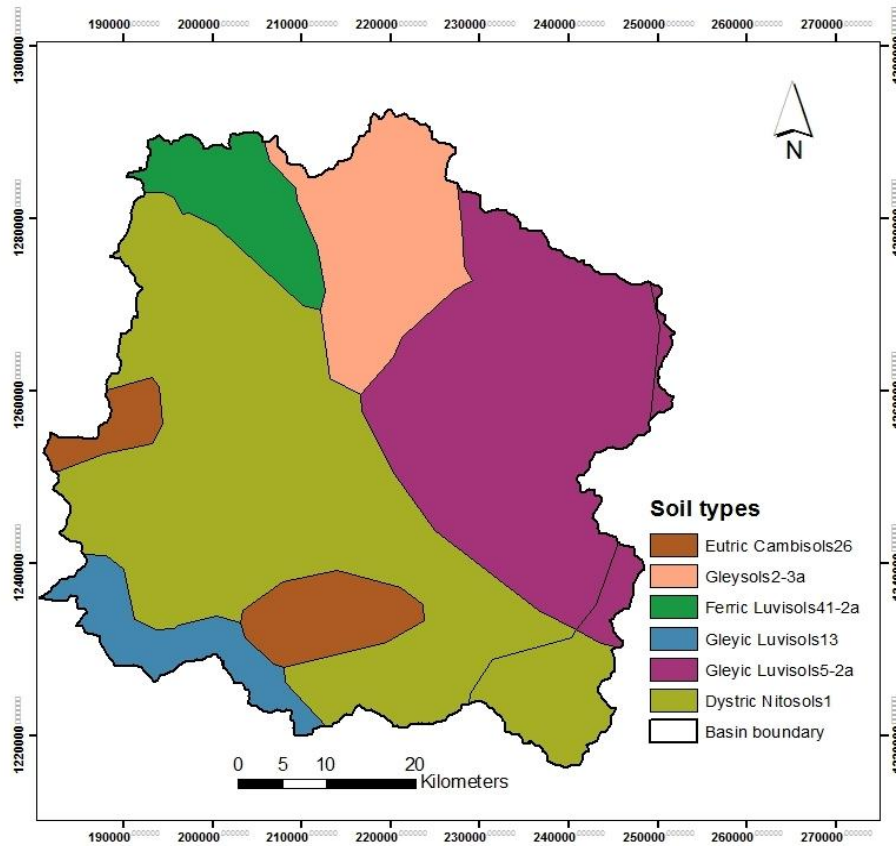
Figure 0.16 Soil types map of the Klela basin (Map source FAO-Unesco, 1974)

CHAPTER 3: DATA, MATERIALS AND METHODS

3.1.   Introduction

All the data used in this thesis are collected from different sources such as field, National and Regional Directions, remote sensing, etc. These data were used over the period of this study to run all the groundwater resource estimation methods and models. Details on all data used in this study are given in this section. The materials and methods were also applied to quantified groundwater recharge and simulated groundwater dynamics of the Klela basin.

3.2.   Data

3.2.1. Climate data

Climate data recorded on the field come from the synoptic station installed in the city of Sikasso. This station is able to record all the climatic data such as precipitation, maximum and minimum temperature, relative humidity, the wind, solar radiation, etc. In this study, only precipitation and temperature were required as climate data. Other climate data used in this study were provided by CORDEX.

3.2.1.1.   Precipitation data

The daily precipitation data, measured by the synoptic station, used in this study was collected from the National Hydraulic Direction (DNH) and ranged from 1970-2013. This daily precipitation data was used in most of the chapters in this study. In chapter 0, it was used to characterize the climate in the Klela basin. In chapter 0, (a) for WTF method; to compare to the weekly groundwater level fluctuation; (b) for CMB method, to estimate recharge estimation; and (c) for EARTH model, to run the model. The monthly rainfall data provided by CORDEX was ranged from 1950-2005 as historical rainfall data and from 2006-2050 as projected rainfall data. Projected climate scenario data in CORDEX was for RCP4.5 and RCP8.5; this data was only used in chapter 0 to assess the impact of climate change on groundwater resources. Some other monthly precipitations data were

collected in the field and used in chapter 0, for CMB method, which ranges from 1993-2013. These rainfall data were measured by the agents of Regional Directions of CMDT (Compagnie Malienne pour le Développement du Textile) and IER (Institut d'Economie Rurale, IER) using traditional pluviometers.

3.2.1.2. Temperature data

The monthly temperature used was collected from DNH and ranged from 1970-2013 as well as precipitation dataset. These data was used in chapter 0. CORDEX provided the same range of temperature data as in precipitation and was used in chapter 0.

3.2.1.3. Evapotranspiration data

The daily potential evapotranspiration data from 2012-2013 was deducted from the daily temperature based on Blaney and Criddle (1962) method.

3.2.2. Topographic data

The information on the topography of the basin is deducted from Digital Elevation Model (DEM) provided by HydroSHEDS. The HydroSHEDS (Hydrology of data and map based on SHuttle Elevation Derivatives at multiple Scales) data, which is derived from elevation data of Shuttle Radar Topographic Mission (SRTM), was used in this study to extract surface elevation data. The HydroSHED has a resolution of five-degree by five-degree tiles (or 90 m * 90 m approximatively). Prior to using it in this current study, it was reconverted to 300 m* 300 m, which is the model cell size. DEM was used in chapter 0 (in the topography of the study area) and chapter 0 (to facilitate groundwater modeling).

3.2.3. Hydrological data

In this part, the daily discharge data of the Lotio station was collected and used in chapter 0. This data range from 1980-2014 with many missing data, often the whole one or two months data over a year.

3.2.4. Hydrogeological data

The hydrogeological data used in this study was very important for groundwater modeling. It gathers two essential points which are detailed below.

3.2.4.1. Pumping test data

In the field area, historical pumping test data (from 34 boreholes) collected were measured in 1985, 1986 and 2005, which were used to calculate the transmissivity data and then hydraulic conductivity data ($T = K*e$). These data were used in chapter 0 for groundwater modeling. Pumping test data was also used to calculate the specific yield in chapter 0.

3.2.4.2. Drilling log data

More than 100 drilling boreholes data were collected and used to estimate the historical groundwater level in chapter 0 and were used as starting hydraulic head in steady-state simulation in chapter 0. These data were also used in chapter 0 to estimate the number of aquifer layer for modeling purpose of the study area.

During the fieldwork, 12 boreholes water level data were collected at the basin scale in July and in November 2014 and were used in chapter 0 to simulate groundwater level in steady-state calibration.

Three weekly piezometers (F7, F15, and F18) data were collected and used in this study in chapter 0 (to estimate groundwater level rise in WTF method) and chapter 0 (to simulate the hydraulic heads in transient simulation). The data ranged from 2010-2014.

3.2.5. Geological data

The geological map was collected from the DNH Direction and was used in chapter 0 to characterize the aquifer features.

3.2.6. Hydrochemical data

The hydrochemical data related to the chloride concentration of both: groundwater and precipitation.

Groundwater samples data were collected in May and October 2014 from eight equipped boreholes and wells over the study area.

The samples of rainwater were collected during the rainy season in July and August 2014. As the study area is a cotton cultivation zone, the existing pluviometers were used to collect rainwater for analyses in the laboratory. Initially, the pluviometers installed by Cotton Company were suitably cleaned to avoid any eventual chemical reaction. In total eight locations (Figure 0.1), the same as in groundwater samples were chosen throughout the basin scale, based on the availability of pluviometers.

These chloride samples data were analyzed in the Malian National Water Laboratory (Laboratoire National de l'Eau, LNE) in order to determine the chloride concentration containing in the water samples. This data was used in chapter 0 to estimate the recharge in CMB method.
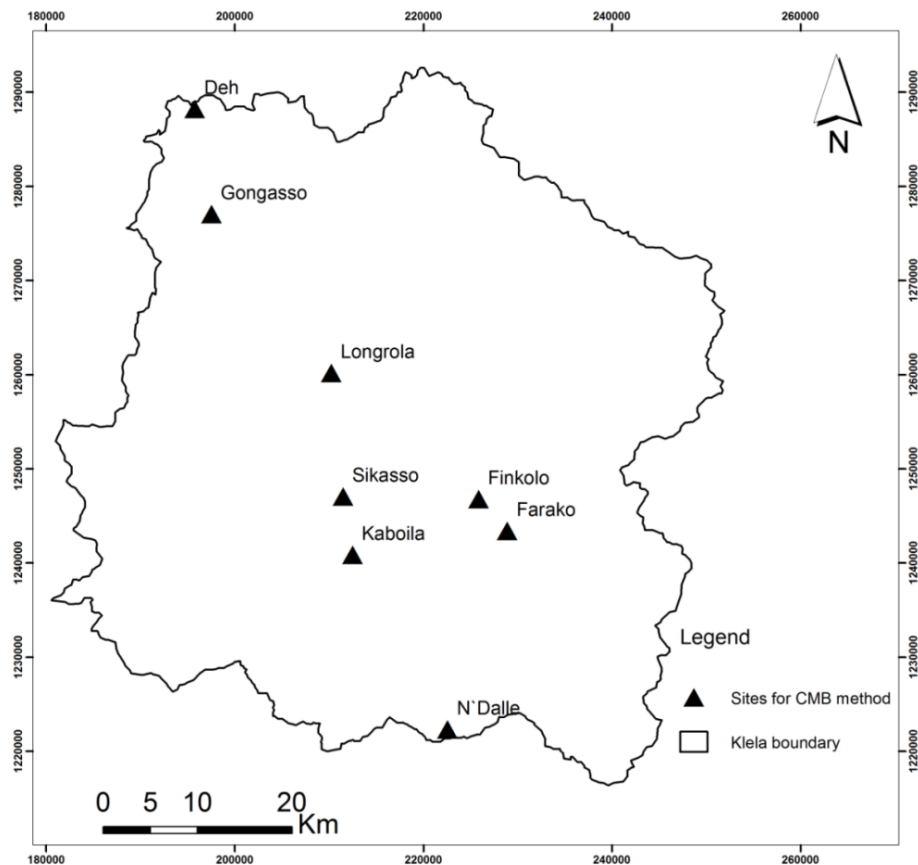
Figure 0.1 Location of the water sampling sites in the Klela basin

3.2.7. Population data

According to RGPH (2009), the population of the Klela basin was estimated to approximately 462,544 in 2009, with 3.6% of growth rate (N'Djim and Doumbia, 1998). This population data was used in chapter 0 and in chapter 0 to assess the impact of climate change and population growth on groundwater resources.

3.2.8. Water demand data

Water demand per person in Mali is highly dependent on the state of urbanization, which in turn is based on a number of inhabitants per area. For example, in the village (less than 2000 inhabitants) the water need is 20 liter per capita per day (lpcpd) (N'Djim and Doumbia, 1998; WHO, 2003), it is 31 lpcpd in semi-urban area (between 2000-10000 inhabitants) and in urban area (> 10000 inhabitants), it is 45 lpcpd (N'Djim and Doumbia, 1998; WWAP, 2006). Since most of the population in Klela basin is living in the villages, therefore, 20 lpcpd has been used as their need in the water. The remainder of the population living in town receives water via SOMAGEP. Water demand data was used in chapter 0.

3.3. Materials

The materials used in this study are:
- **ArcGIS**, used in all the chapters to map most of the figures used in this study and interpolated some data using Kriging method.
- **Camera** used to take some photos over the period of fieldwork
- **Computer** used to run all the models used in this study
- **Container for a water sample**, used in chapter 0 to collect rainwater and groundwater samples from the field area to the laboratory for analysis.
- **EARTH model**, this model was used in chapter 0 to simulate groundwater recharge for the three piezometers (F7, F15, and F18)
- **Excel spreadsheet**, used to prepare the data for all the models
- **GPS** used to measure the geographical position of the data point.
- **Processing MODFLOW for windows (PMWIN 5.3)**, used in chapter 0 to simulate groundwater dynamics in steady and transient conditions

- **Pluviometers** used to collect rainwater for chloride analysis.
- **Standard Precipitation index (spi_sl_6)**, this program was used to compute the standard precipitation index for the Klela basin
- **Surfer 8 and Surfer 11**, used for mapping some figures in this study
- **Thornthwaite model**, used in chapter 0 to simulate the future groundwater recharge
- **Water level meter**, this was used to measure the water level for boreholes and piezometers
- **WEAP model**, used in chapter 0 to assess the impacts of climate change and population growth on groundwater resources

3.4. Methods

3.4.1. Groundwater recharge estimation

3.4.1.1. Water table fluctuation (WTF) method

The water table fluctuation method was applied in the study area considering three piezometers (Figure 0.2). Since the 1920s, the Water Table Fluctuation (WTF) method has been used for estimating groundwater recharge (Meinzer, 1923), and from that time until today it is one of the most widely used techniques on all weather climatic conditions (Healy and Cook, 2002; Scanlon *et al.,* 2002; Risser *et al.,* 2005; Maréchal et al., 2006; Ordens *et al.,* 2011; Diouf *et al.,* 2012). This method has been used by various studies that can be due to the simplicity to use it, and large data availability concerning groundwater level. Groundwater level and specific yield (S_y) are essential for WTF method. According to Healy and Cook (2002), changes of water level depend on three time scales: (1) long-term fluctuations due to natural climatic change (change in land use/land cover) and anthropogenic effects (pumping, irrigation); (2) seasonal fluctuations related to evapotranspiration, precipitation and irrigation; and (3) short-term fluctuations attributed to rainfall, pumping, *etc.* The WTF method is well suited for shallow aquifers with short-term water table fluctuations (Healy and Cook, 2002).

Some assumptions are required by applying the WTF method such as the only reason of increase in groundwater level in unconfined aquifers is due to recharge of water

reaching the water table, and all other components (evapotranspiration from groundwater, base flow to streams and springs, lateral flows, *etc.*) from the water balance are negligible during the period of recharge (Healy and Cook, 2002; Scanlon *et al.,* 2002). The recharge can be calculated as being the product of groundwater level over time by specific yield (equation 3.1) (Scanlon *et al.,* 2002):

$$R = S_y \frac{dh}{dt} = \frac{\Delta h}{\Delta t} \tag{3.1}$$

where R is recharge (mm/s), Sy is specific yield (dimensionless), Δh is change in water

table height (mm), and t is time (s).

According to Delin *et al.* (2007), there are some three other assumptions using this technique: (i) in shallow unconfined aquifers, groundwater recharge and discharge are directly linked to the rise and fall in groundwater levels ; (ii) during the period of fluctuation in groundwater table, the value of specific yield (Sy) of aquifer is known and invariable ; and (iii) "the pre-recharge water level recession can be extrapolated to determine water level rise". The WTF method permits to calculate total recharge by using equation 3.1. Some of the difficulties arising from this technique are the identification of the cause of water level fluctuation because the fluctuations are not always due to recharge and discharge; and also the calculation of specific yield (Healy and Cook, 2002).
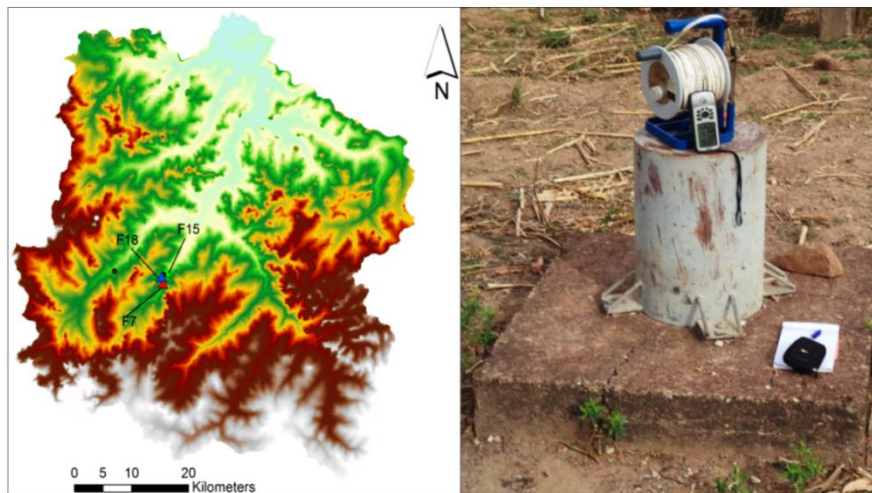
Figure 0.2 DEM and location of the three piezometers in the left, and example of the piezometer F15 used to measure the piezometric level in the Klela basin in the right

As reported by Crosbie *et al.* (2005), rainfall is not the only parameter that causes the rising of the water table. Groundwater level rise is mainly influenced by river stage; the increased gas pressures in the vadose zone can also be a cause (Heliotis and DeWit, 1987 cited in Crosbie *et al.*, 2005). The second case occurs generally when trapping air in the vadose zone between the wetting front and the water table due to the events of high intensity of rainfall, and other causes of water table fluctuations are due to earth tides, pumping, and lateral flow (Crosbie *et al.,* 2005). Crosbie *et al.* (2005) suggested removing an eventual cause of rising water table different from rainfall before estimated recharge to avoid overestimation. As this study area is located in the south of Mali where there is no sea, the only principal cause of rising water table would be rainfall since the Klela basin is set to the no-flow boundary.

The WTF method requires the estimation values of Δh, which is the difference between the top of the rise of water level and the lowest point at the time of top of the extrapolated antecedent recession curve (Healy and Cook 2002). The recession curve is the trace that the well hydrograph would have followed without the presence of any rising of precipitation (Healy and Cook 2002; Delin *et al.,* 2007) (Figure 0.3).

As a result of the difficulty in estimating groundwater level rise, different approaches, including master recession curve (MRC) and the graphical extrapolation, were developed in order to minimize the errors in this calculation. The MRC approach used in the WTF method is an automated procedure for calculating groundwater level rise, while in the graphical extrapolation method the recession curve is extrapolated manually (Delin *et al.,* 2007). This last approach is based on the visual examination, and it is more subjective than other approaches. When this approach is applied by different users, they provide slightly different recession curves, therefore, different recharge estimation results. Refer to Delin *et al.* (2007) for more details on different approaches regarding recession curves calculation.

Among various approaches for estimating groundwater level rise, the graphical extrapolation (Figure 0.3) is the simplest approach and was used in this study to estimate water level rise in each of the observed piezometers. After determining Δh through

graphical extrapolation approach as showed in Figure 0.3, there is a need to calculate specific yield (S_y) in order to determine the recharge.
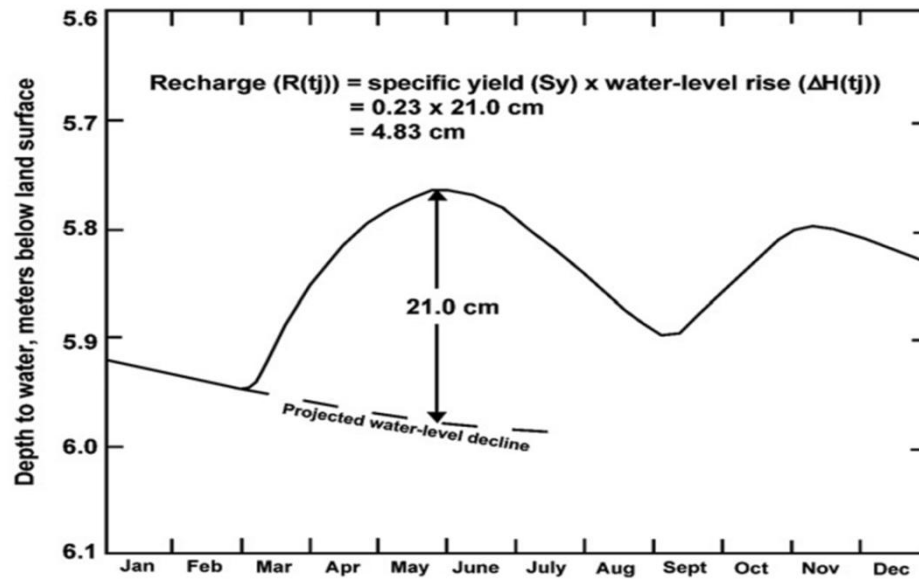
Figure 0.3 Recharge estimated using the graphical approach to the WTF method, illustrated with hypothetical data (Delin et al., 2007)

Meinzer (1923); Johnson (1967) defined the specific yield of a rock or soil, with respect to water, as "the ratio of the volume of water that will drain by gravity from a saturated rock to totally volume of the rock". The specific yield plays an important role in estimating groundwater recharge (Sophocleous, 1985).

The specific yield can be calculated knowing porosity and specific retention as follows in equation 3.2 (Healy and Cook, 2002):

$$S_y = \phi - S_r \tag{3.2}$$

where ϕ is porosity and S_r is specific retention ("the volume of water retained by the

rock per unit volume of rock" (Healy and Cook, 2002)).

The specific yield is considered as constant in theory, while in practice it is dependent of the geology and there may be differences in the stratigraphy depending on the water level. S_y varies as a function of depth to water table (Childs 1960 cited in Delin *et al.,* 2007). According to Healy and Cook (2002), there are many methods (Laboratory methods, field methods such as aquifer tests, water budget methods, volume balance

methods, geophysical methods) to estimate the value of specific yield, may be because of the difficult to determine its value. Even with the same textural class, there is a large difference between the values of specific yield determined in the laboratory and field methods. This is because of the difference period used for each method. For determining S_y, laboratory methods are more time consuming than aquifer pumping tests. Lerner *et al,* (1990) suggested using the value of specific yield from laboratory methods, which is more reliable than others. They recommended also using the value from literature when laboratory measurement values of specific yield are not available. In this current study, the specific yield values for the aquifer material in the study area were determined using Ramsahoye and Lang (1961) method, which use the pumping tests data. This method of specific yield calculation is based on the simple equation 3.3 below:

$$S = \frac{Q \times t}{7.48 \times V} \tag{3.3}$$

where S is specific yield; Q is discharge rate of pumping well, in m³/hour; t is time since pumping began, in hour; V is the volume of dewatered material, in m³ which is determined from the following equation 3.4

$$V = \frac{Qr^2 e^{4\pi Ts/Q}}{4T} \tag{3.4}$$

where r is horizontal distance from the axis of the pumped well to a point on the cone of depression, in meters; s is drawdown at distance r, in m; T is the coefficient of transmissibility of the aquifer, in m²/hour.

Rearranging equation 3.3 and 3.4, the equation 3.5 will be:

$$S = 0.5 \frac{Tt}{r^2} e^{-4\pi Ts/Q} \tag{3.5}$$

Pumping tests data from Regional Hydraulic Direction (DRH) of Sikasso from ten boreholes was used to estimate the specific yield, which value ranged from 0.011-0.081, with a mean value of 0.042 (

Table 0.1).

Table 0.1 Estimation of specific yield values using pumping test data in sandstone (sandy loam, clay and silty) material (T: transmissivity (m²/h), Q: discharge (m³/h), r: radius (m)) (data source from DRH of Sikasso)

$T(m^2/h)$	$Q(m^3/h)$	t(h)	Drawdown(m)	r(m)	Specific yield
0.072	1.65	6	9.5	0.125	0.081
0.9	3.42	6	2.46	0.125	0.054
1.98	6.54	4	2.31	0.125	0.042
2.664	3.5	6	1.05	0.125	0.024
0.54	6.26	6	7.27	0.125	0.042
1.224	2.67	6	1.47	0.125	0.053
0.072	1.2	6	11.35	0.0625	0.011
0.144	1.5	6	7.39	0.0625	0.016
0.0153	1.05	4	29.68	0.07	0.029
0.087	3.3	4	15.42	0.125	0.072

3.4.1.2. Chloride mass balance method

The chloride mass balance method (CMB), which is developed by Eriksson and Khunakasem 1969 cited in Ting *et al.* (1998), is based on the simple calculation of the ratio between the total chloride deposition at the surface from rainfall and chloride concentrations from groundwater. To date, the CMB method is becoming widely used in recharge estimation, mainly in arid and semi-arid areas (Bazuhair and Wood, 1996; Mazor, 2004; Wheater, 2010; Diouf *et al.,* 2012.). This method is essentially based on the chloride behavior in nature. It is a conservative ion; chloride does not contribute in water-rock ion exchange interactions; and it cannot be removed from groundwater by any process when it reaches groundwater table (Mazor, 2004). This means that the chloride concentration is neither decreased nor increased with chemical reactions in the soil. Its concentration is still constant if climate, soil, and other conditions near the ground have been stable for a sufficiently long time (Sumioka and Bauer, 2004). There are two principal chloride sources: chlorides from atmospheric (Guan *et al.,* 2009) salts and halite rock. The dissolution of halite rock is limited because it involves only the areas where this mineral is present in the rocks passed by water (Mazor, 2004). The atmospheric salts are the common sources of chlorine in groundwater and the most important source. The other sources of chloride from human (septic system) and animal (*e.g.,* cow manure) can contribute to increasing the amount of chloride depending on the study area. As this study

area is conducted in a rural zone, human activities could affect the chloride concentration. Since there is no data available to estimate the quantity of human contribution, these other sources of chloride were neglected in this study. The Cl⁻ is used as a conservative tracer in recharge calculations in many studies, but the Chloride mass-balance method is probably the most reliable approach to recharge estimation in semi-arid and arid regions (Allison *et al.,* 1994, Edmunds, 2010). Furthermore, the CMB method is easy to use and less expensive.

Estimating groundwater recharge applying the chloride mass balance method is founded on the simple "principle that a known fraction of chloride in precipitation and dry atmospheric deposition is transported to the water table by the downward flow of water" (Sumioka and Bauer, 2004).

A mass balance of chloride from precipitation, surface runoff, and groundwater is expressed in the following equation 3.6 (Maurer *et al.,* 1996; Prych, 1998; Sumioka and Bauer, 2004)

$$P \times Cl_p^- = R \times Cl_{gw}^- + RO \times Cl_p^- \qquad (3.6)$$

where P is annual precipitation, in mm; Cl_p^- is concentration of chloride in

precipitation, in mg/l; R is annual groundwater recharge, in mm; Cl_{gw}^- is concentration of chloride in groundwater, in mg/l; RO is annual surface water runoff, in mm.

By rearranging the terms of equation 3.6 and assuming that the chloride from surface runoff is null because of lack of data, groundwater recharge will be equation 3.7

$$R = P \times \frac{Cl_p^-}{Cl_{gw}^-} \qquad (3.7)$$

As surface runoff should be removed from the precipitation, therefore, neglecting this value in groundwater recharge estimation could lead to overestimating the recharge. This is true in the study performed by Martin (2005) who estimated the error, by neglecting runoff from above equation, to be less than 10%.

Some necessary assumptions must be taking into account applying this technique successfully: (i) the source of chloride in soil or in groundwater is from rainwater all

other sources such as anthropogenic (wastewater) and dissolution of minerals are negligible; (ii) chloride is conservative in the system, *i.e.,* the ion Cl⁻ does not exchange (dissolution or absorption) with aquifer sediments, nor participates in any particular chemical reaction (Marei *et al.,* 2010); (iii) steady-state conditions are considered by using long-term precipitation and chloride concentration in that precipitation (Bazuhair and Wood, 1996); (iv) surface runoff does not present in the system; and (v) the groundwater table should be prevented against groundwater evaporation (Marei *et al.,* 2010). In addition, Bonsor and MacDonald (2010) suggested applying this technique in the area where annual rainfall amount is less than 600 mm/year. Although the annual amount of rainfall in this study is greater than 600 mm, the method was applied. Obuobie (2008) also used this technique to estimate recharge with a mean annual rainfall of 990 mm. The CMB technique is still applicable even if the chloride is taken up by growing vegetation because it will be released as long as possible by decaying vegetation at the same rate.

3.4.1.3.   EARTH modeling

EARTH (**E**xtended model for **A**quifer **R**echarge and soil moisture **T**ransport through the unsaturated **H**ardrock) model is a lumped parametric model that is used to estimating groundwater recharge (Van der Lee and Gehrels, 1990). This model has been developed in a project in Botswana by Van der Lee *et al.* in 1989 and used to be tested under various climatic conditions (Van der Lee and Gehrels, 1990). The EARTH model is better indicated for semi-arid regions and associates both direct and indirect methods (Van der Lee and Gehrels, 1990). From the atmosphere toward the soil zone, the direct method describes the recharge process, and the indirect method uses groundwater table fluctuations as an indicator of the quantity of recharge process calculation (Van der Lee and Gehrels, 1990). Base on physical procedures above the groundwater table, the direct method may estimate the recharge, but the indirect method uses the recharge estimated from the direct part to simulate groundwater table (Van der Lee and Gehrels, 1990). The EARTH model has five modules (Figure 0.4). The direct part of the model (MAXIL, SOMOS, LINRES) might simulate recharge to the unsaturated zone and the measured time series of soil moisture data can be used to calibrate it (Belay 2009). The indirect part

of the model (SATFLOW) computes groundwater level from the recharge simulated by the direct part; and SUST calculates the surface runoff, Figure 0.4 (Van der Lee and Gehrels, 1990).

EARTH model can be used for the recharge estimation with certain accuracy in arid and semi-arid regions (Xu and Beekman, 2003). It has been used in different hydrogeological conditions throughout the world by many authors (Paralta and Oliveira, 2005; Lubczynski and Gurwin, 2005; Usher et al., 2006; Toure et al., 2014) for recharge estimation.

Details concerning the five modules according to Van der Lee and Gehrels (1990).

MAXIL (Maximal Interception Loss)

Precipitation excess is a quantity of water which reaches the Earth surface from total precipitation and is calculated with only one parameter: the maximal interception loss (MAXIL). MAXIL is the remaining water retained by surface features such as leaves, steams, depression storage, *etc.* The precipitation excess is estimated using the equation 3.8:

$$Pe = P - MAXIL - E_0 \qquad (3.8)$$

where *Pe* is precipitation excess (mm), *P* is total precipitation (mm), *MAXIL* is total surface retention (mm) and E_0 is total evaporation (mm)

SOMOS (Soil Moisture Storage)

"The soil moisture storage (SOMOS) describes water storage in the root zone that represents the root zone depth" (Van der Lee and Gehrels, 1990). In this section, infiltration from precipitation excess (P_e) is divided into different components such as actual evapotranspiration, percolation, evaporation, ponding and/or surface runoff. The remaining part of P_e is the changed in soil moisture storage, which is calculated using the mass balance in equation 3.9.

$$\frac{dS}{dt} = P_e - AET - Rp - E_0(SUST) - Q_s \qquad (3.9)$$

where $\dfrac{dS}{dt}$ is a change in water storage over time (mm), S= WD is defined by volumetric

soil moisture content (W) and an effective root zone thickness (D), AET is actual

evapotranspiration rate (mm/d), R_p is the percolation flux below root zone

(mm/d), E_0 (SUST) is evaporated fraction of ponding water (mm/d), and Q_s is

surface runoff (mm/d).

The actual evapotranspiration (AET) is linearly linked to the soil moisture content (S) (Van der Lee and Gehrels, 1990), and AET can be estimated knowing potential evapotranspiration and soil moisture content through this equation 3.10

$$AET = PET \left| \frac{S - S_r}{S_m - S_r} \right| \tag{3.10}$$

where *PET* is potential evapotranspiration (mm/d), S, Sm and Sr represent actual,

maximum and Residual soil moisture content respectively (mm)

The soil moisture continues downward after passing the root zone to reach the saturated zone, this is called percolation and is expressed by the Darcy equation in EARTH as in equation 3.11:

$$R_p = K \left| \frac{dh_p}{dz} + 1 \right| \tag{3.11}$$

where R_p is percolation (mm/d), K is hydraulic conductivity that is a function of soil

moisture Content (mm/d), and $\dfrac{dh_p}{dz}$ is the hydraulic head gradient taken positive

downward

When the pressure head remains constant over depth, then, the equation 3.11 can be reduced as equation 3.12:

$$R_p = K \tag{3.12}$$

The relationship commonly used for hydraulic conductivity is:

$$K = K_s \left| \frac{S - S_{fc}}{S_m - S_{fc}} \right|^n \tag{3.13}$$

- 49 -

where K_s is saturated hydraulic conductivity (mm/d), n is a soil constant, and S_{fc} is the

soil water at field capacity (mm)

SUST (Surface Storage)

The ponding and/or surface runoff occurs when the quantity of water in SOMOS reaches a certain threshold defined as saturation ($S=S_m$), and the infiltration rate is greater than the percolation rate. In the EARTH model, surface storage is represented by the reservoir SUST. This reservoir uses a parameter giving by $SUST_{max}$ that is the maximum amount of ponding water that can be stored at the surface. When $SUST_{max}$ is equal to zero, all ponding water will become surface runoff, which is considered as a loss for recharge calculation and runoff is negligible if $SUST_{max}$ is large. It is expressed in the equation 3.14 below:

$$SUST_t = S_t - S_m + SUST_{t-1} - E_0 \tag{3.14}$$

where S is actual soil moisture content (mm), S_m is maximum soil moisture content

(mm), and E_0 is open water evaporation from the pond (mm), "which is limited to the actual presence of water at the surface" (Van der Lee and Gehrels, 1990).

LINRES (Linear Reservoir Routing)

After SOMOS zone, the water percolates from this reservoir to the LINRES, and thereafter, the water cannot be lost by evapotranspiration. LINRES redistributes the output of SOMOS in time using a parametric transfer function. It needs only two parameters, the number of reservoirs (n) and unsaturated recession constant (f). LINRES part of the model EARTH is important and presents the accurate optimization to fit the simulated groundwater level with the measurements (Van der Lee and Gehrels, 1990).

SATFLOW (Saturated Flow)

SATFLOW is the last reservoir of the EARTH model; it is a one-dimensional parametric model where the parameters have a semi-physical meaning. SATFLOW calculates the groundwater level with the estimated recharge of the direct part of the model from the percolation zone (Gebreyohannes, 2008). It uses this equation 3.15

$$\frac{dh}{dt} = \frac{R}{STO} - \frac{h}{RC} \qquad (3.15)$$

where *h* is groundwater level above the local base level (mm), *R* is recharge (mm/d),

STO is storage coefficient, *RC* is saturated recession constant, and *dh/dt* is a change in groundwater level over time (mm/d).

According to Van der Lee (1989), "the recession coefficient is proportional to the storage coefficient and the drainage resistance described" as in equation 3.16:

$$RC = \beta \cdot STO \cdot DR \qquad (3.16)$$

where β is the coefficient of proportionality, and *DR* is specific drainage resistance (day).

The drainage resistance can be determined using this formula:

$$DR = \frac{L^2}{\beta T} \qquad (3.17)$$

where L is the flow path (m), T is aquifer transmissivity (m^2/d) and β is a shape factor varying from 2 for radial flow to 4 for parallel flow.
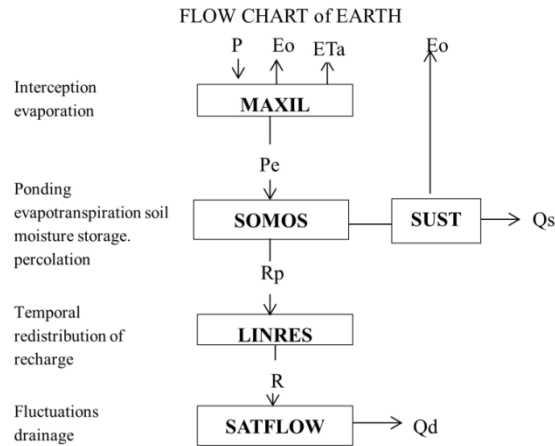
Figure 0.4 Flow chart of EARTH model (modified from Van der Lee and Gehrels, 1990). E0 = potential evapotranspiration, Eta = actual evapotranspiration, P = precipitation, Pe = precipitation excess, Rp = percolation, R= recharge, Qs = surface runoff, Qd = drainage

Model input and calibration

EARTH model requires daily precipitation and potential evapotranspiration as input data. In addition, daily groundwater level and soil moisture storage may be used for

model calibration purpose. Other eleven input parameters are needed to calibrate the model such as "maximum, initial and residual soil moisture, soil moisture at field capacity, saturated hydraulic conductivity, unsaturated reservoir coefficient, saturated recession constant, number of reservoirs, storage coefficient, initial groundwater level and local base level" (Van der Lee and Gehrels, 1990). These parameters can be determined either from field measurements or from optimization of the model (Belay, 2009). In this study, daily precipitation and potential evapotranspiration were used as input data to the EARTH model to estimate the recharge. The potential evapotranspiration was calculated using Blaney and Criddle (1962) method. As the field soil moisture storage was not available, then the daily observed groundwater levels were used to calibrate the model. EARTH model was applied to three location piezometers (F7, F15 and F18) at Sikasso commune inside the basin (see Figure 0.2), where the groundwater levels were monitored from January 2012 to December 2013.

The main objective of the calibration is to minimize the difference between the simulated and measured variables and obtain the best fit. The performance of the model can be assessed by using the calibration process of the model and established the acceptance of the model as an image of reality or not. Due to the unavailability of the model optimization program, EARTH model was calibrated by a trial and error procedure by adjusting model parameters manually in this study. The important parameters changed in this calibration process were maximum soil moisture content, MAXIL and unsaturated recession constant. The calibrated results for the three piezometers show some differences between simulated and observed groundwater level. Three calibration procedures were carried out during the calibration process: "first change the parameter value that causes the largest deviation, change just one parameter in each run; determine if the change of the parameter cause negative or positive effect on other parts" (Anderson and Woessner, 1992; Lu and Zhou, 2011),

3.4.2. Groundwater modeling

The groundwater model is defined by Middlemis (2004) as "a computer-based representation of the essential features of a natural hydrogeological system that uses the laws of science and mathematics". Generally, groundwater model is applied in an area in

order to estimate the groundwater dynamic regime (quantity), and/or identify the elements responsible for groundwater pollution (quality). In the current study, only the quantification of the groundwater dynamic regime was taking into account, as it presents a real problem for every aquifer and difficult to estimate. Groundwater flow model uses two equations: Darcy's law equation and the equation of continuity, which, associated, give partial differential equation (equation 3.18) that allow evaluating groundwater flow dynamic regime. Another purpose of groundwater modeling is the prediction of the future groundwater flow systems by using groundwater models as a predictive tool or as a generic tool to investigate groundwater flow process. As it is known today that groundwater plays an important role in terms of mitigation and adaptation face to climate change; therefore, its modeling can be a powerful tool for water resources management, groundwater protection and remediation. Groundwater models can be classified into physical or mathematical models.

"Physical models such as laboratory sand tanks simulate groundwater flow directly", while by the means of a governing equation a mathematical model simulates groundwater flow indirectly "to represent the physical processes that occur in the system; together with equations that describe heads or flows along the model boundaries" (boundary conditions) (Anderson and Woessner, 1992). Although physical models are useful and easy to set up, they cannot handle complicated real problems, whereas mathematical model can be used to solve simple or complicated equations problems using analytical or numerical method respectively (Essink, 2000).

Mathematical model solutions may be either analytical or numerical (Baalousha, 2009; Kouli *et al.,* 2009). Analytical methods were first used in hydrogeology to solve the equations (*e.g.,* determination of transmissivity), as they are not able to solve complicated equations, then, their application is limited (Simmons *et al.,* 2010). Though the analytical methods are limited by application, they are often very useful because they can serve as verification of solutions of more complex systems obtain by numerical methods (Essink, 2000, 2001). In addition, they can "provide exact solutions to the governing differential groundwater equations for simple boundary conditions" (Shelton, 2011). When the equations (*e.g.,* partial differential equation) become very complex, the use of numerical methods is recommended because they might treat more complicated

problems than analytical solutions (Baalousha, 2009). Numerical models are actually more effective and easy to use due to the rapid development of computer processors. They "are generally used to simulate problems which cannot be accurately described using analytical models" (Mandle, 2002). Unlike numerical solutions, analytical solutions give a continuous output at any point in the problem domain. The most numerical methods widely used for solving mathematical model equations are the finite difference and finite element methods (Baalousha, 2009). Only the finite difference methods were applied in this study because they are easy to understand and program (Kinzelbach, 1986). The finite difference methods are also used in many computer codes such that MODFLOW and produces reasonably good results. Basically, the finite difference method consists of substituting differential expressions by quotients of differences (Bundschuh and Arriaga, 2010). Therefore, the partial differential equation solution is performed by means of a system of algebraic equations that can be solved using different techniques because the numerators of these quotients are the differences that include the values of the unknowns (Bundschuh and Arriaga, 2010). Furthermore, the finite difference method consists of discretizing the problem area into regular elements that are identified with discrete points or nodes (Essink, 2000). The use of finite difference methods, although widely used, introduces some disadvantages (Baalousha, 2009). For example, they do not fit properly to an irregular model boundary, and output accuracy of the finite difference methods is not good in the case of solute transport modeling (Baalousha, 2009). Groundwater modeling requires some steps that must be followed over the period of modeling (Figure 0.5).
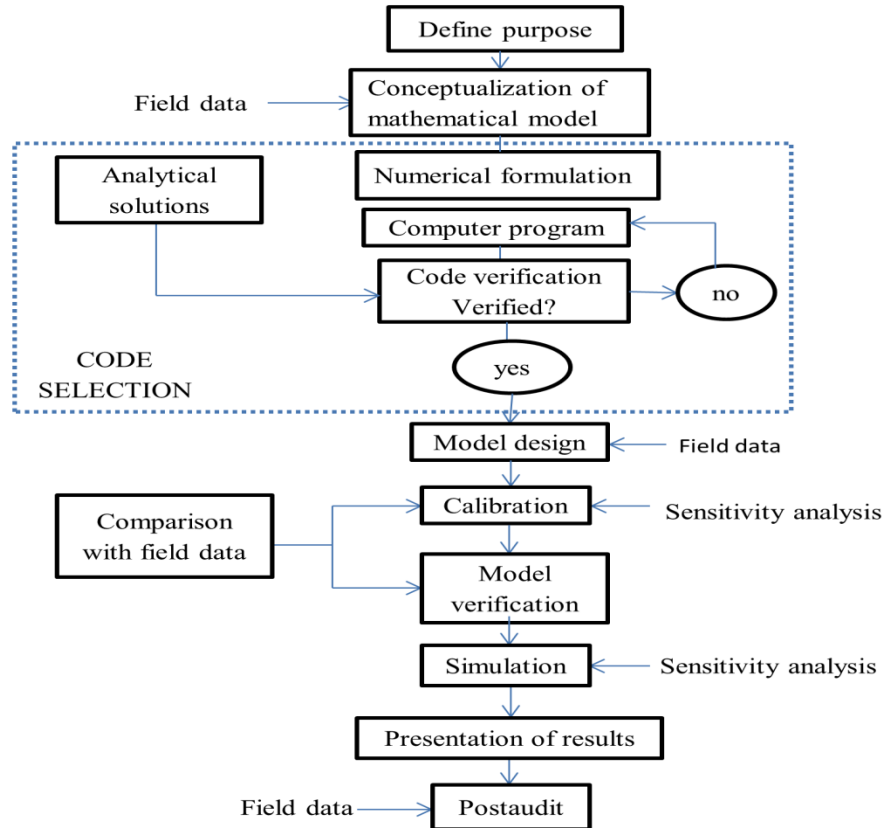
Figure 0.5 Different steps for model application (modified from Anderson and Woessner, 1992)

The purpose of this modeling was to simulate groundwater flow and heads for the aquifer system of the study area in order to establish water balance.

3.4.2.1.　Modeling process

3.4.2.1.1.　Conceptual model

The conceptual model is defined by Baalousha (2009) as "a descriptive representation of a groundwater system that incorporates an interpretation of the geological and hydrological conditions". In hydrogeology study, one of the important challenges is how to organize the hydrological field data (*e.g.,* pumping test data, drilling logs, piezometric level data, *etc.*) for analyzing, while a conceptual model is built in order to simplify the field reality and organize the associated field data to be easily analyzed (Anderson and Woessner, 1992). In a modeling study, it is very necessary to simplify the

field reality, since the identical reproduction of the field system is very difficult, or even impossible. Development of conceptual model is the most important part of modeling process because theoretically, the numerical model accuracy depends on a good conceptual model (Anderson and Woessner, 1992). This was proved by Council (1999), who affirms that model conceptualization should be re-examined when the model cannot be calibrated to match the calibration data. Furthermore, the conceptual model involves the understanding of aquifer characteristics and their quantification in time and space. A good conceptual model is a simple way to summarize the understanding of groundwater flow behavior. It requires necessary information on geology, hydrology, boundary conditions, and hydraulic parameters. The conceptual model is the basis of the mathematical model and plays an important role for selecting a type of computer code to be used in modeling as well as the design and priority of site characterization activities (Council, 1999). In this current study, the real system was simplified to facilitate groundwater flow modeling. This simplification involved all important features and processes such that geological data (*e.g.,* drill logs), pumping test data, groundwater levels, rainfall data, topography, groundwater extraction, *etc.*

Modeling purpose cannot be done without deep information on hydrogeological, topography data, surface-water bodies, hydraulic head data, hydraulic conductivity data, and groundwater recharge and discharge (Mandle, 2002). In addition, Anderson and Woessner (1992) state that building a conceptual model requires three steps: (1) "defining hydrostratigraphic units; (2) preparing a water budget; and (3) defining the flow system". Usually, in practice, it is very difficult to obtain all these information in any study area, and this case study was not an exception. Thus, the field information collected was not sufficient but represented the essential data, which could allow reproducing as well as possible the natural groundwater system in the study area. Since the study was focused on regional groundwater flow system that does not require excessive details (Seneviratne, 2007), then, the data (particularly hydrogeological) may use with some uncertainties.

Hydrological logs of boreholes data collected from Regional Hydraulic Direction (DRH) of Sikasso were used to characterize the lithology of the study area. The principal geologic unit of the study area is sandstone known as "grès de Sikasso", however, there is

some dolerite formation. Investigations of borehole logging data in the study area, one can say that more than 80% display only a single layer with facies of sand-clayey, weathering rock, sandstone schist, *etc.* For simplification, the aquifer of the study area was set as a single numerical layer under unconfined condition. The study area was characterized by shallow aquifer because most of the water table falls between 20 m below ground level (see Figure 0.7 in chapter 0). The aquifer thickness estimation is critical because it is one of the parameters that influence the hydraulic heads calculated by the model. Based on the data collected in the field, the aquifer thickness was ranged from 40 m and exceeded 200 m in some cases. The topographic data from Shuttle Radar Topography Mission: (SRTM[4]) Digital Elevation Model (DEM) was used to delineate the Klela Basin. Only the surface-water bodies (*e.g.,* stream and river flows) have been considered in this delineation. The subsurface drainage delineation was still unknown. The available hydrogeological data in the study area could not provide enough information in order to acquire the detail in subsurface delineation. Therefore, the lateral flow exchange between Klela basin and its surrounding aquifers was neglected and the whole basin was assigned as a no-flow boundary. The pumping test data was investigated to estimate the value of hydraulic conductivity based on Cooper-Jacob method (Cooper and Jacob, 1946). Hydraulic conductivity is a very good important parameter in modeling groundwater flow and is defined by Hendrickx *et al.* (2003) as"a representative volume of the porous medium". Its variability (increase or decrease) affects directly groundwater flow rates estimation (Moore, 2002; Healy and Scanlon, 2010). In this study, hydraulic conductivity data collected in the field varies from 0.04 m/d to 40 m/d. Groundwater recharge was estimated in chapter 0. Groundwater recharge is essential in groundwater modeling study, but it is one of the most difficult hydrological fluxes to be quantified (Wheater, 2010). The values of recharge previously calculated were used in this modeling. Groundwater extraction from the aquifer through drilling boreholes and traditional dug wells is mostly related to human domestic activities, livestock water needs and irrigation. The approximate quantity of water withdrawn from the Klela basin aquifers will be detailed afterward.

---

[4] SRTM DEM can be downloaded from srtm.usgs.gov.

3.4.2.1.2. Model software selection

After developing a model conceptualization, the code of model should be selected. The main objective of selecting a model code is to transform the model conceptual to computer code. The selected model must be susceptible to simulate the conditions encountered at the site. Due to the complexity of groundwater flow system and the spatiotemporal variation of groundwater directions, and sources and sinks, the numerical model was used in the study area instead of analytical model (Mandle, 2002). There is numerous groundwater flow model available, but the widely used, since the 1990s, over time and space is MODFLOW (Harbaugh, 2005), and was selected in this study.

MODFLOW

MODFLOW "is a modular three-dimensional finite-difference groundwater model that was developed by the United States Geological Survey (USGS)", and first published in 1984 (McDonald and Harbaugh, 1988). "The model code is written in FORTRAN and divides input data into modules known as packages" (Ahern, 2005). MODFLOW uses groundwater flow equation that is the combination of continuity equation and Darcy's law (Harbaugh, 2005). In a porous medium, the partial-differential equation (equation 3.18) is used to simulate the movement of the three-dimensional groundwater flow (Harbaugh, 2005):

$$\frac{\partial}{\partial x}\left(k_{xx}\frac{\partial h}{\partial x}\right)+\frac{\partial}{\partial y}\left(k_{yy}\frac{\partial h}{\partial y}\right)+\frac{\partial}{\partial z}\left(k_{zz}\frac{\partial h}{\partial z}\right)-w=s_s\frac{\partial h}{\partial t} \tag{3.18}$$

where K_{xx}, K_{yy}, and K_{zz} are values of hydraulic conductivity along the x, y and z coordinate axes, which are assumed to be parallel to the major axes of hydraulic conductivity (LT^{-1}); h, is potentiometric head (L), W is a volumetric flux per unit volume and represents sources and/or sinks of water (T^{-1}); S_s is the specific storage of the porous material (L^{-1}); and t is time (T).

This governing equation 3.18 can be solved either analytically or numerically. Dependent on their approaches, assumptions and capability, both methods (analytic and numeric) may be used to solve the equation (Belay, 2009). Together with initial

conditions for potentiometric head and various boundary conditions, at each model cell in time steps within every simulated stress period, MODFLOW uses a discretized algebraic of equation 3.18 to solve the potentiometric head. The code MODFLOW is a groundwater flow simulation model and has been applied successfully in fractured rock (Cook, 2003). It is a widely model used through the world by many authors (Brassington, 2004; Valerio, 2008; Banning, 2010; Saatsaz et al., 2011; Sehatzadeh, 2011; Toure et al., 2016) for modeling groundwater flow dynamics. MODFLOW is known as one of the best tools to describe and predict groundwater flow system. It is able to simulate both, steady-state and transient flow conditions in unconfined aquifers, confined aquifers and variably confined/unconfined aquifers (Kim *et al.,* 2008). Groundwater dynamics may be simulated by using different sources and sinks such that "rivers, streams, drains, springs, reservoirs, wells, evapotranspiration, and recharge from precipitation and irrigation" (Alexander and Palmer, 2007). The wide use of the MODFLOW model is probably due to its aptitude and extensive to simulate a broad variety of systems and the freely availability of documentation respectively, and its rigorous USGS peer review (Scientific Software Group, 1998 cited in Alexander and Palmer, 2007).

These reasons below were recognized by the USGS for the widespread use and popularity of MODFLOW (USGS, 1997): (i) "the finite-difference method used by MODFLOW is relatively easy to understand and apply to a wide variety of real-world conditions; (ii) MODFLOW can be applied as a one-dimensional, two-dimensional, or quasi-or full three-dimensional model; (iii) each simulation feature of MODFLOW has been extensively tested; (iv) data input instructions and theory are well documented; (v) a wide variety of programs are available to read output from MODFLOW and graphically present model results in ways that are easily understood, and (vi) MODFLOW has been accepted in many court cases in the United States as a legitimate approach to analysis of ground-water systems".

Several versions of MODFLOW are available; for example, Visual MODFLOW, GMS MODFLOW and Processing MODFLOW for Windows (PMWIN). The last one, which is free of charge and downloadable at www.simcore.com/pm53, was used in this study. PMWIN is a simulation system for modeling ground-water flow and transport processes with MODFLOW (Chiang and Kinzelbach, 2001; 2005).

3.4.2.1.3.   Model construction

Construction of the numerical model is a more complex and time-consuming process, even when using one of the many graphical user interfaces (Middlemis, 2001). In groundwater flow model construction, groundwater flows and heads are simulated based on the process of modifying the conceptual model into a mathematical form (Middlemis, 2001). MODFLOW can be used to simulate groundwater flow and heads. In this study, the version of the numerical model used was PMWIN 5.3., developed by Chiang and Kinzelbach (1998). Model construction involved grid design, the setting of boundary and initial conditions, assigning aquifer geometry and properties, time parameters, and recharge values.

a.   Spatial discretization

"In numerical groundwater modeling, an aquifer system is replaced by a discretized domain consisting of an array of nodes and associated finite difference blocks (cells). In PMWIN, the model domain is divided into rectangular mesh comprising columns, rows and layers" (Toure *et al.,* 2016). The spatial discretization of an aquifer system can be seen in Figure 0.6.
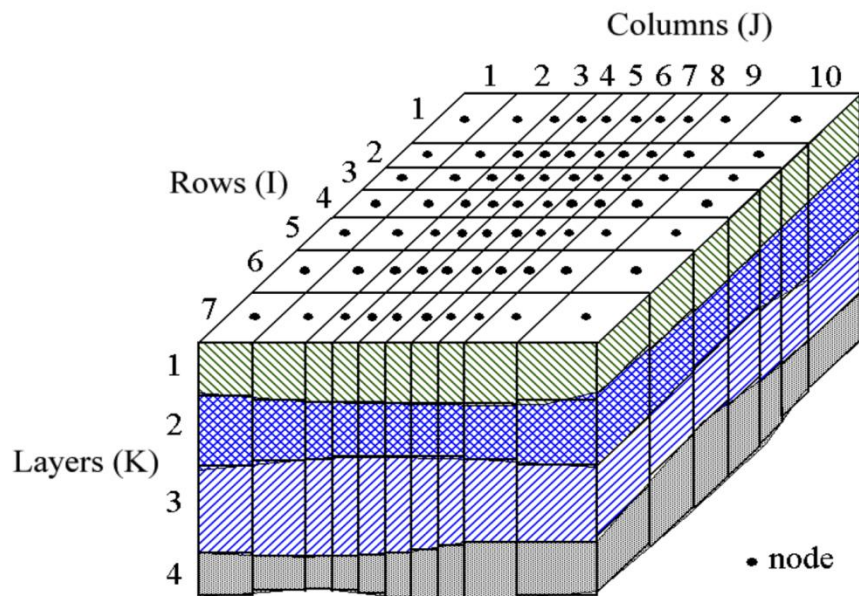
Figure 0.6 Spatial discretization of an aquifer system and the cell indices (source Chiang and Kinzelbach (1998)

In this study, the model grid was discretized into 239 columns and 256 rows, resulting in a total grid cell number of 61,184 with a grid size of 300 m * 300 m, taking into account of aquifer extension and hydrogeological data availability. The total number of active grid cells describing the active model domain was 40,992. These sizes were taken to minimize as well as possible numerical errors in the model domain.

b.   Aquifer geometry

The aquifer geometry step establishes the top and bottom of an aquifer. Determination of aquifer geometry is critical in numerical modeling because it influences model calibration results (Middlemis, 2001). Drilling logs data and an SRTM-based Digital Elevation Model (DEM) from HydroSHED.org were combined to estimate the top and bottom of the aquifer thickness in the study area. The DEM was used as the aquifer top (see Figure 0.6 in chapter 0) and the aquifer thickness was arbitrarily set to 300 m. The aquifer bottom elevation is displayed in Figure 0.7.
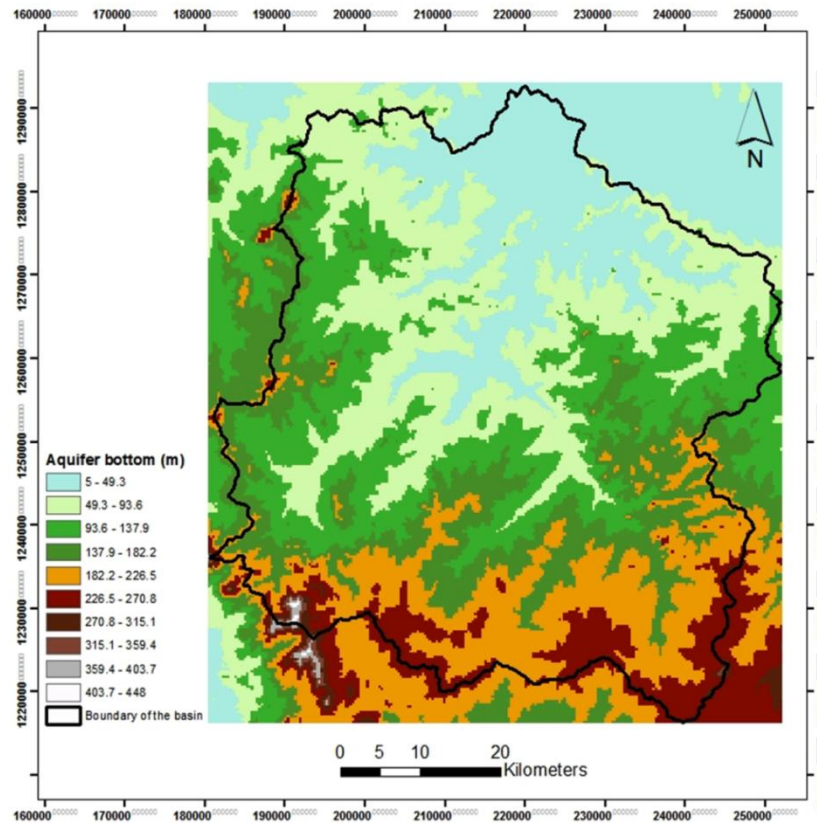
Figure 0.7 Aquifer bottom assigned to the model in meters above mean sea level

As discussed above, there is a strong possible interaction between groundwater and surface water bodies within the basin because the scatter plot of surface elevation and water table (see Figure 0.7 in chapter 0) indicate that in most of the wells the water table is up to 20 m below ground level. For this reason, the surface water and groundwater interaction were analyzed in this study.

c.   Aquifer properties

Aquifer properties are the most important part of the modeling groundwater flow system. The hydraulic properties of an aquifer, including transmissivity, hydraulic conductivity and storativity, determine water movement through the aquifer as well as storage in the aquifer. Different methods such as Theis, Jacob and Theim are commonly used to determine the aquifer properties from pumping test data (Singhal and Gupta, 2010). In this study, the horizontal hydraulic conductivity value was calibrated until a good correlation between simulated and observed heads was obtained. For this reason, the model domain was arbitrarily divided into 6 hydraulic conductivity zones due to the lack of details in hydrogeological information in the study area.

The data of storativity was not available in the study area. Therefore, specific yield data was estimated using a simple Ramsahoye-Lang method (Ramsahoye and Lang, 1961) and was used in transient calibration.

d.   Boundary conditions

According to Owais *et al.* (2008), "boundary conditions specify how an aquifer interacts with the environment outside the model domain". There are three major types of boundary conditions such as specified-head, specified-flow and head-dependent flow. The boundary selected type should be compatible with the conceptual model and the water budget (Middlemis, 2001). This boundary type "should be located and oriented consistent with the physical features it represents" (Middlemis, 2001). The choice of boundary conditions in model design is very useful step because they significantly control flow pattern (Anderson and Woessner, 1992; Ahern, 2005). As explained in the conceptual model, the topographical limits of the basin were taken as the groundwater divides (a no-flow boundary), *i.e.,* there is no hydrogeological interaction between the

aquifer inside and outside the basin. Drainage of the basin was limited to groundwater-surface water interaction.

In MODFLOW, two categories of cells (constant-head and no-flow cells) can be used to simulate boundary conditions. "Constant-head cells are those for which the head is specified for each time and the head value does not vary as a result of solving the flow equations. No-flow cells are those for which there is no flow into or out of the cell (Harbaugh, 2005)". The value 1 was set to constant-head cells inside the basin and the value -1 was assigned to no-flow cells outside the basin (Figure 0.8).
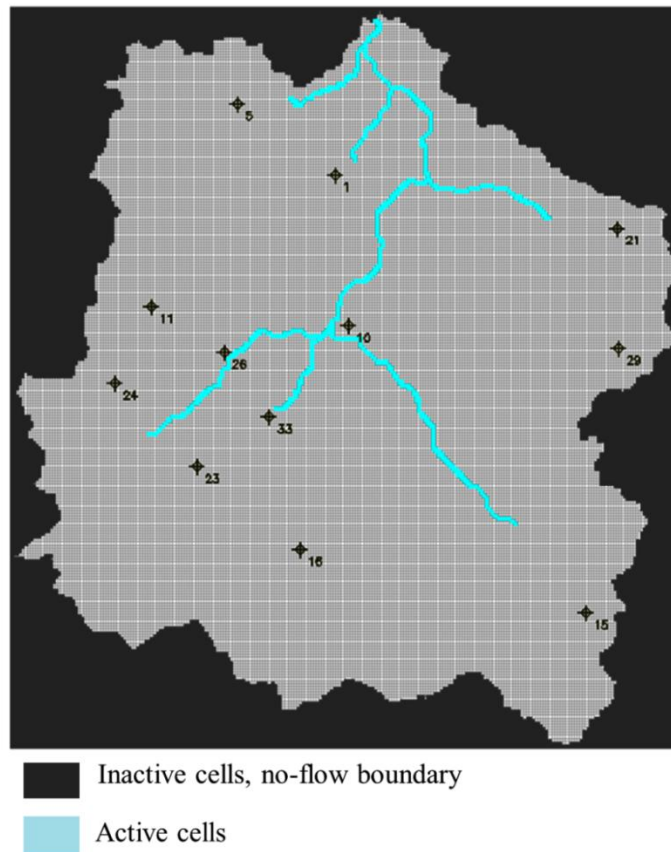
Figure 0.8 Boundary conditions of the Klela basin, and location of the wells used in steady-state simulation

e.   Initial hydraulic head

Initial hydraulic heads are a starting data inside the boundary of which MODFLOW requires at the beginning of a flow simulation. In practice, it is common to use a steady-state calibration in order to develop a large hydraulic conductivity

distribution by matching against a measured head distribution (Middlemis, 2001). Transient simulation needs initial conditions closely matching natural conditions at the beginning of the simulation (PDP, 2002 cited in Belay, 2009). Since the results from calibrated steady-state provide calculated heads, then, this was used in transient simulation as the starting heads conditions. In this study, historical water level data from more than hundred boreholes and data interpolated using the Kriging method were assigned to the model as initial hydraulic heads in the steady-state simulation. The head distribution computed using the calibrated steady-state simulation was used as the starting head distribution in the transient simulation.

f.   Groundwater recharge

As previously explained, the average recharge value (0.00046 m/day = 168 mm/a) estimated by the EARTH model was assigned to the entire model domain in steady state simulation.

g.   Pumping wells

In the study area, the only way to withdraw groundwater is from wells. The real quantity of water extracted from wells is not well known due to the presence of various traditional wells, which are not monitored. In order to estimate the extracted water quantity, each village was considered has one well. In total, a number of 150 pumping wells were distributed through the model domain. The total annual water extracted from the aquifer and assigned to the model is approximatively 57.3 Mm^3. See the detail below on water extraction per person.

3.4.2.2.   Surface water and groundwater system

Surface water and groundwater are both originally generated by precipitation. In some hydrological conditions and during the drought or low precipitation period, the surface water in streams and rivers is provided by groundwater via the drainage. Therefore, the surface water and groundwater are intimately linked through the hydrologic cycle component system. Although surface water is hydraulically connected to groundwater, their interaction is poorly known due to the fact that it is difficult to observe and measure, and usually have been ignored in water management considerations

and policies (Winter *et al.,* 1998). In the past, groundwater and surface water interactions were sometimes treated separately, but actually, several recent studies have considered water and material exchanges between stream water and groundwater, using numerical modeling and direct seepage flux estimation (Wroblicky *et al.,* 1998; Lee *et al.,* 2013). Because of the complexity of the interactions between surface water and groundwater, Sophocleous (2002) has suggested a sound hydrogeoecological framework to better understand these interactions in relation to climate, landform, geology and biotic factors. A better understanding of the interactions between the two water bodies is a key in effective water resources management for inhabitants of the Klela basin because the surface water is quasi-inexistent during the drought period. The interactions between both water resources follow this simple process.

As explained in Taft *et al.* (1997), a small amount of water can infiltrate below the ground and continue downward until it reaches an impermeable layer where the gravity effect is negligible. During the downward travelling, water fills any subsurface pore spaces, cracks, or crevices before arriving the impermeable layer. This process will continue in a subsurface area until an important quantity of water is stored and can be exploited as an aquifer. Depending on many factors in an area such as soil types, slope, vegetation, etc., the water downward can be rapid or slow. For example, in an area where the material is characterized by coarser grained water will transmit more rapidly than in a finer grained material area. Over time, water will leave from groundwater to the surface through various ways such as the formation of natural springs, discharge to river and stream banks, discharge under the river and stream beds, or direct discharge into the ocean. This discharging of groundwater from the aquifer to the surface water depends on the water tables and stream stages. When water tables intersect the ground surface, surface flow occurs as spring or drain flow.

Groundwater surface-water interactions are complex and constitute a critical component of the water budget. The combination of field and theoretical modeling studies have further contributed to our understanding of groundwater-surface water processes (Sophocleous, 2002). Therefore, many computer codes were recently developed to be applied in modeling surface-groundwater system. For example, "when a

head-dependent flow boundary is used, flow is computed at the surface-groundwater interface as a function of the relative water levels at any time and a conductance term at the boundary interface with the conductance term becoming a calibration parameter" (Middlemis, 2001). Also, the simplest and most common code is a special case where the discharge only occurs from groundwater to surface water during surface-water groundwater interaction process. In this modeling, the most common codes used such that drain, river, *etc.,* were not suitable in the study area, then, the streamflow-routing code was applied to model the interaction between stream-aquifer.

3.4.2.2.1.   Streamflow-Routing Package

Due to the "strong influence that streams can have on the flow and transport of contaminants through many aquifers, a new Streamflow-Routing (SFR1) Package was written for the use of the U.S. Geological Survey's MODFLOW-2000 groundwater flow model" (Harbaugh *et al.,* 2000; Prudic *et al.,* 2004). In this study, the streamflow-routing package was used to simulate the exchange of fluxes (sources and sinks) between surface water and groundwater.

The Streamflow Routing within the SFR1 Package is based on the continuity equation and assumption of piecewise constant function, uniform (location is still the same), and constant-density streamflow such that, the water budget equal to zero (*i.e.*, there is a balance between water inflow and outflow) and "no water is added to the or removed from the storage in the surface channels" during all times (Prudic *et al.,* 2004). In groundwater flow model, the direction of the streamflow is constant along the channels and is invariable for each time step (Prudic *et al.,* 2004). "The Streamflow-Routing Package is designed to account for the amount of flow in streams and to simulate the interaction between surface streams and groundwater" (Prudic, 1989; Chiang and Kinzelbach, 1998). This package requires ten parameters data such as segment, reach, streamflow, stream stage, streambed hydraulic conductance, elevation of the streambed top, elevation of the streambed bottom, width of the stream channel, slope of the stream channel and manning's roughness coefficient n/c. For more details, see Chiang and Kinzelbach (1998).

The most important part of modeling stream-aquifer interaction is ordering and numbering of streams. The stream network within the SFR1 Package is divided into reaches and segments. A stream reach is "a length of a stream within a particular finite-difference cell used to model ground-water flow and transport". A segment is "a group of reaches that are uniform in term: (i) of surface flow and precipitation amount to them; (ii) of evapotranspiration rates from them; and (iii) of change properties (for example; streambed elevation, thickness, and hydraulic conductivity, and stream depth and width)" (Prudic *et al.,* 2004). Only, the first reach contains the tributary flows or specified inflow or outflow and the diversions from the last reach (Prudic *et al.,* 2004). In this study, the model area was divided into 11 segments and 523 reaches.

In MODFLOW, the flow from streams to an aquifer (losing stream) or from an aquifer to streams (gaining stream) (Figure 0.9) is calculated depending on the groundwater table and stream stage. When groundwater table is above the stream stage, the volumetric flux between from their reaction is calculated using equation 3.19 (Brunner *et al.,* 2010)

$$Q = c_{STR} \times (h_S - h) = \frac{KLW}{M} \times (hs - h) \quad , \quad \text{with } C_{STR} = \frac{KLW}{M} \quad (3.19)$$

where Q is the volumetric flux (L^3/T), C_{STR} is streambed hydraulic conductance (L^2/T), is hydraulic conductivity K (LT^{-1}), L is the length of the river within a cell (L), W is the width of the stream (L), M is the thickness of the streambed (L), h_S is the head in the stream (L) and h (L) is the groundwater head.

"When the groundwater table h is below the elevation of the streambed bottom z, the volumetric infiltration flux from the river to the aquifer is calculated using equation" 3.20 (Brunner *et al.,* 2010).

$$Q = c_{STR} \times (h_S - z) \qquad z > h \qquad (3.20)$$

The value of C_{STR} was determined to be 500 m^2/d. The hydraulic conductivity of the streambed is unknown; therefore, it was set to 0.5 m/d based on the dominant soil material in the study area. The length L within the cell is 300 m, the width is 10 m, and the streambed thickness is 3 m.
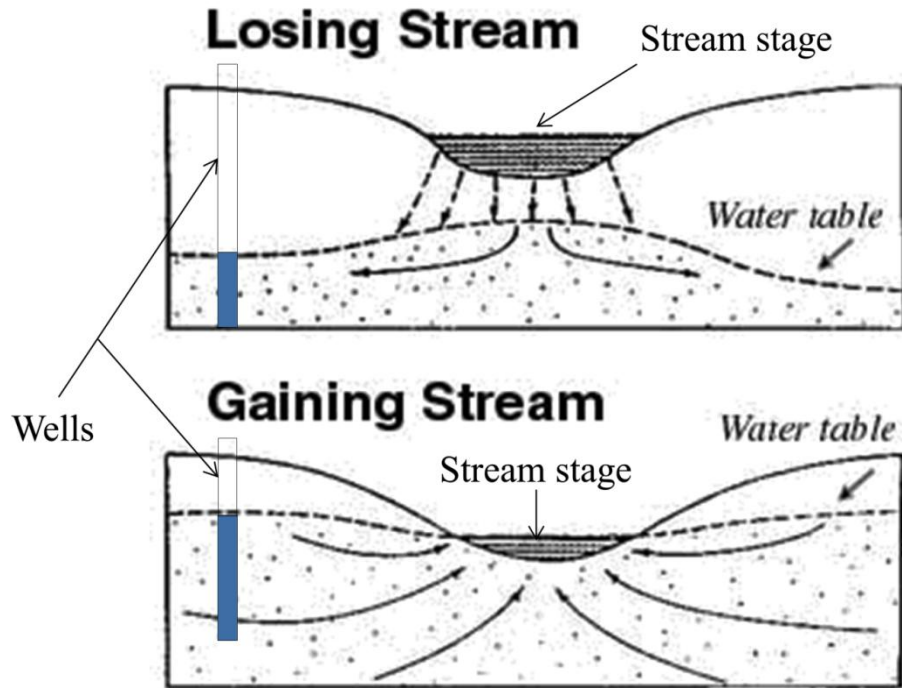
Figure 0.9 Interactions between surface-water and groundwater (figure adapted from Csaba and Csaba (2011))

3.4.2.3.   Calibration of the model

In groundwater modeling study, the real values of aquifer properties (*e.g.,* transmissivity, hydraulic conductivity, storativity, *etc.*) are generally not well known or unknown. For that reason, after the first run of the model simulation, it is noticed that the model simulated results are different from the field measurements. Thus, the model is always run with some errors. According to Konikow and Reilly (1998), these errors can be due to a bad conceptualization, the numerical solution error, or a poor set of field parameter values. In order to estimate the unknown parameter values, or reduce errors between computed and measurement parameters, the model calibration is used. Fetter, (2001); Moore, (2002) explained the calibration as "the process of fitting a model to a set of observed data by changing unknown or uncertain model parameters systematically within their allowable ranges until the best fit of the model to the observed data is achieved". In other words, model calibration solves a problem using inverse modeling by adjusting the unknowns (parameters and fluxes) until the solution matches the knowns (heads) (Genetti, 1999; Middlemis, 2001). During the calibration process, model input

parameters (aquifer geometry and properties, initial hydraulic heads and boundary conditions and stresses) are adjusted in order model simulated results match related head measurements (Hill and Tiedeman, 2007). Calibration is one of the most important steps in groundwater modeling because it is the only way that allows reducing errors between simulated and observed heads. Model calibration can be performed under steady-state and transient conditions. Usually, in steady-state calibration, the transmissivity or hydraulic conductivity is the parameter that is modified until head calculated matches measured heads, while changed of storativity or specified yield value can be applied for transient calibration. The steady-state is calibrated based on matching hydraulic heads, whereas that of the transient is based on groundwater fluctuation. Generally, the flow model is said to be calibrated when it can reproduce the hydraulic heads and groundwater fluxes of the natural system being modeled with some acceptable errors (Genetti, 1999).

Calibration can be performed using two methods a manual trial-and-error calibration and automated calibration (Anderson and Woessner, 1992; Hill, 1998; Genetti, 1999; Essink, 2000; Middlemis, 2001; Hill and Tiedeman, 2007).

3.4.2.3.1. Trial-and-error calibration

Trial and error calibration is a manual way to change initial parameter values until the best correlation between simulated and observed heads is obtained. Modification of parameter values depends on the degree of certainty. When the parameter value is known with a high degree of certainty, it does not need to be changed in calibration. Typical steps followed in trial and error calibration can be found in Figure 0.10. The trial and error calibration gives useful information for the parameter to be adjusted during the calibration process and also provided an appropriate trend of the observed and simulated results. Trial and error technique is subjective and inefficient; this may be due to a large number of interrelated factors affect the output (Konikow and Reilly, 1998). Although this process is not sufficient for calibration, but it demands a high level of understanding of the model physics and the inner exchanges among model components (Duan, 2003). Calibration using only trial-and-error methods is more common. This may be due to lack of familiarity with model calibration using inverse modeling and the perception that they require more time than trial-and- error methods (Hill and Tiedeman, 2007). In this study,

the trial and error method was used to obtain a range of horizontal hydraulic conductivity in the steady-state simulation.
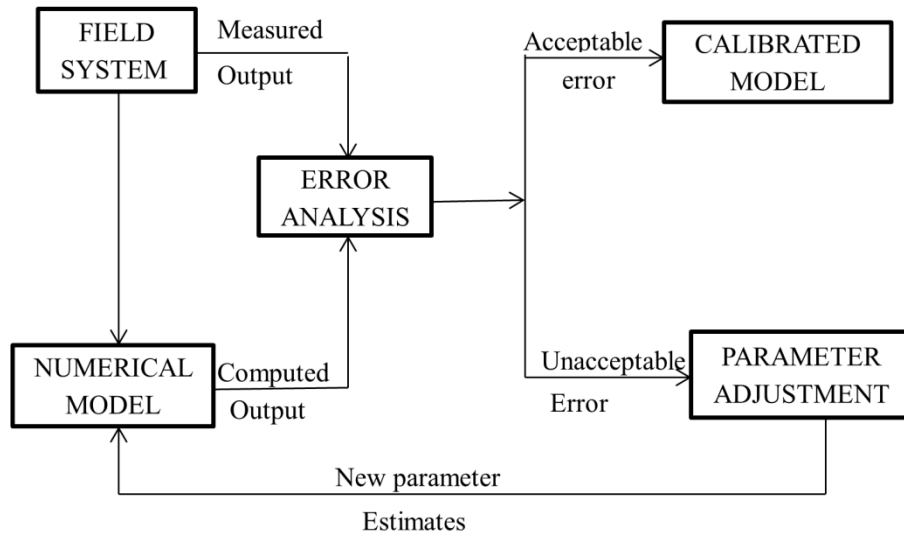
Figure 0.10 Trial and error calibration procedure (modified from Seneviratne, 2007)

3.4.2.3.2. Automated calibration

As the trial and error calibration is subjective and inefficient, the automated calibration must be applied to correct a large error made by manual calibration. Computer-based optimization methods are usually used to optimize model parameter in automatic technique (Duan *et al.*, 2003). The objective of automatic calibration is to obtain the closest match possible (minimizes deviations) between observed data and model output (Konikow and Reilly, 1998). The success of automatic calibration depends heavily on four factors: model structure, calibration data, calibration criteria and optimization method. Although the automatic calibration is based on single objective, it does not necessarily lead to satisfactory hydrological calibrations. There are many different types of automatic calibration, but PEST (Parameter ESTimation), incorporated into PMWIN, was used in this study to calibrate the model in steady-state simulation.

3.4.3. WEAP model

Because of increasing of water demand related to increasing of population, reduction of freshwater availability, climate variability and change, all the world's

governments are worried face to these new challenges. Integrated water resources management (IWRM) tools may be used to help decision makers to better overcome this issue. One of these tools applied in water management is Water Evaluation And Planning system (WEAP). It is an exemplary application, which links supply and demand site requirements (Höllermann *et al.,* 2010). WEAP is a software tool developed by Stockholm Environment Institute for integrated water resources planning (SEI, 2001) and an integrated decision support system (DSS) that is aimed to support water planning system by comparing water supplies generated from surface water (*e.g.,* streamflow, lake, seepage, spring, *etc.*) and groundwater (*e.g.,* natural and artificial recharge) of a basin scale, or municipal scale and multiple water demands and environmental requirements characterized by spatially and temporally variable allocation priorities, and supply preferences (Rosenzweig *et al.,* 2004; Yates *et al.,* 2005). According to Haddad *et al.* (2007), the DSS for water resources management system involve three major components (1) stakeholders survey to define key planning issues; (2) database system to facilitate data management; and (3) the WEAP model that simulates and predicts water resources management using multiple alternative scenarios. It is straightforward and easy to use, free of charge for organizations and institutions in developing countries and downloadable at: www.weap21.org.

The WEAP model can be used to simulate both natural hydrological processes and anthropogenic effects on natural water resources to evaluate the availability of water within the basin and human impact on water use respectively (Yates *et al.,* 2005; McCartney and Arranz, 2007). These simulations within the WEAP model are constructed as a set of scenarios, where simulation time steps are monthly based with a time horizon of a single year to more than 100 years (Yates *et al.,* 2005).

In WEAP, the future behavior of water availability and demand is compared to the current or a baseline year, which is based on a snapshot of actual water demand and supplies, known as Current Accounts. Basically, the baseline year is chosen to determine the recent eventual potential water accessibility of a system; and then, to assess the impact of different alternative scenarios for future water availability. Generally, the baseline year is the year where there is enough information on all input data such as hydrology, precipitation, natural infiltration, temperature, demography, socio-economic,

agriculture, *etc.* The adaptability of the WEAP model to different levels of data availability and its simple graphical user interface make it the suitable tool to be used in all climatic conditions (Hoff *et al.,* 2011) including Klela basin case, where data availability is very scarce. Water Evaluation And Planning System has been chosen in this study in order to evaluate the impact of human action on groundwater resources and climate change effects, by developing multiple alternative scenarios based on population growth rate and precipitation variation over time. Climate scenario data, RCP4.5 and RCP8.5, from CORDEX, used in this study will be developed throughout this document.

3.4.3.1.   Model structure

The WEAP model structure comprises five different views (SEI, 2005 2015); it is similar to other water allocation decision system support tools, for example, HEC-ResSim developed by US Army Corps of Engineers (2007).

Schematic

The schematic view is a spatial physical feature of the water supply and demand system. It permits to connect all supply and demands by using nodes and transmission links. This linking can easily be changed or modified at any moment during modeling process by dragging and dropping method. Its graphical interface allows importing GIS layers (vector and raster) and using them as background layers. The WEAP model schematic of the Klela basin can be seen in Figure 0.11. Red points in this figure represent water demands in the study area. These water demands include irrigation, industry, livestock, rural and urban, which explain the quantity of water use in each sector; urban and rural indicate domestic water use. The green square is groundwater source, which furnishes water to other sectors via a transmission link, in the green arrow.
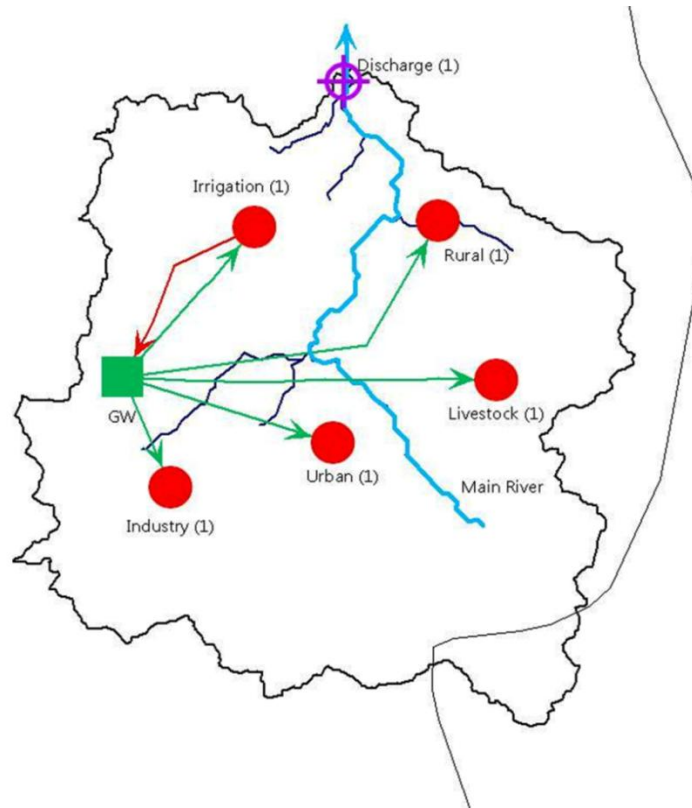
Figure 0.11 Schematic of the WEAP model for the Klela basin, GW is groundwater. Red points represent water demands in the study area, the green square is groundwater source, and green arrow is transmission link

Furthermore, the WEAP has a dynamic capability to be linked to other models and spreadsheets such as LEAP, MODFLOW, MODPATH, QUAL2K, Excel, *etc.* It is therefore recommended to improving groundwater modeling by linking WEAP to MODFLOW. In this current study, the fractured sandstone aquifer of the Klela basin was first calibrated and validated with PMWIN 5.3 version, and then the results were used for calibration in WEAP.

3.4.3.2.   Modeling process of WEAP

The modeling process within WEAP follows some steps: (i) creation of a geographic representation of the study area on which all the features (supply and demand sites) are represented, (ii) establishment of current account; this involves choosing a reference year (baseline) in which all or the maximum of data are available. In this part,

the reference scenario is naturally created which shows the probable evolution of the system during the simulation period without any modification, and (iii) development and evaluating of model scenarios; it is the most important part of modeling allowing predicting an eventual change on water resources exploring the model with a wide range of questions. For example, what if demographic or economic patterns change? What if the mix of agricultural crops changes? What if groundwater is more fully exploited? How might climate change alter demand and supplies? How does pollution affect water quality? How will land use changes affect runoff? In this case, the question is what will be groundwater resources in the Klela basin under population growth and climate change? The answer to these questions allows evaluating the model scenarios.

3.4.3.3.   Scenarios development

In this study, the scenarios have been developed for the time interval 2013-2050, with the year 2013, the current account (baseline). The baseline (2013) was chosen based on the availability of consistent and reliable data. Six scenarios were developed such as Reference scenario, socio-economic scenarios (E1 and E2), high population growth scenario, and climate change scenarios with RCP4.5 and RCP8.5.

a. Reference scenario: scenario 1

This scenario refers to the current account scenario in which the socio-economic is used "business as usual". Climate (precipitation) data is based on current account year (2013). Therefore, the recharge was constant over time from 2013-2050.

b. **Population growth scenario**

Like many African countries, Mali has a high population growth. According to the last census in Mali (Traore *et al.,* 2011), the average population growth rate was estimated at 3.6%. The average rate is increasing from one census to another; *e.g.,* it was 1.7% from 1976 to 1987, and it achieved 3.6% from 1998 to 2009, or an increase of 1.9% in 33 years. With this growth rate, the population could double each 20 years. Moreover, Traore and Sissoko (2010) argued that the population of Mali could be doubled in 2050, but the projection made by DAES, cited in Traore and Sissoko (2010) suggested that the growth rate will decrease from 2010 and will reach 1.43% between 2045 and 2050. Besides population growth, the increasing trend of urbanization rate is also noticeable in

Mali. In 1998, urbanization rate was approximatively 27%, and it was estimated to exceed 40% in 2015 (PNUD cited in Keïta and Konaté, 2003). All these (population growth and urbanization evolution) increase the water demand for the population. What are the implications for groundwater resources face to this pressure of population growth? The question comprises various variables including the closeness and accessibility of groundwater resources, groundwater system vulnerability, the consistency and comprehensiveness of existing governance regimes, type of current stresses, and climate change impacts.

Since the population growth rate is the average for all Mali, the same growth rate (3.6%) will be considered in the Klela basin. The population of Klela basin is estimated to 462,544 in 2009. It was calculated to be 532,834 in 2013 (baseline for the model) and in 2050, it is projected to reached 1,971,982 if the growth rate remains constant. The population scenario is as follows:

- **Higher population growth scenario:** scenario 2, the present growth rate (3.6%) will be increased by 2%, and to be 5.6% in 2050. Other parameters: socio-economic is used "as usual"; and the climate (precipitation) data is based on current account year (2013).

c. **Socio-economic scenario**

In order to consider all eventual socio-economic development in the future for the Klela basin, two socio-economic scenarios (E1 and E2) were evaluated in this study. For both cases, the climate was set as that of reference scenario.

- **Socio-economic scenario E1**: scenario 3, in this scenario, all the water demand data is moderately increased, except livestock which is the same as in reference scenario and population growth decreases (based on DAES, Nations Unies projection see above) slightly compared to the reference scenario.
- **Socio-economic scenario E2**: scenario 4, this is high water demand scenario with slightly decrease of population growth but greater than that in scenario E1. All the socio-economic data was increased as much as possible.

d. **Climate change scenario**

In this study, climate data series (present and future) were taken from the GCM ECHAM downscaled to a 0.44° resolution by the Swedish Meteorological and Hydrological Institute (Sveriges Meteorologiska och Hydrologiska Institute, SMHI) and provided by CORDEX (Coordinated Regional Climate Downscaling Experiment) initiative which was used to assess the impacts of climate change on groundwater resources in the Klela basin. CORDEX is a program funded by World Climate Research Programme (WCRP), of which the main aim is to develop a framework allowing the use of downscaled global climate projections and assessing regional climate downscaling techniques and finally using them into impact and adaptation studies within the IPCC Fifth Assessment Report (AR5) timeline (Ozturk *et al.,* 2012). "The first part of this framework is a set of common regional domains" (Evans, 2011). Therefore, CORDEX domains cover most of the land surfaces of the world. Based on regional focus and improved resolution, it is expected that the CORDEX dataset will provide a link to the effects and adaptation community (Evans, 2011). Unlike former IPCC assessments based on SRES GHG scenarios, CORDEX is focused on the GCM experiments applying emission scenarios that are based on Representative Concentration Pathways (RCPs). For most land regions of the world including Africa, CORDEX data provide a coarse resolution of 0.44° (approximatively 50 km) ensembles of downscaled regional climate projections. An ensemble of dynamical and statistical downscaling models will be produced in the framework of CORDEX applying multiple forcing GCMs as input (Ozturk *et al.,* 2012). Africa was designated as the first region to be tested with CORDEX data for the simple reason that it is the region that is most vulnerable to climate change due to the dependence on seasonal agriculture and also on the relatively low adaptive capacity of its economies. In addition, climate change could have an important impact on temperature and precipitation patterns over Africa, which can interact with land-use change, desertification and aerosol emissions (Giorgi *et al.,* 2009). The Representative Concentration Pathways (RCPs) are four greenhouse gas concentration trajectories adopted by IPCC for its fifth assessment report in 2014, which replace the Special Report Emission Scenarios projections in 2000. The RCPs describe an emission trajectory and concentration by the year 2100, unlike SRES that starts by socio-economic from which emission trajectories and climate impacts are projected (Wayne, 2013). A set of four

pathways were created based on radiative forcing degrees of 8.5, 6, 4.5 and 2.6 W/m^2 corresponding to RCP8.5, RCP6, RCP4.5 and RCP2.6 respectively by the end of 2100. The RCPs dataset cover the period 1950-2100 (van Vuuren *et al.,* 2011). Only the two scenarios (RCP4.5 and RCP8.5) were taken into account in this case study and are described below.

RCP4.5: the scenario RCP4.5 is an intermediate pathway that is around the stabilization level of approximatively 4.5 W/m^2 (Moss *et al.,* 2008). Thus, the RCP4.5 is a stabilization scenario that supposes that all the world countries undertake emission mitigation policies (Thomson *et al.,* 2011). For RCP4.5, the radiative forcing reaches 4.5 W/m^2 (Figure 0.12) when the stabilization is achieved in 2080. From 2080-2100, the radiative forcing is constant in the RCP4.5, but the greenhouse gas concentrations and those emissions are still varying in the underlying scenario. Compared RCP4.5 to GCAM (General Circulation Atmospheric Model) reference scenario, it has been demonstrated in Thomson *et al.* (2011) that the population and income drivers are the same, but they are different from the policy applied to greenhouse gas emissions to stabilize atmospheric radiative forcing. The main anthropogenic gas emission for RCP4.5 is carbon dioxide (CO_2) and constitutes the largest contribution to total radiative forcing followed by methane (CH_4) and others. The maximum value of anthropogenic CO_2 emissions for the RCP4.5 top around 42 GtCO (gigatonnes of carbon dioxide) per year corresponds around 2040. In order to decrease greenhouse gas emissions into the atmosphere and stabilize radiative forcing by 2100, the RCP4.5 scenario is projected to inform research on the atmospheric consequences (Thomson *et al.* 2011).

RCP8.5: The worst case scenario RCP8.5 is a reference scenario and representing the highest RCP scenario regarding GHG emissions without any explicit climate policy. According to Wayne, (2013), most non-climate policy scenarios projected emissions by the end of the century achieving the order of 15 to 20 GtC (gigatonnes of carbon), which is not far from the emission degree of the RCP6. RCP8.5 is a rising radiative forcing pathway leading to 8.5 W/m^2 in 2100 (Figure 0.12). In RCP8.5, increasing global population (approximatively 12 billion by 2100) and economy associated with a lower rate of technology development lead to increasing a primary energy demand (Riahi *et al.,* 2011). An increasing global population in RCP8.5 is mostly due to increase use of

cropland and grasslands (van Vuuren *et al.,* 2011). The RCP8.5 is similar to the original IPCC A2 SRES scenario storyline (Nakićenović *et al.,* 2000). It is mentioned in Riahi *et al.* (2011) that in RCP8.5, the greenhouse gas emissions continue rising due mainly to the high intensity of fossil energy as well as growing population and also high demand for food. Most of the GHG emissions rising are due to those of CO_2 from energy sector; but from agriculture sector it is principally attributed to increasing use of fertilizers and intensification of agricultural production, giving rise to the main source of nitrogen dioxide (N_2O) emissions. Riahi *et al.* (2011) compared the GHG emissions in RCP8.5 CO_2-eq per year; they found more than double by 2050 compared to 2000 and continue rising and reach triple by 2100 to about 120 $GtCO_2$-eq (Figure 0.12). Besides the principal responsible for radiative forcing such as CO_2, CH_4, NO_2, *etc.,* there are some others additional tropospheric ozone in RCP8.5, which are expected to increase the radiative forcing by an additional 0.2 W/m^2 by 2100 (Lamarque *et al.,* 2011). In addition, bioenergy increases from about 40 EJ in 2000 to more than 150 EJ by 2100 in RCP8.5 scenario (Riahi *et al.,* 2011).

The data from stabilization scenario RCP4.5 and high scenario RCP8.5 were used in this study to evaluate the impact of climate change.

- **Climate change scenario with RCP4.5:** scenario 5, in this scenario, only the climate (precipitation) data from RCP4.5 scenario was used. The population and other demands were not changed.
- **Climate change scenario with RCP8.5:** scenario 6, like in scenario 5, only the climate from RCP8.5 scenario was used. The other parameters were used like in reference scenario.

The raw climate data from CORDEX were used directly to the model without any bias correction because its historical mean datasets of precipitation and temperature were nearly fitted to the observed dataset measured from the field (Figure 0.13-Figure 0.16). The correlation coefficient of 0.802 for temperature shows a good correlation between observed measurements and simulated from CORDEX (Figure 0.16). In addition, the bar graph (Figure 0.14) indicates that the sum of mean monthly precipitation from measurements is close to that from CORDEX.
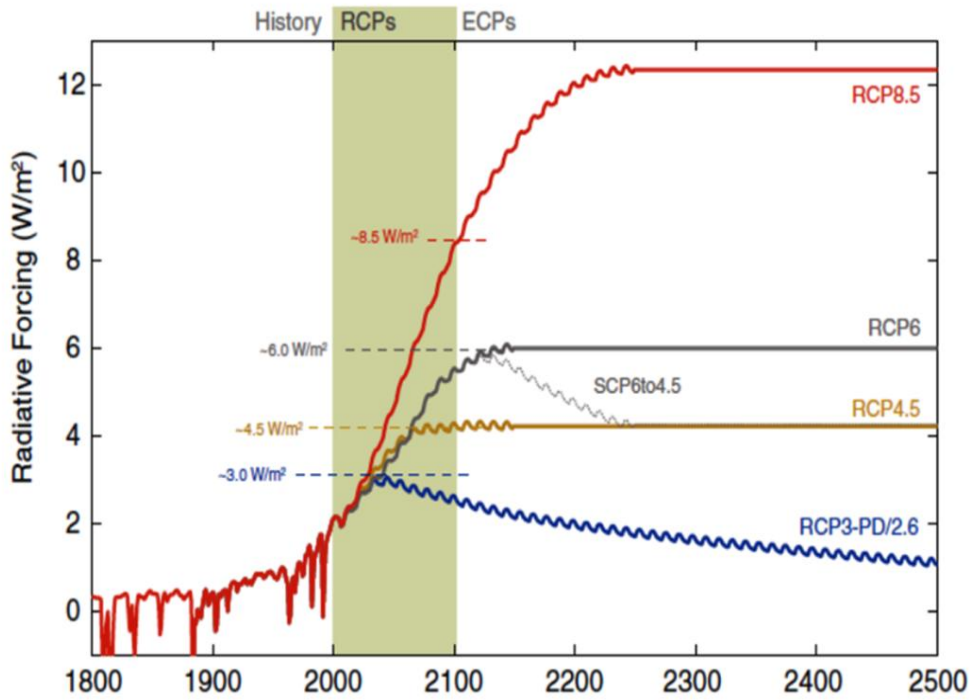
Figure 0.12 Total radiative forcing (anthropogenic plus natural) for RCPs (figure adapted from (Meinshausen et al., 2011)
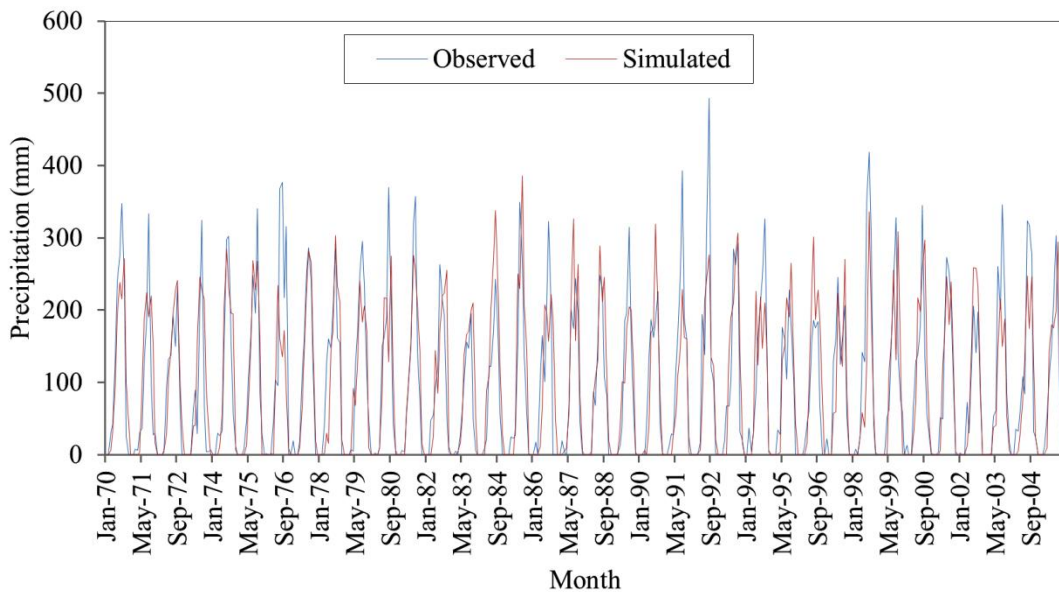
Figure 0.13. Monthly precipitation (mm) of observed and simulated historical data from CORDEX (1970-2005)
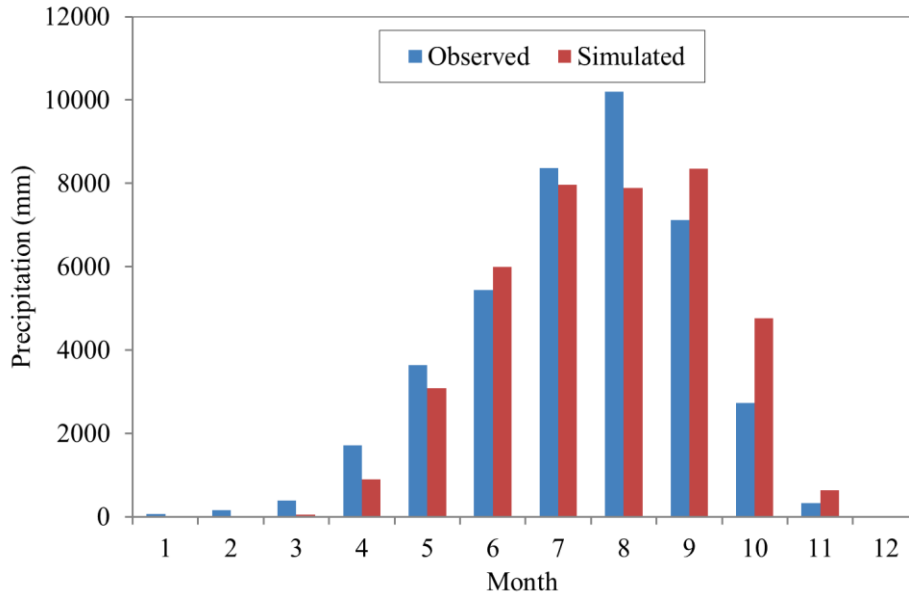
Figure 0.14 Sum of mean monthly precipitation (mm) between observed and simulated from CORDEX (1970-2005)
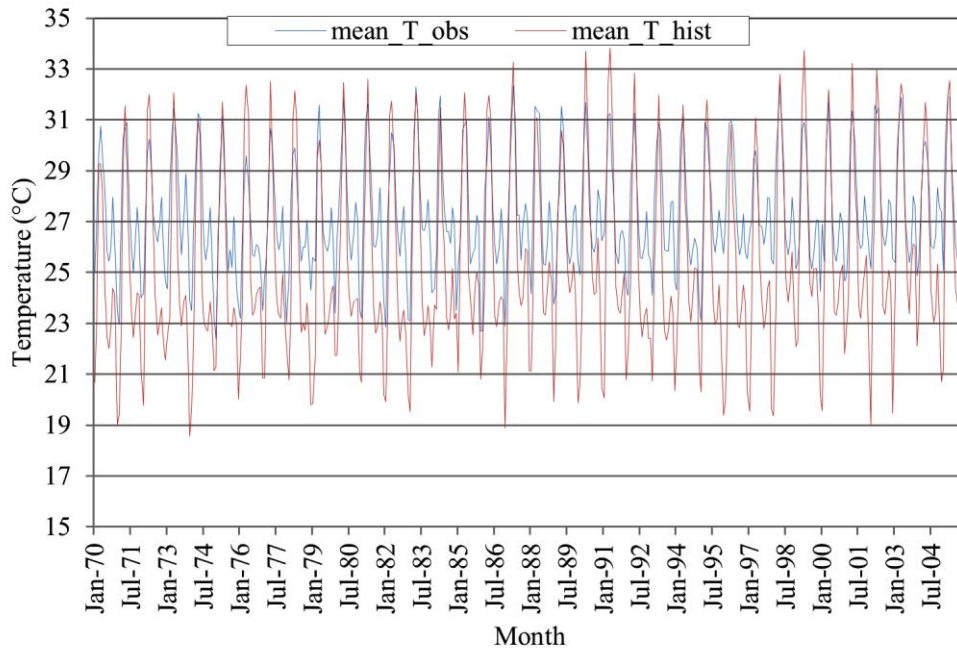
Figure 0.15 Monthly temperature (°C) of observed and simulated form CORDEX (1970-2005)
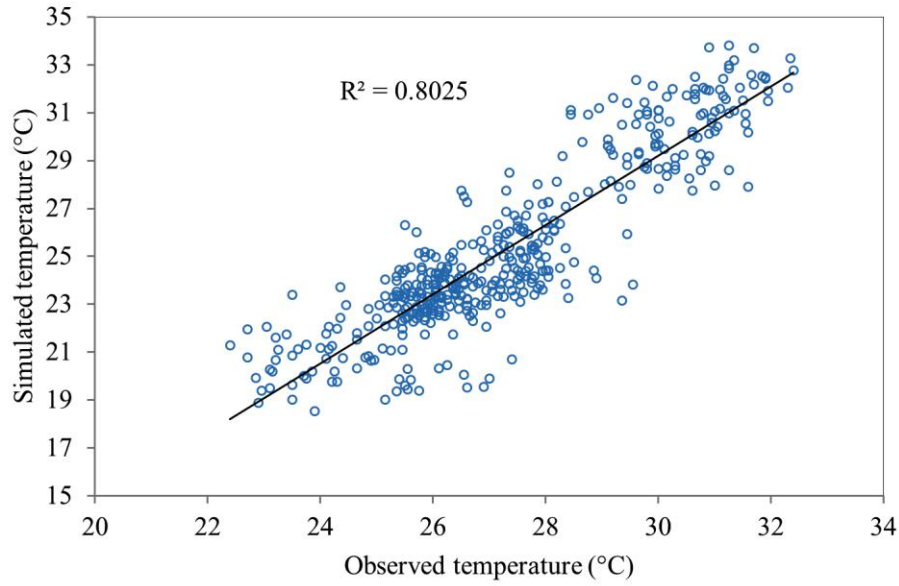
Figure 0.16 Comparison between observed and simulated temperature (°C) from CORDEX (1970-2005)

3.4.3.4.   Groundwater-surface water within WEAP

As explained above, groundwater interacts with surface water depending on the water table in the well. The results from MODFLOW show that groundwater is hydraulically connected to surface-water. In general, groundwater fluctuations respond to natural recharge from precipitation and often from irrigation, where a portion of this water may recharge the aquifer, both contribute to increase groundwater levels; and also from pumping that draw down groundwater levels.

In WEAP (see detail in Yates *et al.* (2005)), there are four options to simulate groundwater-surface water interactions: (1) specify directly the amount of groundwater inflow to a particular river or reach; (2) groundwater "wedge" connected to river; (3) deep soil layer of Soil Moisture method catchment; and (4) link WEAP to MODFLOW. In this study, the option 2 was used to model the interaction between groundwater and surface water.

A stylized representation is used to simulate groundwater-surface water interactions (Figure 0.17). In this case, groundwater is represented as a wedge, which is

symmetrical about the river. Recharge and extraction from one side of the wedge will, therefore, represent half the total rate.
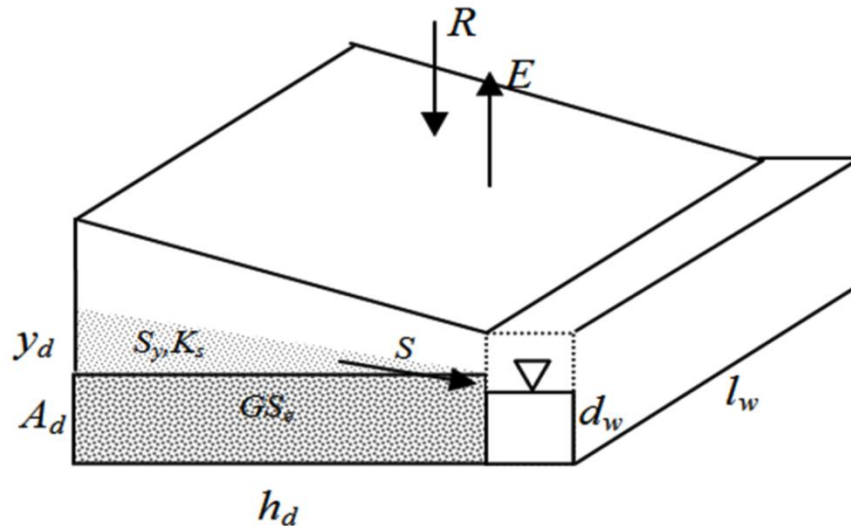
Figure 0.17 A stylized representation of groundwater system and its associated variables (figure source from SEI 2011)

The first parameter estimated is total groundwater storage in which it is supposed that the groundwater table is in equilibrium with the river. Equation 3.21 allowing calculating equilibrium storage is given as follows:

$$GS_e = h_d \times l_w \times A_d \times S_y \qquad (3.21)$$

where GS_e is equilibrium storage for one side of the wedge (m^3); h_d is the distance that extends in a direction horizontally and at a right angle to the stream (m); l_w is the wetted length of the aquifer in contact with the stream (m); A_d is the aquifer depth at equilibrium (m); and S_y is the specific yield of the aquifer.

The initial storage in the aquifer is given in equation 3.22 at t=0 as:

$$GS(0) = GS_e + y_d \times h_d \times l_w \times S_y \qquad (3.22)$$

where $GS(0)$ is initial storage (m^3), and y_d is the vertical height of the aquifer above or below the equilibrium position (m) which is given in equation 3.23 below:

$$y_d = \frac{GS - GS_e}{h_d \times l_w \times S_y}$$ (3.23)

The total seepage from the aquifer to the streams or vice versa depending on water table position (rises or falls relative to stream channel) is estimated using equation 3.24:

$$S = 2\left(K_s \frac{y_d}{h_d} \right)(l_w)(d_w)$$ (3.24)

where S is total seepage (m^3/time), K_s is saturated hydraulic conductivity of the aquifer (m/time), and d_w is an estimate of the wetted depth of the stream (m).

After estimating the total seepage, the groundwater storage at the end of the current time step is estimated as indicated in equation 3.25:

$$GS_{(i)} = GS_{(i-1)} + 0.5\left(R - E - S \right)$$ (3.25)

where R is recharge from precipitation (m^3/time), and E is the anthropogenic extraction from the aquifer (m^3/time). Refer to Sieber *et al.* (2005) for more information.

3.4.3.5.   Recharge estimation with thornthwaite model

As the climate data available from CORDEX were precipitation and temperature, then, the recharge calculation is needed because the WEAP version 3.4 cannot take directly these parameters. The Thornthwaite model (McCabe and Markstrom, 2007) developed by the U.S. Geological Survey was applied for this purpose, which used monthly total precipitation (in millimeters) and temperature (in degrees Celsius) as input data to estimate the recharge. The Thornthwaite model is based on the monthly water-balance model that is driven by graphical user interface.

The water-balance model calculates the water amount of the various components of the hydrological cycle (Figure 0.18) using a monthly accounting procedure. Seven other "input parameters (runoff factor, direct runoff factor, soil-moisture storage capacity, the latitude of the location, rain temperature threshold, snow temperature threshold, and maximum snow-melt rate of the snow storage)", incorporated in the model, were changed during the model calibration process McCabe and Markstrom, (2007). The model was calibrated to fit the groundwater recharge previously simulated using EARTH model in

the past. To calibrate this model, monthly precipitation and temperature from RCP4.5 and RCP8.5, from 2012 to 2013 were used as input data, direct runoff was set to zero because local scale surface runoff infiltrates on the way to the river system. There is no direct runoff contribution to the discharge of the basin. The soil moisture storage capacity was calibrated to be 375 mm by comparing the groundwater recharge of the two models (EARTH and Thornthwaite). All other parameters were unchanged. More detail on this model can be found in McCabe and Markstrom, (2007). After calibration, the model was applied to simulate groundwater recharge from 2006 to 2050, as well as potential evapotranspiration, actual evapotranspiration, soil moisture storage and runoff.
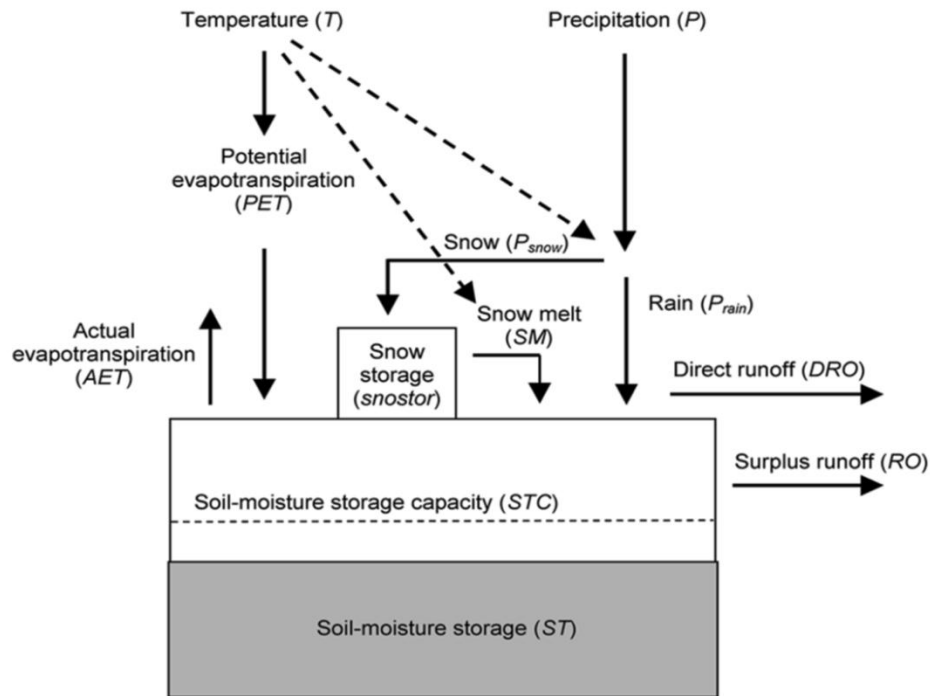
Figure 0.18 Diagram of water-balance model (figure source from McCabe and Markstrom, (2007))

3.4.3.6.   Water supply and demand, and current and future data sources

Most of the data used in this modeling are collected from the different National Directions, but some have been computed by models (EARTH, MODFLOW and CORDEX) applied in previous sections in this study. The data was divided into two parts

water supply resources (surface water and groundwater) and water demand (agriculture, domestic, industry, *etc.*).

3.4.3.6.1.   Water supply sources

The main source of water in the Klela basin is groundwater, which is acceded through wells and boreholes. These groundwater sources are principally replenished by local precipitation through the infiltration. This infiltration has been estimated (chapter 0) by the EARTH model to be approximatively 13.9% of mean annual precipitation. The precipitation data from DNM for the current account (the year 2013) and from CORDEX for the scenarios (2014-2050) were used in this study. As explained in chapter 0, the groundwater dynamic has been simulated and that showed that more than 90% of groundwater resources are leaving to the streams by seepage. Therefore, the assessment of the future water availability is worthwhile for the population in the Klela basin.

Other water sources, which are seasonally important, are stream flows. These resources are notably useful for irrigation and for livestock, and available mostly during the rainy season.

3.4.3.6.2.   Water demands

Like many rural zones in Mali, four types of water users are known in Klela catchment: households, irrigation, industry and livestock. Population uses water from three different sources: water supplied assured by SOMAGEP (Societe Malienne de Gestion de l'Eau Potable), water from wells or hand-pumps or water tower, and water from rivers. Water demand per person in Mali depends strongly on the state of urbanization, which is in turn based on the number of inhabitants per region. For example, in the village (less than 2000 inhabitants) the water need is 20 liter per capita per day (lpcpd) (N'Djim and Doumbia, 1998; WHO, 2003), it is 31 lpcpd in semi-urban area (between 2000-10000 inhabitants) and in urban area (> 10000 inhabitants), it is 45 lpcpd (N'Djim and Doumbia, 1998; WWAP, 2006). Since most of the population in Klela basin is living in the villages, therefore, 20 lpcpd has been used as their need in the water. The remainder of the population living in town receives water via SOMAGEP.

During the rainy season, the rivers contribute to satisfying water demand in rice irrigation and in livestock water need.

The fourth and last census that Mali has experienced was conducted in 2009 (RGPH, 2009). This population data was used to estimate the domestic annual water use. The data for irrigation was provided by DRGR Sikasso (Direction Régionale du Génie Rural de Sikasso) and PCDA (Projet pour la Compétitivité et Diversion Agricole). In fact, two major types of the crop (rice and potato) that consume a huge quantity of water were retained as water demand in irrigation. Of course, there are other types of crops, but the data are not available and the quantity of water used are certainly small compared to the two cited above. Rice cultivation is carried out during the rainy season from June to October. The main water resources that reach the irrigated area (Bas-fonds and Pond) are the runoff and groundwater discharge. Concerning the potato, it is irrigated in the cool dry season from November to February. Groundwater is the principal source exploited for this need (Diakité and Zida, 2003). This source is extracted from wells manually or through motor pump depending on the extension of the irrigated surface. The industry is not well developed in this rural study area. In contrast, there are some small factories that withdraw water from groundwater (source DRI: Direction Régionale Industrie). The statistical detail on the current situation, 2013 is in Table 0.2.

Table 0.2: Statistics information on current situation (data sources: DRI, DRGR, RGPH and PCDA)

Population		Demand per capita $(m^3/year)$		Irrigation (ha)		Livestock	Number of factories
Urban	Rural	Urban	Rural	Potato	Rice		
260,059	272,775	15	7.5	576	4,612.2	363,270	12

The details on water demands and their sources are mentioned in Table 0.3.

Table 0.3 Water demand data for current account for the year 2013 in million cubic meters (Mm^3)

Demand site		Annual water demand (Mm^3)	Sources
Domestic	Urban	3.90	DNSI, RGPH, (N'Djim and Doumbia, 1998)
	Rural	2.05	(WWAP, 2006)
Livestock		3.31	DRSV
Irrigation	Rice	62.26	DRGR
	Potato	4.49	(Diakité and Zida, 2003), PCDA,

		Fiche technique pomme de Terre
Industry	0.05	DRI
Total	76.06	

3.5.   Conclusion

Like in most of the developing countries, hydrogeological and soil characteristic data availability in the Klela basin is very limited. This may affect some results in this study. Sometimes, even the acquisition of existing data is not easy due to its high cost, especially the daily climate data from the DNM of Mali. Despite the serious problems associated with the lack of data available in the study area, it is recommended to try the hydrological models in such kind of areas to find out the true problems. Materials and methods used in this study show that they might be applied in a catchment even with low data availability. Those tools are well known in hydrological domains and used in many aquifers.

CHAPTER 4: GROUNDWATER RECHARGE ESTIMATION

4.1.   Introduction

Groundwater recharge has been widely applied by many authors through the world in various climate conditions. The recharge is defined as any water fluxes which arriving the water table downward, or laterally. The water balance components traverse different processes from the atmosphere to the aquifer. Various water resources reach water table including precipitation, irrigation water, surface water bodies (ponding, surface storage), the interaction between aquifers and lateral flow. Most of the recharge studies throughout the world are focused on the relationship between groundwater recharge and precipitation (Lee and Risley, 2002; Weiss and Gvirtzman, 2007). This present study was not an exception, thus, it was based on the contribution from the precipitation to the aquifer. Before reaching the aquifer, water passes through the soil surface, unsaturated zone, and saturated zone. Recharge is a sensitive function of the climate (precipitation and temperature regimes), local geology and soil, topography, vegetation, surface water hydrology, surface-groundwater interactions, coastal flooding and land-use activities such as urbanization, woodland establishment, crop rotation, and irrigation practices (de Vries and Simmers, 2002; Holman, 2006; McMahon *et al.,* 2006; Candela *et al.,* 2009). Spatial variability of any of these factors can produce localized effects (Henry, 2011). Many studies have shown the uncertainties and limitations of the methods used for estimation of groundwater recharge, especially in arid and semi-arid areas. Among different techniques used for estimating the recharge, one can note physical unsaturated and saturated zones methods, cumulative rainfall departure (CRD), saturated volume fluctuation- water balance (SVF), hydrograph separation, lysimetry, water table fluctuation (WTF), Extended model for aquifer recharge and soil moisture storage through the unsaturated hard rock (EARTH), and chemical tracer methods (chloride mass balance (CMB), groundwater dating, environmental isotopes). Due to the high uncertainty on recharge estimation, it is recommended to use multiple methods in the same area for estimating groundwater recharge in order to obtain more reliable results

(Lerner *et al.,* 1990; Scanlon *et al.,* 2002). The errors and uncertainties linked to recharge estimation can be due to an unreliable technique used in an area include spatial and temporal variability, an inappropriate conceptual model, field measurement errors and calculation errors (Simmers, 1997 cited in Henry, 2011). The recharge can be considered as potential or actual depending on the sources of water that replenish the aquifer. For example, when the recharge is computed considering surface water and unsaturated data, it is called potential recharge because the fluxes can be lost by many factors (evapotranspiration, *etc.*) before achieving the water table (Obuobie, 2008). In contrast, the recharge is generally known as actual recharge, when the data are provided from groundwater as this is based on the water that has already reached the water table (Scanlon *et al.,* 2002; Belay, 2009). As mentioned before, the recharge can be classified by using a physical method or tracer technique.

The physical method can be divided into two important parts, direct and indirect measurements. The direct measurements include, for instance, lysimetry, while the indirect measurements involve water balance methods and numerical modeling. The direct measurements are costly and difficult to implement the material and most of the studies completed do not use this method. In contrast, the indirect measurements are based on the simple reason that the other components of the water balance (precipitation evapotranspiration, runoff, *etc.*) can be easily measured and allow the estimation of recharge. The accuracy of the recharge calculated from water balance method depends on the precision on measurements. If the measurements are performed with major errors, obviously the recharge generated from that equation will be the same errors. These can be considered as some limitations using water balance method in determining groundwater recharge. Furthermore, the numerical models, which are developed to reduce the errors on recharge calculation, present some limitations, particularly at calibration level.

Additionally, the chemical tracer techniques have been applied to estimate the recharge worldwide. According to Scanlon *et al.* (2002), tracers are grouped into three categories: natural environmental tracers, historical tracers, and applied tracers. The chloride (Cl) is the most natural environment tracer method used in recharge calculation (Allison and Hughes, 1978 cited in Scanlon *et al.,* 2002). Applying the tracer techniques

lead to over- or under-estimate the recharge because tracers do not measure water flow directly (Lerner *et al.,* 1990).

Based on limitations, applicability and rating (accuracy, ease of use and cost), Xu and Beekman (2003) have summarized in Table 0.1 diverse methods of recharge usually applied in semi-arid regions, the case of Southern Africa, from surface water to saturated groundwater.

Very few studies have been accomplished in Mali to estimate the recharge and even less in the southern part. Although there is no significant study in the south of Mali including the Klela basin for recharge estimation, Henry (2011) had investigated on different methods to estimate the recharge. Particularly, his study was focused on numerical modeling HELP (Hydrologic Evaluation of Landfill Performance Code). The result from this model shows that groundwater recharge is about 12.6% of the annual rainfall.

Due to the limitation of data availability and the ease to use, only three methods were selected, in this study, among others common used in arid and semi-arid areas. These methods are chloride mass balance method CMB, water table fluctuation WTF and EARTH model. The aim of selecting these methods was to tempt to obtain a reliable recharge value in the study area as recommended by many authors to use multiple techniques in recharge estimation.

Table 0.1 Review of commonly used recharge methods for (semi)-arid Southern Africa, SW. surface water; HS. Hydrograph separation; CWB. Channel water budget; WM. Watershed modeling; UFM. Unsaturated flow modeling; ZFP. Zero flux plane; CMB. Chloride mass balance; CRD. Cumulative rainfall departure; EARTH. Extended model for aquifer recharge and soil moisture storage through the unsaturated hard rock; WTF. Water table fluctuation; GM. Groundwater modeling; SVF. Saturated volume fluctuation; EV-SF. Equal volume-spring flow; GD. Groundwater dating (Xu and Beekman, 2003)

Zone	Method	Limitations	Applicability[1]			Rating[2]		
			Flux (mm/a)	Area (km²)	Time (yrs)	Accuracy	Ease	Cost
SW	HS	Ephemeral rivers	400-4000 (0.1-1000)	10^{-4}-1300 (10-1000)	0.3-50 (1-100)	2-3	1-2	1-2
	CWB	Inaccurate flow measurement	100-5000	10^{-3}-10	1d-1yr	2-3	2	3
	WM	Ephemeral rivers	1-400	10^{-1}-5*10^5	1d-10yr	2	2-3	3
Unsaturated	Lysimeter	Surface runoff	1-500 (0-200)	0.1-30m²	0.1-6	2	3	3
	UFM	Poorly known relationship hydraulic conductivity moisture content	20-500	0.1-1m²	0.1-400	3	2	2
	ZFP	Subsurface heterogeneity; periods of high infiltration	30-500	0.1-1m²	0.1-6	3	2	2
	CMB	Long-term atmospheric deposition unknown	0.1-300 (0.6-300)	0.1-1m²	5-10^4	2	1	1
	Historical	Poorly known porosity; present ^{3}H levels almost undetectable	10-50 (10-80)	0.1-1m²	1.5-50	2-3	2-3	3
Saturated-Unsaturated	CRD	Deep (multi-layer) aquifer; sensitive to specific yield (Sy)	(0.1-1000)	(1-1000)	(0.1-20)	1-2	1-2	2
	EARTH	Poorly known Sy	1-80	(1-10m²)	(1-5)	1-2	2	1
	WTF	In/Outflow and Sy usually unknown	5-500	510^{-5}-10^{-3}	0.1-5	2	1	1
	CMB	Long-term atmospheric deposition unknown	0.1-500	210^{-6}-10^{-2}	5-10^4	2	1	1
Saturated	GM	Time-consuming; poorly known transmissivity; sensitive to boundary conditions	(0.1-1000)	(10^{-6}-10^6)	(1d-20yr)	1-2	3	3
	SVF	Flow-through region; multilayered aquifers	(0.1-1000)	(0.1-1000)	(0.1-20)	1-2	1-2	2
	EV-SF	Confined aquifer	(0.1-1000)	(1-100)	(1-100)	1-2	1-2	1-2
	GD	^{14}C, ^{3}H/^{3}He, CFC: poorly known porosity/correction for dead carbon contribution	^{14}C: 1-100 ^{3}H/^{3}He, CFC: 30-1000	^{14}C, ^{3}H/^{3}He, CFC: 210^6-10^{-3}	^{14}C:200-210^5 ^{3}H/^{3}He, CFC: 2-40	3	2-3	3

[1] data in brackets are those estimated in South Africa, the others have been given by Scanlon *et al.* (2002) and represent global values. Rainfall may be up to 2000 mm/yr.

[2] Ratings for methods applied to semi-arid Southern Africa. "Ease of application is related to data requirements and data availability and is rated from 1: easy to use to 3": difficult to use. Cost is rated from 1: inexpensive to 3: expensive Xu and Beekman (2003).

4.2.   Recharge estimation using Water table fluctuation method

In total, five piezometers are installed in the study area and are monitored by the DRH of Sikasso Region. All these monitoring wells are Casagrande piezometers drilled on sandstone aquifer, through which the probe allows measurement of the water level. Groundwater level data measurement has been performed manually at weekly time step. Due to lack of data, three piezometers (F7, F15 and F18) (see Figure 0.2) were selected to be used in this study. Unfortunately, the selected piezometers are the very close one to another, which will not permit to spatially interpolate the result through the entire basin.

As the water level is critical in estimating recharge applying WTF method, then, the hydrograph extrapolated approach was used in this study to estimate groundwater level rise (ΔH).

The water level for all piezometers starts rising during the period of the rainy season (Figure 0.1). This implies that the recharge in the study area is mostly due to the precipitation. However, the highest monthly rainfall occurred in August for both years 2013 and 2014 in the study area, while the highest water level is measured in September and October (Figure 0.2). Therefore, there is some lag between the first precipitations and water level rise, which is normal in reality, because when the first rain falls, the soil was dry and needs to be wetted before water continues to reach the groundwater table. Another cause may be due to the frequency of rainy days; before July there are many days without rain, while after this month, the number of rainy days is high (Figure 0.1). For that reasons above, the water level takes a while before rising at the beginning of the rainy season (generally from May). Except in 2013, where the highest daily rainfall was measured in April, and that for F15 and F18 the water level started rising in May. This early rising of water level for F15 and F18 may be explained by their proximity to the streamflow (see Figure 0.2 in chapter 0). Furthermore, large-scale groundwater flow may also influence local-scale groundwater dynamic. As this early water level rise occurs only in 2013, it can be concluded that groundwater recharge is chiefly depending on local rainwater.

Even though the mean annual rainfall (1,341.6 mm) in 2014 is greater than the mean annual rainfall (1,262.7 mm) in 2013, the seasonal water level fluctuation slightly

decreases for all the piezometers (Figure 0.1); this is probably due to the increase in water extraction by population. The estimated annual water level rises from 3,400 mm to 4,200 mm in 2013 and that in 2014 range from 3,600 mm to 5,700 mm (Table 0.2). The highest water level is recorded at piezometer F18, while the lowest is recorded at F7 for both years (Figure 0.1a, Figure 0.1c). The overall average of water level rise is 3,900 mm and coefficient of deviation is 0.11 in 2013 and 4,933 mm and 0.23 for those in 2014.

As indicated in equation 3.1, the groundwater recharge was estimated in this study for each piezometer by multiplying the water level rise by specific yield. The estimated mean annual recharge ranged from 120.7 mm to 149.1 mm, representing 9.6 to 11.8% of annual mean rainfall, in 2013; whereas in 2014, the calculated annual mean recharge ranged from 127.8 mm to 195.3 mm, or 9.5 to 14.6% of annual mean rainfall (Table 0.2). The highest annual mean recharge, 202.4 mm or 15.1% of the mean annual rainfall in 2013, is recorded in the piezometer F18 and the lowest annual mean recharge, 120.7 mm or 9.6% of annual mean rainfall in 2014, is recorded in the piezometer F7. The overall annual mean recharge is calculated using the arithmetic mean to be 156.8 mm, representing 12% of the overall annual mean rainfall. As the study was performed in the consolidated sandstone aquifer of which the material has low porosity, the specific yield was chosen from 0.011 – 0.06.
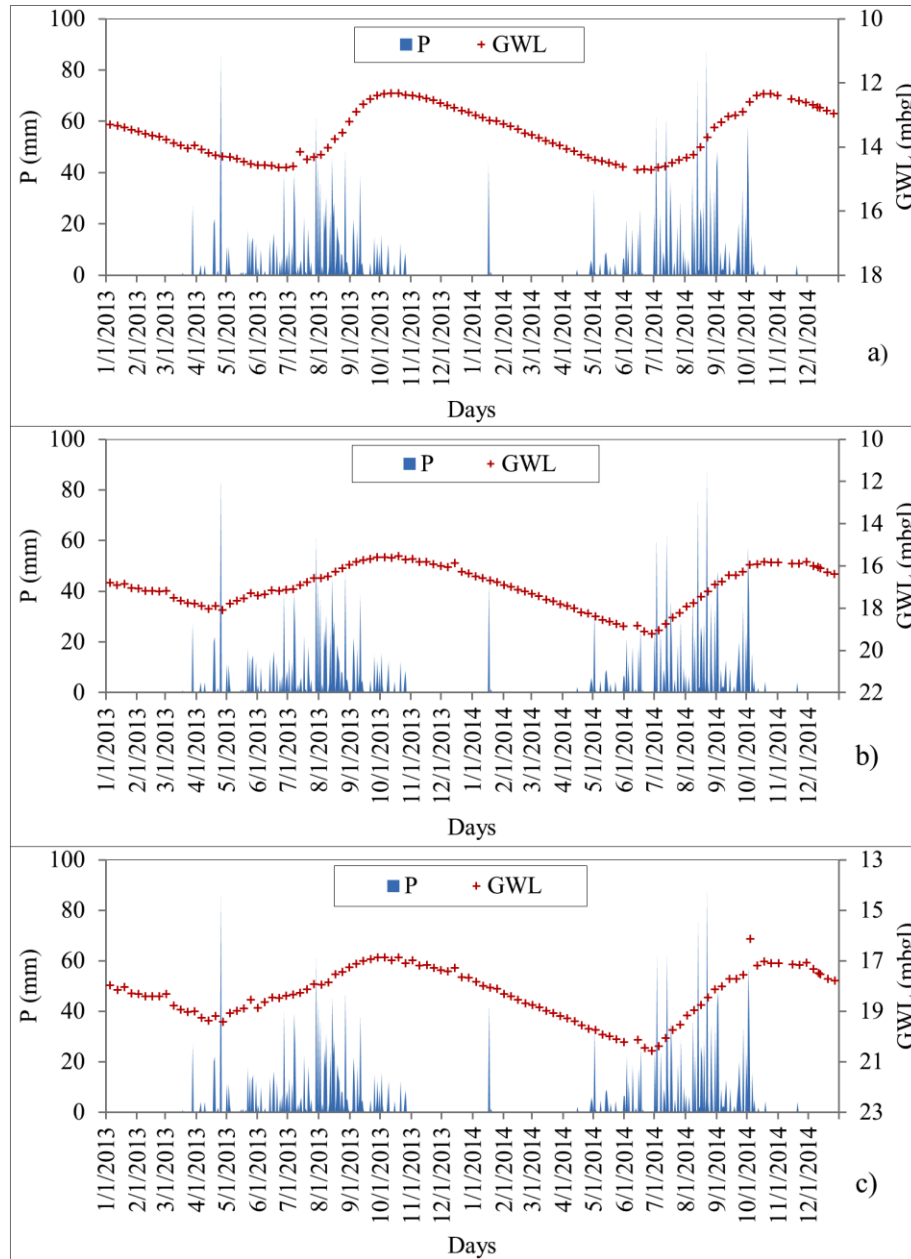
Figure 0.1 Groundwater hydrograph in meters below ground level and daily rainfall at Sikasso in the Klela Basin, (a) Piezometer F7; (b) Piezometer F15; and (c) Piezometer F18

Compared to other study results applied WTF method through the world particularly in West Africa, the results of this study seem to be reliable. As an example, Krautstrunk (2012) has used WTF method in his study in the Cambrian-Precambrian

fractured sandstone aquifer, in Northern Region in Ghana to estimate the recharge and found a range of 1-13% of mean annual rainfall. In the same region, Lutz *et al,* (2014) obtained a range larger of recharge, from about 1-20% of mean annual rainfall, but he used large values of specific yield (0.00-0.30). In the same manner, Jassas and Merkel (2014) used WTF technique in the sandstone aquifer in the semi-arid Al-Khazir Gomal basin, north Iraq, and acquired 17% of average annual rainfall, as mean annual recharge.
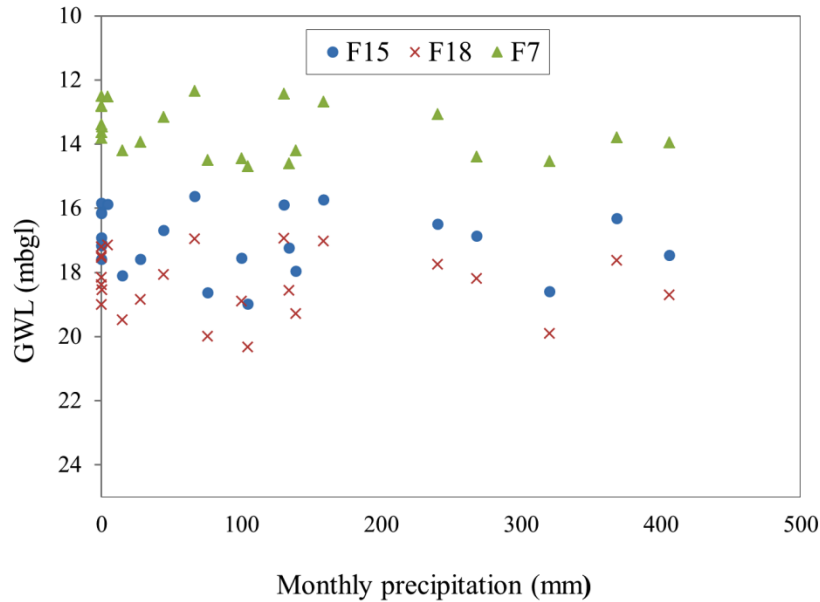
Figure 0.2 Monthly precipitation and groundwater table in meters below ground level for the three piezometers in the Klela basin from 2013-2014 (data source from DNM and DNH respectively)

Table 0.2 Estimation of annual recharge values using WTF method in the Klela basin, in 2013 and 2014; P annual precipitation (mm), ΔH water level rise (mm), R recharge in mm and percentage of P, Sy specific yield

Pezo meter	Aquifer	Year	P (mm)	ΔH (mm)	R (mm)		R (%P)	
					$S_y=0.011$	$S_y=0.06$	$S_y=0.011$	$S_y=0.06$
F7	Sandstone	2013	1262.7	3400	37.4	204.0	3.0	16.2
		2014	1341.6	3600	39.6	216.0	3.0	16.1
F15	Sandstone	2013	1262.7	4100	45.1	246.0	3.6	19.5
		2014	1341.6	5700	62.7	342.0	4.7	25.5
F18	Sandstone	2013	1262.7	4200	46.2	252.0	3.7	20.0
		2014	1341.6	5500	60.5	330.0	4.5	24.6

4.3.   Recharge estimation using Chloride mass balance method

The chloride mass balance method is fundamentally based on chloride data from the precipitation and groundwater table and/or vadose zone soil moisture. As stated in Sumioka and Bauer (2004), it is very important to use long-term data for chloride mass balance method. The same author argued that chloride concentration from groundwater can be considered as long-term average, due to the mixing and multi-year residence times of water in most aquifers. In this study, there was no data available in chloride concentration from precipitation in terms of long-term average; in contrast, the long-term average including 2014 of rainfall exists and was used.

Chloride concentration in the rainwater was ranged from 0.9 to 5.0 mg/l with a mean value of 3.3 mg/l. The minimum value of chloride concentration in rainfall is observed in two sites Gongasso and Deh, while the maximum is in Finkolo (Figure 0.3 (left)). In general, the chloride concentration in rainwater was considered higher compared to those found in the study performed by Obuobie (2008) in the Upper East Region of Ghana where the concentration ranged from 0.2 to 2.1 mg/l, after excluding the value (6.8 mg/l) assumed outlier. In contrast, in Diouf *et al.* (2012), a study performed at Dakar, the capital of Senegal, the chloride concentration in rainfall varies from 4.9 to 20.6 mg/l, which are by far higher than those obtained in this current study. Figure 0.3 (left) shows a correlation between rainfall and chloride concentration, *i.e.,* when chloride concentration increases, the mean annual rainfall increases too; the same remark has been observed in the study conducted by Edmunds (2010).

Chloride concentration measured in groundwater from eight samples used in this study ranged from 3.9 to 150.7 mg/l with a mean value of 29.4 mg/l. The higher value was located at Longrola (Figure 0.3(right)), which is by far greater than the mean value. This high value could be due to the anthropogenic effect because the well in which the water sample has been withdrawn was near a house, and was not properly equipped. Except for this high value, the chloride concentration decreases with reducing of rainfall amount in most of the locations (Figure 0.3). These analysis results seem to be reliable compared to others in Africa. For example, in his study in Zimbabwe, Sibanda *et al.*

(2009) have found the chloride concentration in the sandstone aquifer ranging from 2.5 to 76.5 mg/l.
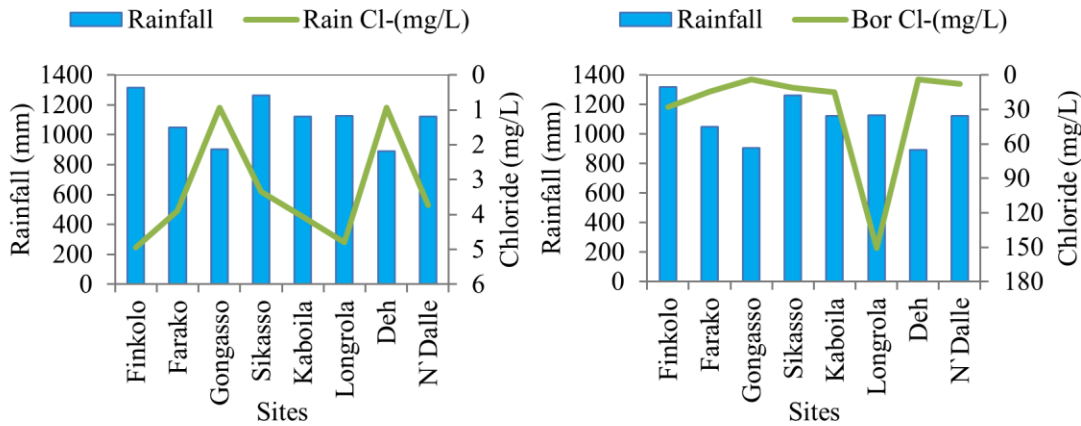
Figure 0.3 Chloride concentration (mg/l) in rainwater and annual rainfall bar graph (mm) (left), and chloride concentration (mg/l) in groundwater and annual rainfall bar graph (mm) (right)

The recharge was estimated based on chloride concentration measured in the laboratory from both sources (rainwater and groundwater). The values of recharge were estimated using the long-term average annual rainfall (approximatively 1,068.6 mm/yr) for all the sites in the study area, and the individual value of chloride concentration for each site. The estimated annual recharge varies from 34 to 513.7 mm (with 3.0 to 45.7% of mean annual rainfall) (Table 0.3). Compared these results from the other two methods (WTF and EARTH), those two extreme values (34 to 513.7 mm) were supposed to be under- and overestimated, respectively. Particularly, the maximum value, which is localized in the south of the basin at N'Dalle, represents almost half of mean rainfall. In reality, this is very difficult to demonstrate, especially in the area where the overlying formation is dominated by the facies sandy loam, clay and silt (see Figure 0.16 in chapter 0), and aquifer bedrock belongs to consolidated sandstone. Therefore, the value 513.7 mm of annual recharge was considered as an outlier and was excluded. Excluding the outlier, the recharge was ranged from 3.0-29% (with a mean of 21.7%) of overall mean annual rainfall. The correlation between rainfall and the estimated recharge is low (Figure 0.4). These results of recharge seem to be reasonable compared to other studies in semi-

arid regions in Africa (Table 0.4). The results applying this technique would be improved when long-term data of chloride concentration was used instead of two average months.
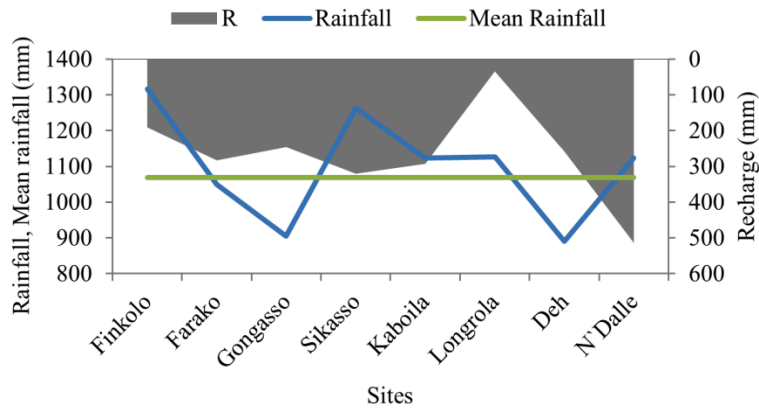
Figure 0.4 Mean annual rainfall and groundwater recharge (mm) calculated with CMB method for 2014

Table 0.3 Mean chloride concentration in rainfall and groundwater and recharge estimated in the Klela basin, in 2014

Sites	Cl⁻ in Rainfall (mg/l)	Cl⁻ in GW (mg/l)	Recharge (mm/yr)	Recharge (%)
Finkolo	4.9	27.8	190.5	14.5
Farako	3.9	14.7	282.9	26.9
Gongasso	0.9	4.1	245.7	27.1
Sikasso	3.3	11.1	320.2	25.3
Kaboila	4.1	14.8	292.4	26.0
Longrola	4.8	150.7	34.0	3.0
Deh	0.9	3.9	257.8	29.0
N'Dalle	3.7	7.8	513.7	45.7*

*considered as outlier in this study

Table 0.4 Estimated groundwater recharge value (minimum and maximum) with CMB method from previous studies in semi-arid regions, Africa

Location	Climate	Estimated recharge		Reference
		mm/a	Rainfall (%)	
Upper East Region/Ghana	Semi-arid	22.0-182.8	2.2-18.5	Obuobie (2008)
South Africa	Semi-arid		1.0-25.0	Bredenkamp and Xu (2003)
Springbok Flats/South Africa	Semi-arid	5.5-99	1.0-17.3	Bredenkamp *et al.* (1995)
Nyamandhlovu/Zimbabwe	Semi-arid	19-62		Sibanda *et al.* (2009)
Ghana	Semi-arid	30-61	3.0-6.2	Martin (2005)
Zimbabwe	Semi-arid	62-117	4.0-25.0	Nyagwambo (2006)

The interpolated map, using kriging method, shows a spatial distribution of groundwater recharge over the study area. This reveals a decreasing trend of recharge from south to north with the lowest value in the center at Longrola not far from the Sikasso town (Figure 0.5).
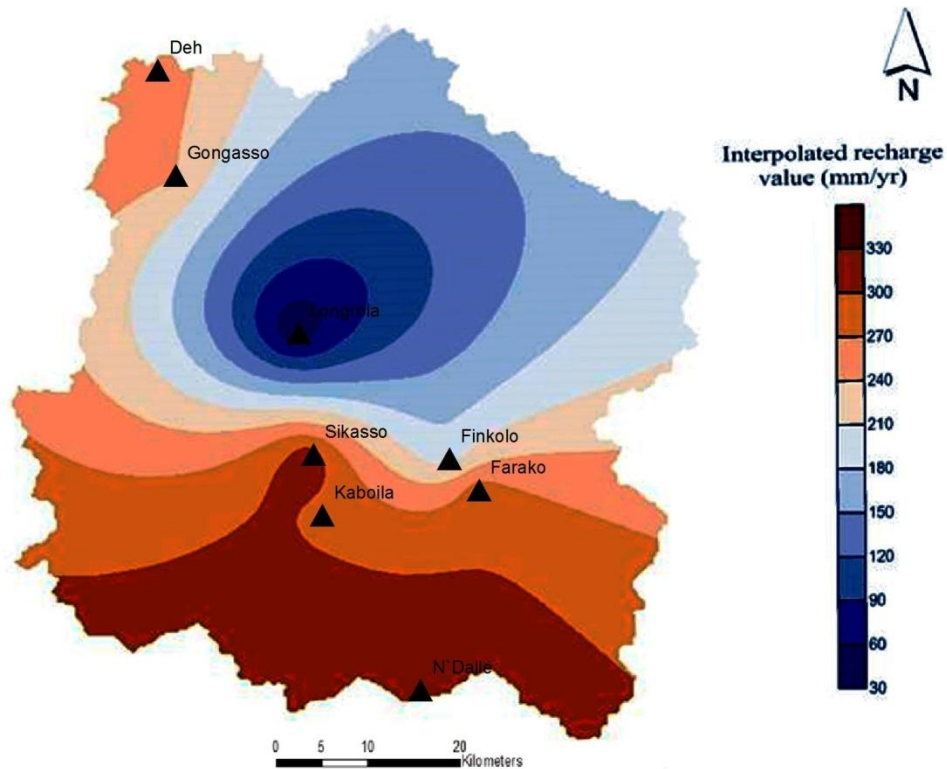
Figure 0.5 Mean annual recharge interpolated with CMB method

4.4.   Recharge estimation using EARTH model

The model was able to simulate groundwater level from the beginning to the end of the simulation period (Figure 0.6 - Figure 0.8). After calibration, the model results provide some outputs. The parameters set to the model for calibration can be seen in Table 0.5. The main outputs provided by EARTH model are actual evapotranspiration and daily groundwater recharge, which are represented graphically in Figure 0.6 - Figure 0.8, and other outputs are quantitatively represented in Table 0.5.

The relationship between groundwater level fluctuation and rainfall has been well discussed in the section WTF method. In all the piezometers, there is a lag between the beginning of rainfall and groundwater level rise. In general, groundwater level rise takes

two to three months late after the first rainfall during the rainy season. This may be explained by the increase of actual evapotranspiration during the rainy season (Figure 0.6 - Figure 0.8), which will evaporate most of the first amount of precipitation. The exception was made in 2013 for F15 and F18 where groundwater level rise immediately after the first rainfalls; because of this anomaly, the model was not able to simulate reasonably these parts (Figure 0.7 - Figure 0.8).

Furthermore, the daily actual evapotranspiration computed by the model ranged from 0.2 mm/day to 3.8 mm/day as minimum and maximum values for the piezometer F7 and F15, respectively. The variation between the mean annual actual evapotranspiration for the two simulation periods (2012-2013) was not significant and was found to be 1.5, 1.8 and 1.8 mm/day for F7, F18 and F15, respectively.

The results from EARTH model show that groundwater recharge starts occurring in July for all the three piezometers and reaches their maximum value in August/September. The daily recharge calculated from piezometer F7 extends over more months compared to the other two (Figure 0.6 - Figure 0.8). The maximum daily recharge occurs at F18 to be 5.4 mm/day in 2012. The temporal variation between the mean daily recharge is insignificant, which is about 0.5, 0.47 and 0.48 mm/day for F7, F15 and F18, respectively. Moreover, the maximum mean annual recharge was recorded at piezometer F7, which was 190.2 mm/a, or 14.9% of mean annual rainfall, in 2012; while the minimum was registered at F15 in 2013 and equal to 163.0 mm/a, or 12.9% of mean annual rainfall. The overall mean annual recharge was estimated to be 13.9% of the overall mean annual rainfall (Table 0.6).
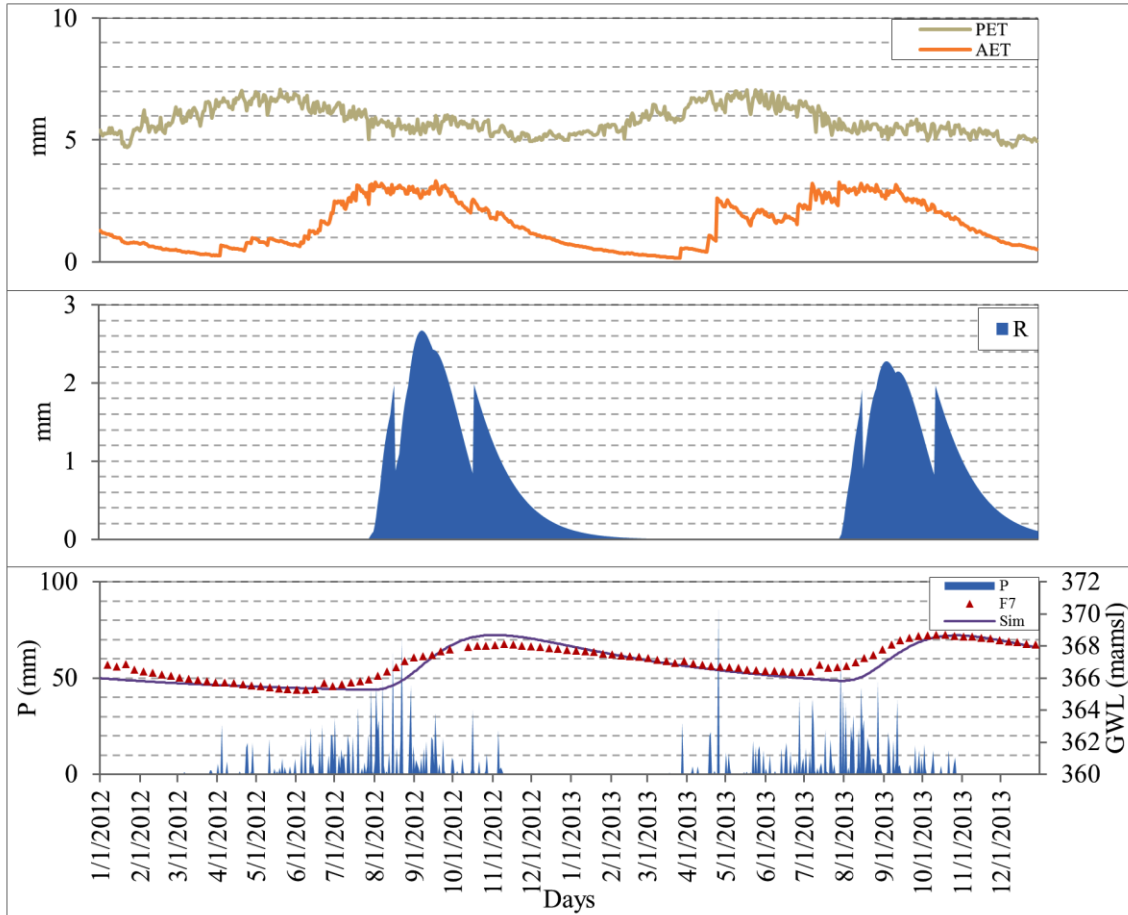
Figure 0.6 EARTH results for the piezometer F7, From top to bottom, potential and actual evapotranspiration (mm); recharge (mm); and precipitation (mm) and simulated and observed groundwater levels meter above mean sea level for the Klela basin, from 2012-2013
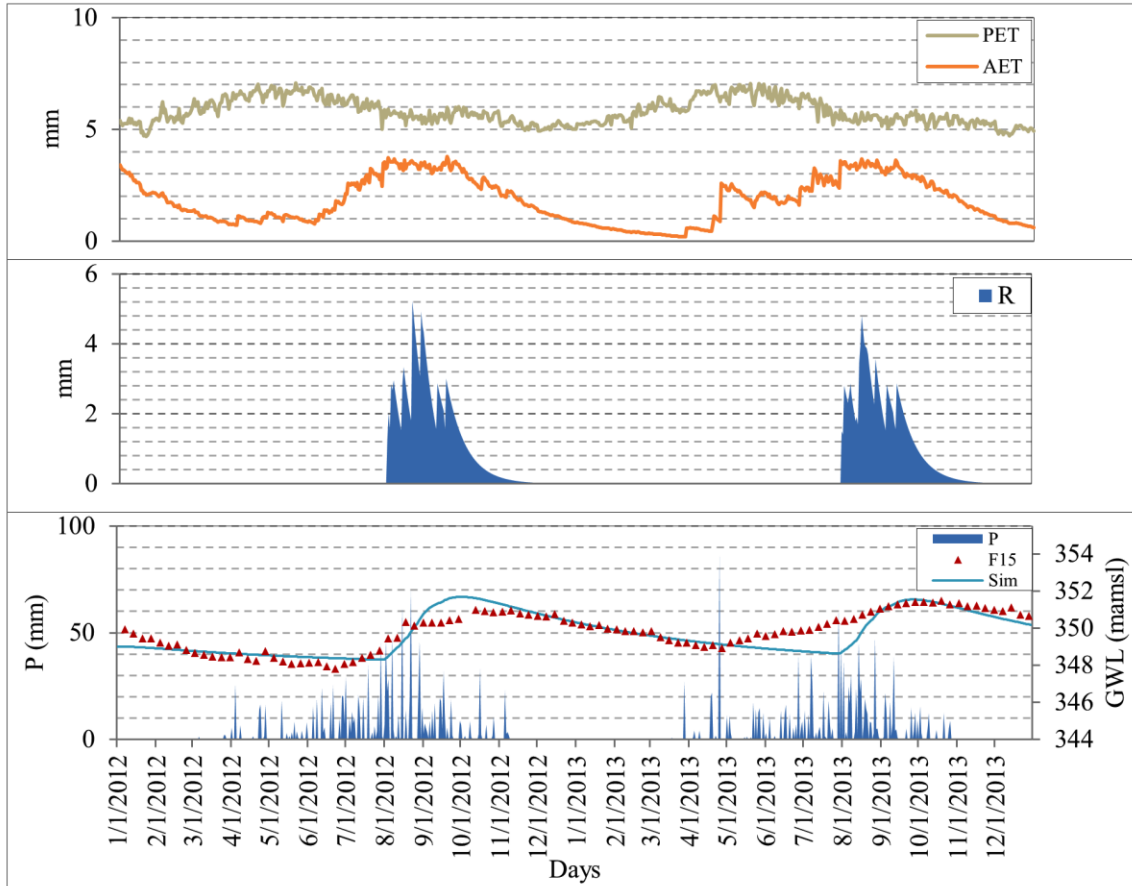
Figure 0.7 EARTH results for the piezometer F15, From top to bottom potential and actual evapotranspiration (mm); recharge (mm); and precipitation (mm) and simulated and observed groundwater levels meter above mean sea level for the Klela basin, from 2012-2013
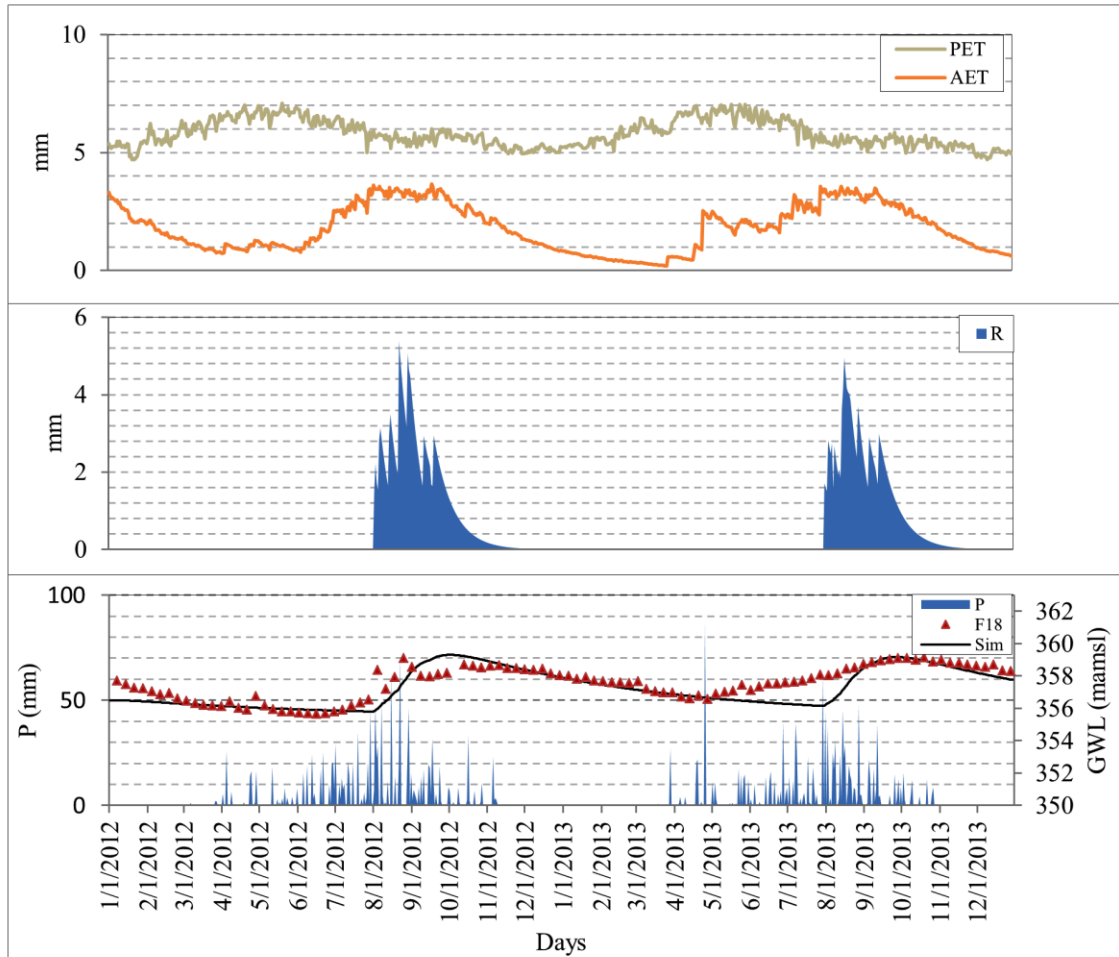
Figure 0.8 EARTH results for the piezometer F18, From top to bottom, potential and actual evapotranspiration (mm); recharge (mm); and precipitation (mm) and simulated and observed groundwater levels meter above mean sea level for the Klela basin, from 2012-2013

Furthermore, the qualitative and quantitative comparison was used to assess the calibrated output by comparing the simulated and observed hydraulic heads. Visual comparison between simulated and observed hydraulic heads in qualitative comparison (Nyende, 2013) and the quantitative model calibration was carried out using correlation coefficient (R^2), Root Mean Square Error (RMSE) and Nash-Sutcliffe coefficient (Nr). The correlation coefficient was used to evaluate the model performance.

Table 0.5 Parameters for the EARTH model simulation at representative piezometers, Sm. maximal soil moisture content (mm); Sr. residual soil moisture content (mm); Si. initial soil moisture content (mm); S_{fc} Soil moisture at field capacity (mm); S_{smax}. maximum surface storage (mm); MAXIL. maximum interception loss (mm); K_s. saturated hydraulic conductivity (mm/day); f. unsaturated recession constant (day); n. number of reservoirs; RC. saturated recession constant (day); S_{to}. storage coefficient; Lbl. the local base level

Piezometer	S_m	S_r	S_i	S_{fc}	S_{smax}	MAXIL	K_s	f	n	RC	S_{to}	Lbl
F7	320	30	100	190	0	3.2	3500	20	2	160	0.05	365
F15	300	1	200	190	0	3	3000	15	1	160	0.05	348
F18	310	1	200	190	0	3	3000	15	1	160	0.05	355.5

is between 0 and 1. The value of 0 means there is no correlation between observed and simulated data, whereas the value of 1 means the dispersion of the prediction matches that of the observation. The correlation coefficient is calculated as:

$$R^2 = \left(\frac{\sum_{i=1}^{n}\left(h_{o_i} - \overline{h_o}\right)\left(h_{s_i} - \overline{h_s}\right)}{\sqrt{\sum_{i=1}^{n}\left(h_{o_i} - \overline{h_o}\right)^2} \sqrt{\sum_{i=1}^{n}\left(h_{s_i} - \overline{h_s}\right)^2}} \right)^2 \tag{4.1}$$

where h_o is observed head, $\overline{h_o}$ is mean observed head, h_s is simulated head and $\overline{h_s}$ is

mean simulated head

RMSE and N_r were also used to evaluate the quantitative model calibration. When the value of RMSE is close to 0, the difference between simulated and observed groundwater level is low. RMSE is calculated as follows:

$$RMSE = \sqrt{\frac{1}{n}\sum_{i=1}^{n}\left(h_o - h_s\right)_i^2} \tag{4.2}$$

In contrast, when the value of Nr is greater than 0.5, the dynamic of the observed groundwater level is considered as well simulated. Nr proposed by Nash and Sutcliffe (1970) is calculated using:

$$N_r = 1 - \frac{\sum_{i=1}^{n}\left(h_{o_i} - h_{s_i}\right)^2}{\sum_{i=1}^{n}\left(h_{o_i} - \overline{h_{o_i}}\right)^2} \tag{4.3}$$

The results of the third model performance evaluation used in this study are mentioned in Table 0.7 and have shown relatively a good correlation between simulated and observed groundwater level, particularly for piezometer F7 where the value of correlation coefficient was about 0.94. All the values of N_r are greater than 0.6 which also show a good simulation of the model.

Table 0.6 Water balance results for the three piezometers calculated with EARTH model (2012-2013), P. precipitation (mm); Pe. Precipitation excess (mm); PET. potential evapotranspiration (mm); AET. actual evapotranspiration (mm); R. recharge (mm); R (%) percentage of rainfall

Piezo meters	Simulation period	P (mm)	P_e (mm)	PET (mm)	AET (mm)	R (mm)	R (%)
F7	2012	1273.4	789.7	2133.3	552.5	190.2	14.9
	2013	1262.7	789.5	2104.6	560.0	173.1	13.7
F15	2012	1273.4	812.7	2133.3	723.4	179.7	14.1
	2013	1262.7	811.4	2104.6	614.4	163.0	12.9
F18	2012	1273.4	812.7	2133.3	712.6	184.8	14.5
	2013	1262.7	811.4	2104.6	607.0	167.7	13.3

Table 0.7 Summary of EARTH model performance evaluation (R^2: correlation coefficient; RMSE: Root mean square error; Nr: Nash-Sutcliffe coefficient)

Piezometer	R^2	RMSE	N_r
F7	0.937	0.182	0.763
F15	0.859	0.217	0.678
F18	0.843	0.182	0.763

Compared these results of EARTH model to others carried out throughout the world, one can say that they are reasonably acceptable. For example, Usher *et al.* (2005) used the EARTH model in their study in South Africa (Kalkveldarea) in the fractured sandstone aquifer and obtained the recharge rate to 7.4% of mean annual precipitation. In the same manner, Baalousha (2003) applied the same model in Palestine in the calcareous sandstone and sand aquifers to get 36.95% of mean annual rainfall. Other studies were carried out in various aquifer types different from sandstone applying EARTH model which can be seen in Table 0.8.

Table 0.8 Summary of the recharge results for different aquifers using EARTH model

Country	Climate	Aquifers	P (mm/a)	R (%)	Reference
China (Nanjing)		glacial outwash sand and gravel of Quaternary age	1050	29.2-37.7	Lu *et al.* (2011)
China (Wuhan)	Semi-arid	Unsaturated sand	965.6-1463.8	7.2-26.5	Wang *et al.* (2015)
Ethiopia (Lake Beseka)	Semi-arid	Volcanic rock	948.8	8.5-8.9	Belay (2009)
Eastern Uganda (Pallisa District)	Semi-arid	Fractured gneiss and granitic formations	1250	11.4	Nyende (2013)

Sensitivity analysis

Model sensitivity analysis is the best way to assess the relative sensitivity of the model output regarding the changing of model input parameters. It allows quantifying the uncertainty in the estimates of soil and aquifers parameters in groundwater recharge and modeling calibrations. "Sensitivity analyses are also beneficial in determining the direction of future data collection activities. Data for which the model is relatively sensitive would require future characterization, as opposed to data for which the model is relatively less sensitive" (Mandle 2002). In this study, the sensitivity analysis was used to know the most sensitive parameters among other eleven used to calibrate the EARTH model. For that, a normalized sensitivity index was used to calculate for each parameter by the following equation (Belay 2009):

$$S_i = \frac{P_{10} - M_{10}}{B} \tag{4.4}$$

where P_{10} is 10% increased of variables from the simulation output, M_{10} is 10% decreased of variables from the simulation output, and B is the result of the baseline simulation.

By applying equation 3.21, each parameter was increased and decreased by 10 %, in order to calculate the sensitive index (S_i).

The results from this formula can be found in Table 0.9.

Table 0.9. Sensitivity analysis for three location piezometers (F7, F15 and F18) (the degree of sensitivity is defined as (Belay 2009): if S<0.05-low, 0.05<S<0.2-medium, 0.2<S<1-high, and S>1 very high sensitivity). S_i is the sensitivity analysis index.

Parameters	F7		F15		F18	
	S_i	Sensitivity	Si	Sensitivity	Si	Sensitivity
maximal soil moisture content	0.35	High	0.35	High	0.35	High
residual soil moisture content	0.03	Low	0.00	Low	0.00	Low
initial soil moisture content	0.11	Medium	0.23	High	0.23	High
Soil moisture at field capacity	0.21	High	0.22	High	0.22	High
maximum surface storage	0.00	Low	0.00	Low	0.00	Low
maximum interception loss	0.00	Low	0.00	Low	0.00	Low
saturated hydraulic conductivity	3.85	Very High	3.50	Very High	3.40	Very High
unsaturated recession constant	0.02	Medium	0.02	Medium	0.02	Medium
saturated recession constant	0.18	Medium	0.19	Medium	0.18	Medium
Storage coefficient	0.00	Low	0.00	Low	0.00	Low

The overall result of sensitivity analysis reveals that the model is sensitive to maximal soil moisture content, soil moisture at field capacity and hydraulic conductivity for all the three piezometers, but the hydraulic conductivity is the most important sensitive parameter. The initial soil moisture content is also sensitive for F15 and F18. By changing the value of one of these sensitive parameters above, lead to increase or decrease significantly the value of recharge in the Klela basin.

4.5.   Conclusions

Although the findings of the various studies argued that groundwater recharge is poorly investigated, three recharge methods were applied in this present study to attempt quantifying groundwater recharge. The overall results show that the recharge is mainly depending on the local precipitation. Groundwater level rise and specific yield, as well as chloride concentration, were keywords in estimating the recharge.

Rising of groundwater level starts in July, *i.e.,* two months after the first rainfall and decreases in October. The exception is done in 2013 for the piezometers F15 and F18 where the groundwater level rise begins just after the first rainfall. This supposes that other causes are rising groundwater level different from the local rainfall, but unknown. Furthermore, the specific yield is poorly known and pumping test data, allowing determining the specific yield, available in the study area is for short time (4-6 hours).

Despite these uncertainties on the field data, the water table fluctuation method, chloride mass balance technique and EARTH model were used to estimate the recharge. Applying WTF method, the recharge was ranged from 3-20% of the mean annual rainfall. In this method, the principal uncertainties are due to groundwater level rise, which is subjective, and specific yield. The recharge results from CMB technique were ranged from 3- 29% of mean annual rainfall. Because the long-term chloride deposit was not available, these results could be considered as overestimated on the one hand, and underestimated in the area where the chloride concentration is very high due to likely human activities, on the other hand. Finally, the EARTH model has estimated the recharge that ranged from 12-14% of average annual rainfall. Compared to the two previous methods, this method is more reliable, for the simple reason that it uses the calibration process to estimate the recharge and the difference between the minimum and maximum values are not high.

The fundamental difference between the three methods is that: WTF and EARTH are a physical based method and use groundwater level rise in saturated zone to estimate the recharge, while the CMB is tracer technique that uses chloride concentration in unsaturated zone to determine the recharge. The overall mean recharge for the three methods gives 13% of the mean annual rainfall in the study area.

This study suggests for the future studies to investigate more deeply on groundwater recharge estimation in the study area and try to understand other possible causes of groundwater level rise aside from the local precipitation. Another suggestion is the implementation of more piezometers throughout the basin scale in order to better monitor the groundwater level fluctuation

CHAPTER 5: GROUNDWATER MODELING

5.1. Introduction

Based on certain simplifying assumptions, groundwater models describe the groundwater flow and transport processes using mathematical equations (Torak, 1992; Cooley, 1992; Lin *et al.,* 2003; Kouli *et al.,* 2009). However, applying a model requires the understanding of the physical system and simplifying assumptions for the mathematical equations. Nowadays, groundwater modeling is becoming widely used in water supply throughout the world.

5.2. Steady-state calibration

Steady state simulations are used to model equilibrium conditions; in this stage, changes in groundwater storage are insignificant (Middlemis, 2001). Steady-state calibration is used in the area where data (*e.g.,* initial conditions, hydraulic conductivities) availability is insufficient because one of the objectives of steady-state simulation is to estimate the hydraulic conductivity of the study by matching observed against simulated heads. Application of steady-state calibration is easier and less time consuming compared to the unsteady condition, this is due to the fact that dynamic stresses and storage effects are excluded in this process (Middlemis, 2001). The parameters data include aquifer thickness, hydraulic conductivity, recharge and hydraulic heads were used to calibrate the model in steady-state conditions.

In this study, mean water table data collected by the DRH of Sikasso in 1985 and data measured in the field in 12 boreholes in 2014 were used to calibrate the steady-state simulation model. This calibration was first performed via a trial-and-error procedure. Then, the output was optimized using the PEST code integrated into PMWIN. During the calibration process, hydraulic conductivity values, that influence the quality of simulated heads, were modified to obtain an acceptable error between simulated and observed heads. As a result, the basin was arbitrarily divided into six hydraulic conductivity zones (Figure 0.1), as explained above.

The results show that hydraulic conductivity values range from 1.1 m/day to 13.9 m/day (Figure 0.1). The hydraulic conductivity values, in the northern part mostly constituted by sandstone basement (see Figure 0.9 in chapter 0), are greater than that in the other parts of the basin. This signifies that the northern parts are more permeable and that represent the lower parts of the basin. The western part of the basin where the significant quantity of dolerite formation occurs is the lesser permeable.

Approval of the model results is based on model qualitative and quantitative efficiency evaluation. The qualitative evaluation is based on visualization between observed and simulated groundwater level fluctuation curve whereas quantitative is founded on the difference calculation between observed and simulated hydraulic heads.
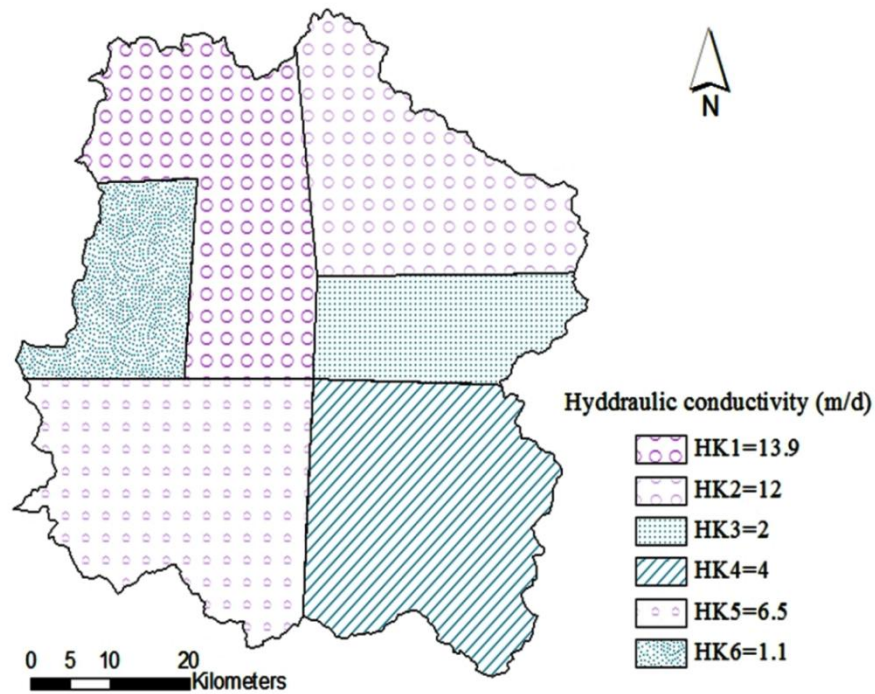
Figure 0.1 Hydraulic conductivity zones of the Klela basin in meters per day

Frequently, the methods used for quantitative are: Mean Absolute Error (MAE), Root Mean Square Error (RMSE), Nash-Sutcliffe Coefficient (E) and Correlation Coefficient (R^2). The model correlation coefficient is displayed in Figure 0.2. Except the beginning of the calibration, all other parts appear visually to be acceptable. The model was also quantitatively evaluated and the results are in Table 0.1.

Table 0.1 Model evaluation results, MAE. Mean absolute error; RMSE. Root mean square error; E. Nash-Sutcliffe efficient; R^2 correlation coefficient

MAE	RMSE	E	R^2
1.6368	5.6699	0.8580	0.9687
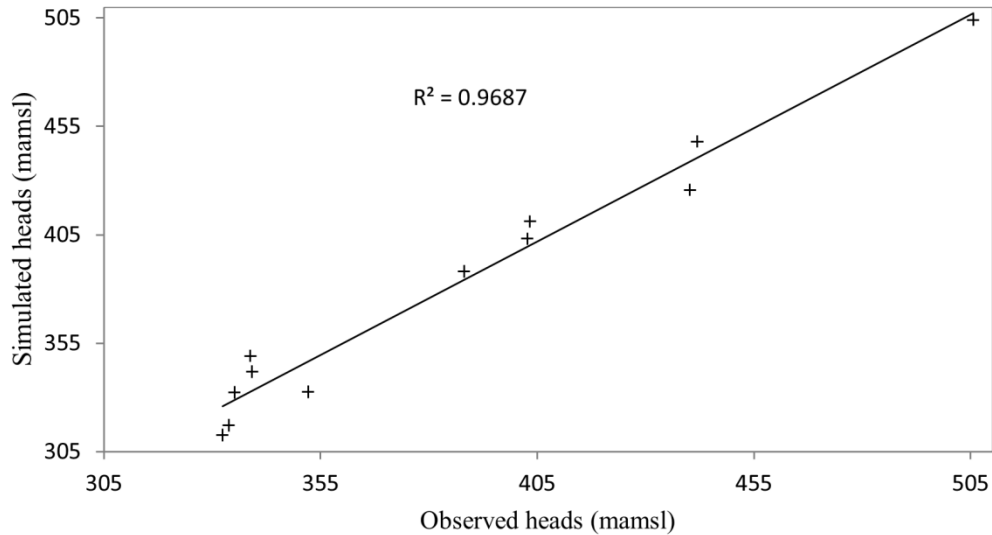
Figure 0.2 Comparison between observed and simulated groundwater levels (mamsl) in steady state calibration in the Klela basin

5.3.   Transient calibration

The transient condition is a system in which inputs and outputs are not in equilibrium. Transient simulations are used to model time-dependent problems, where significant volumes of water are exchanged between the aquifer and its surrounding surface water bodies. Usually, the results (initial head, boundary conditions, and parameters) from the steady-state simulations are used as initial conditions in transient calibration. Only the recharge (include that from precipitation and irrigation) and water extraction are changed over time during the transient simulation process. The unknown parameter is specific yield or storage coefficient, which is used to calibrate the model. Like steady state simulation, trial and error and PEST are commonly used in transient calibration.

In this study, only trial and error method was used in the transient simulation due to technical problems with PEST. The groundwater level of the steady-state simulation was used as the initial hydraulic head in the transient simulation. For the transient calculations, the streamflow-routing package was used to simulate the interaction between streams and groundwater. In the same manner, monthly sources (recharge) and sinks (wells) data were introduced to the model. Specific yield was set to 0.06 for the whole model domain.

The model was run for the period from November 2010 to November 2014 (48 months). Therefore, the simulation time was divided into 48 stress periods (with 32 dry and 16 wet), and each stress period represents one month. The length of a stress period was divided into days resulting in total time steps over 48 months and total simulation time of 1,460 days.

Mean monthly groundwater table data from three piezometers (F7, F15 and F18) was used to calibrate the model. In total, five piezometers are monitoring weekly in the study area, but only three were chosen for modeling purposes. This choice was based on the data quality and data length. Four model efficiency criteria (Table 0.2) were used to evaluate quantitatively the model accuracy. The model efficiency results reflect an acceptable model calibration. However, F7 is not as well simulated as in the others (Table 0.2). The model quality evaluation of the transient calibration is shown in Figure 0.3. The model was able to reproduce the observed groundwater levels for the three piezometers. However, the difference between observed and simulated groundwater levels is relatively higher for certain periods. For example, in October 2013 corresponding to 36th month in Figure 0.3, for piezometers F7 and F15, the difference between the two heads is close to 1 m. Although the model was able to simulate groundwater levels, it found some difficulty in April 2013 for the piezometers F15 and F18, where the observed groundwater level increases and the simulated groundwater level decreases. This was explained previously (in chapter 0, groundwater recharge estimation) by the possible existence of another source that causes the groundwater level rise. In most of the cases, the model tends to underestimate the groundwater level compared to observed measurements.

The spatial distribution of calculated heads for each time step shows a slight difference in values between simulated and observed. For example, Figure 0.4, the difference between the starting head of transient simulation and last simulated head period, exhibits in most of the contour heads, little difference between simulated and observed heads. This figure indicates that where the observed heads are greater than simulated heads, the residual is positive, otherwise, it is negative. Furthermore, the histogram in Figure 0.5 shows the frequency of residuals calculated from observed and simulated heads, and almost of the values fall down between the interval -1 and +1, which indicates an acceptable calibration. These values are obtained by abstracting observed and simulated heads of each month of the simulation period.

Table 0.2 Summary of calibration errors for transient simulation (MAE: Mean Absolute Error; RMSE: Root Mean Square Error; E: Nash-Sutcliffe coefficient and R^2: Correlation Coefficient)

	F7	F15	F18
MAE	0.0248	0.0091	0.0101
RMSE	0.1823	0.0670	0.0741
E	-0.4959	0.2141	-0.4439
R^2	0.7137	0.7889	0.8028
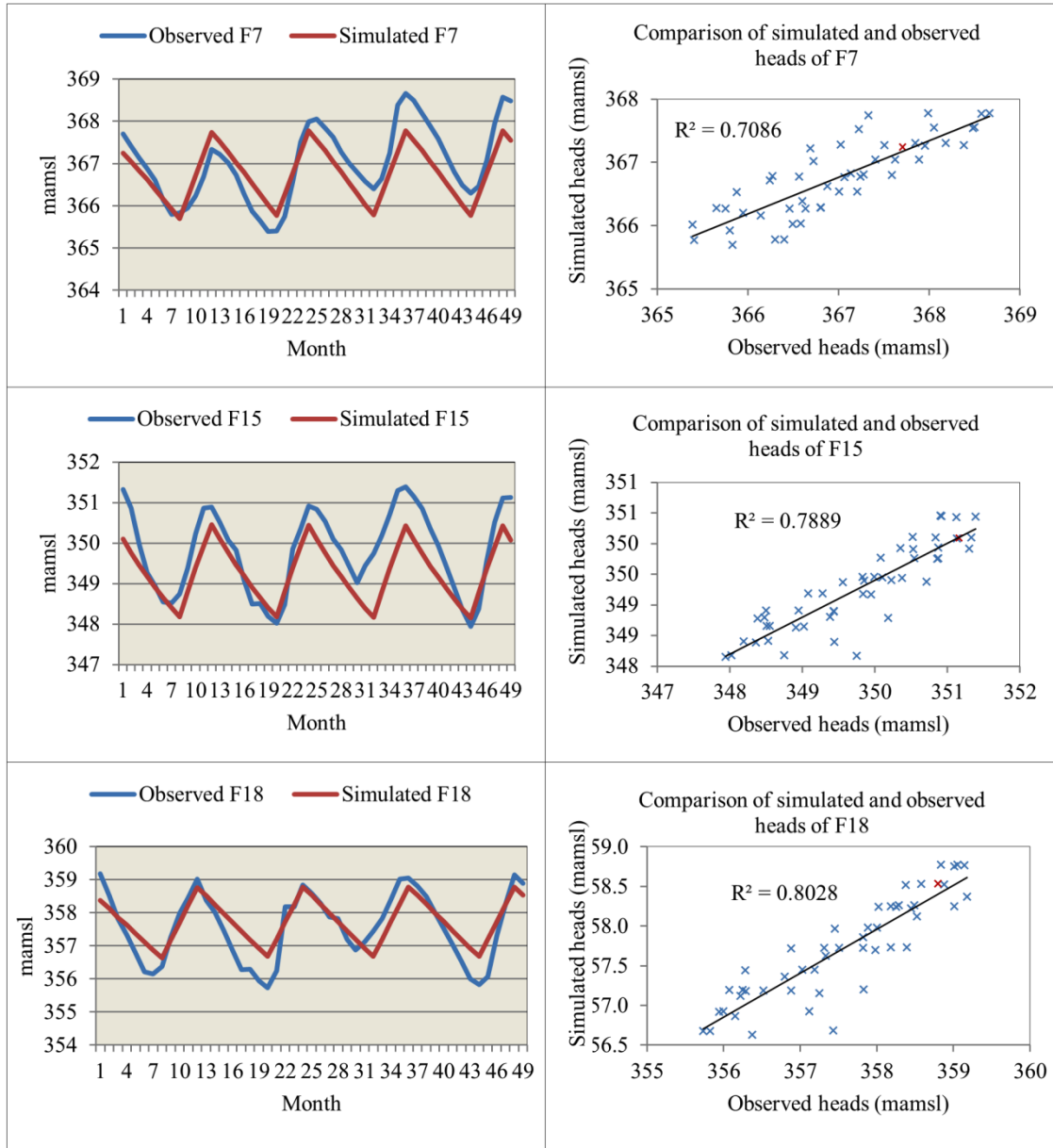
Figure 0.3 Simulated and observed hydraulic heads for the transient calibration in the Klela basin from November 2010-November 2014
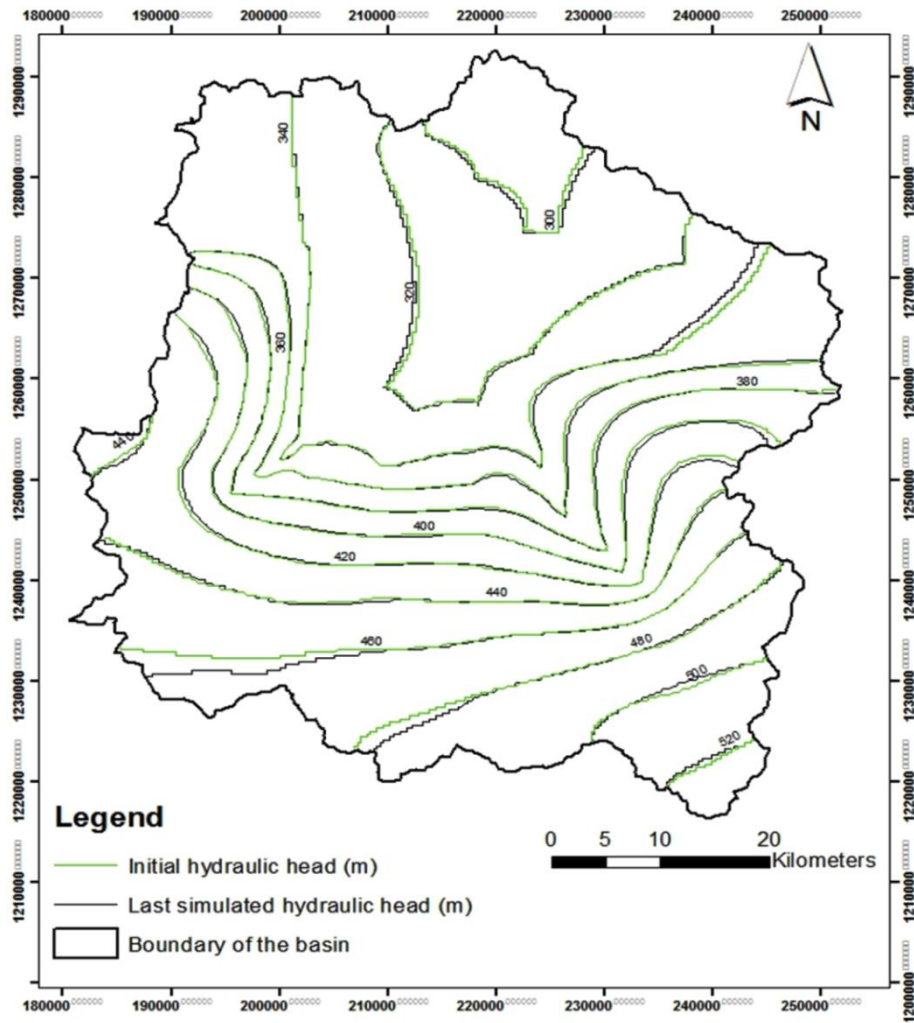
Figure 0.4 Difference between initial hydraulic heads, November 2010 (green contour) and the last simulated head period, November 2014 (blue contour), in meters above mean sea level
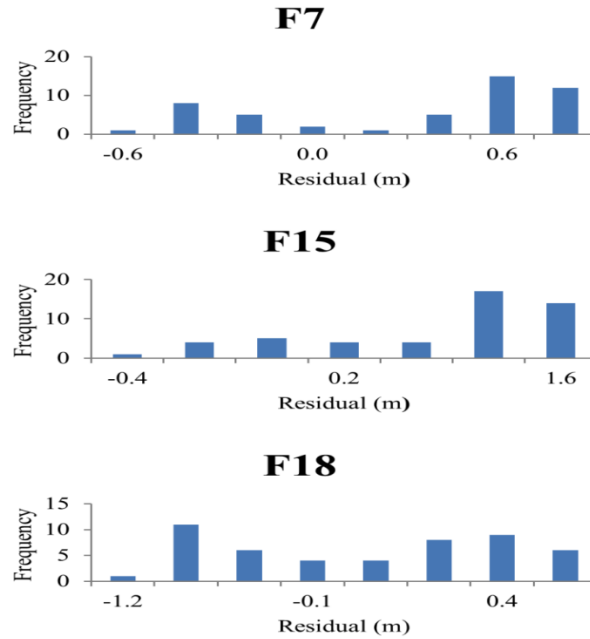
Figure 0.5 Histogram of residuals for each month between simulation and measurement of groundwater levels (m) for the three piezometers

5.4. Water budget

A water budget is a quantitative measurement of the balance between water inflow and outflow of a watershed during a specific period (Seneviratne, 2007). One of the best ways to assess model simulation efficiency is by analyzing the water budget. A water budget provides an indication on acceptability on a numerical model solution. However, a good water balance cannot guarantee a good simulation, a bad water balance indicates problems in the model (Jackson, 2007). In steady state simulation, the difference between total inflow and total outflow should be equal to zero, while it should be a total change in storage in a transient simulation. Although the water budget is used for calibration purpose, it also provides a measure of the relative importance of each component to the total budget (Konikow and Reilly, 1998). The percentage discrepancy that quickly checks the water budget acceptability should be equal to zero in both cases. In this study, the percentage discrepancy of all the stress periods for the model is nearly zero. Thus, the model equations have been correctly solved (Chiang and Kinzelbach, 1998). The average annual water budget is summarized in Table 0.3 and indicates that the

inflow to the streams of the Klela basin is principally due to groundwater seepage. The streams of the basin are gaining and losing water from the aquifer, but losing from the rivers is much lower and can be neglected. The small amount of water flowing from the streams to the aquifer may be explained by over abstraction from pumping wells.

Table 0.3 Mean annual water budget for groundwater in m^3/year in Klela basin from November 2010-November 2014

Flow	Inflow (m^3/year)	Outflow (m^3/year)
Storage	485,869,302	446,718,545
Recharge	635,293,979	0
Wells	0	57,287,607
Stream Leakage	947,401	618,122,906
Total	1,122,110,683	1,122,129,060

Because the boundary condition is a no-flow boundary, the only water source entering the aquifer is the recharge, which is estimated to be approximatively 635 Mm^3/a. Precipitation, the only source of recharge because recharge from irrigation is unknown, is estimated to approximatively 4,162 Mm^3/a (calculated with average value). The annual recharge is slightly greater than groundwater seepage (Table 0.3), *i.e.,* the amount of water that is entering the aquifer is almost the same as the amount exiting the aquifer and entering surrounding streams, which are the discharge points of the study area. According to the boundary condition, groundwater can leave the catchment only via the stream interaction. Inflow from the stream is calculated from the interaction of surface and groundwater throughout the river system. The mean annual water budget shows that groundwater storage slightly reducing by 39 Mm^3/a (approximatively 10.6 mm/a) (calculated from Table 0.3).

The seasonally recharge from July to October was constant and represented the important water inflow entering the aquifer. The stream leakage that is leaving the aquifer and entering streams decreases during the dry season and increases during the rainy season (Figure 0.6).
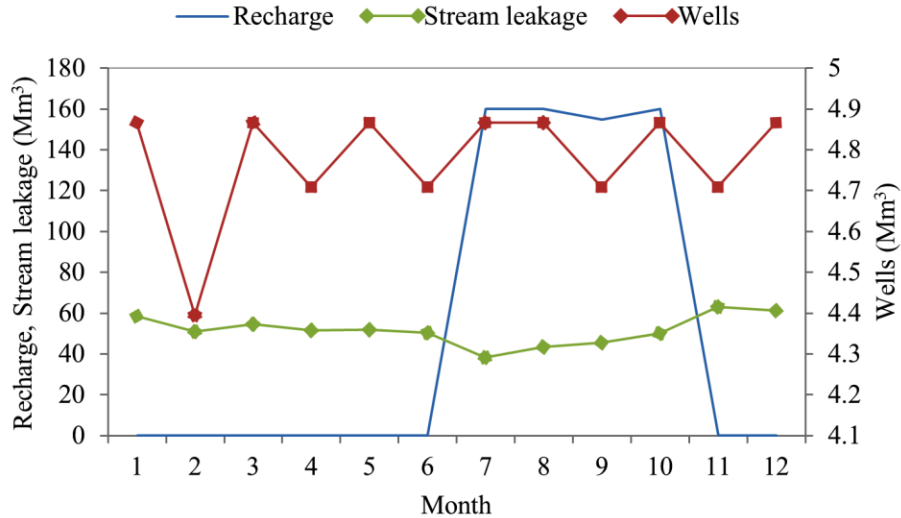
Figure 0.6. Monthly average water budget for the Klela Basin, Mm³/month

MODFLOW results, despite a lack of hydrogeological data, appear to be acceptable by referring to model performance evaluation results. The uncertainty occurs in all domains in groundwater modeling such as aquifer property values, even for a well-calibrated high complexity model, boundary conditions imposed on the finite of a model domain, recharge estimation, and water abstractions (Middlemis, 2001). One of the most important uncertainties in this modeling is in boundary conditions. In this study, the boundary conditions were set as a no-flow boundary. In reality, this is very difficult to prove. For example, Belay (2009) applied the PMWIN model to establish a water balance for Lake Beseka in Ethiopia and concluded that the choice of boundary conditions has a larger effect on the dynamics than does precipitation. Therefore, neglecting lateral outflow in groundwater modeling may considerably affect the water balance.

5.5. Conclusion

The dynamics of groundwater of the Klela basin has been modeled and the water budget was established. In this study, the mean annual recharge that is considered as the only groundwater inflows due to the assumption of a no-flow boundary condition was estimated to be 635.3 Mm^3/year, representing approximatively 13.9% of annual precipitation. The main surface water resources are from precipitation and groundwater seepage. The principal water exiting the aquifer to the surrounding streams is by leakage

and that is approximatively 618.1 Mm^3/year or 97% of annual groundwater recharge. Therefore, groundwater storage decreases about 10.6 mm/year due to the water extraction by population. Furthermore, the map of changed in groundwater storage shows a trend increase of groundwater storage during the rainy season and a trend reduction of groundwater storage during the dry period.

The calibrations of the model in steady state and transient simulations for groundwater system of the Klela basin showed that northern part is characterized by high hydraulic conductivity (varying from 1.1 m/day in the south to 13.6 m/day in the north), then, high permeability. The quantitative and qualitative model performance shows acceptable model results. The piezometric map of the basin indicates a decrease of hydraulic heads from the south to the north. This proves that northern part of the basin, towards Klela town, is a discharging point of the basin. This study concludes that MODFLOW, widely used in modeling groundwater resources, can be applied in the Klela basin to quantify groundwater resources and can support water resources management.

CHAPTER 6: CLIMATE CHANGE IMPACT ON GROUNDWATER RESOURCES

6.1. Introduction

Climate change effect on water resources is the central debate for all the IPCC assessment scenarios, but its impact on groundwater is not well known. Several General Circulation Models (GCMs) (known in other terms as global climate models) have been developed to evaluate the impact of climate change on water resources. There are three principal types of GCMs: atmospheric GCMs, ocean GCMs and a couple of both atmospheric-ocean general circulation models (AOGCMs). These coupled atmospheric-ocean global climate models are usually used for generating climate change projections and scenarios in response to change in greenhouse gas emissions (Mearns, *et al*., 2003; Vasiliades *et al.,* 2009). Different types of GCMs were used by many authors (Serrat-Capdevila *et al.,* 2007; Herrera-Pantoja and Hiscock, 2008; Hiscock *et al.,* 2008; Diallo *et al.,* 2012) in their study, in order to assess the impact of climate change on the hydrologic system (Kabir, 2010). However, the direct application of the GCMs in climate change impact studies is not appropriate due to their coarse and order of 300 km (Mearns, *et al.,* 2003) horizontal spatial resolution (Schmidli *et al.,* 2006). It is therefore difficult to use their outputs to regional or local scale study. In order to apply GCMs data to the local study, the coarse resolution should be enhanced to fine resolution. To solve the resolution issue, three categories of regionalization techniques has been developed to improve the regional information furnished by GCMs as mentioned in Mearns, *et al.* (2003). These techniques are: "(1) High resolution and variable resolution "time-slice" Atmosphere GCM (AGCM) experiments; (2) Nested limited area (or regional) climate models (RCMs); and (3) Empirical/statistical and statistical/dynamical methods". However, the third technique is a widely used may be due to their low computational demand (Wilby *et al.,* 2004).

All the GCMs are associated with some uncertainties (Tebaldi and Knutti, 2007; Giorgi *et al.,* 2008); then, Vasiliades *et al.* (2009) suggested assessing uncertainty by

using different GCMs and Monte Carlo experiments with one GCM beginning with different initial conditions. Because of uncertainty in downscaling techniques, there must be evaluated using different downscaling methods or by varying parameterizations of the downscaling models (Vasiliades *et al.,* 2009).

In this study, the climate (precipitation and temperature) change simulations data provided by ECHAM in the initiative of CORDEX project was directly used without any further regionalization processing. The detail in climate change data used can be found afterward.

6.2.   Recharge estimation with Thornthwaite model

The Thornthwaite model was used to estimate the recharge for RCP4.5 and RCP8.5 scenarios as explained above. The results show that in both scenarios groundwater recharge is decreasing and this is more important in RCP8.5 than in RCP4.5, and in the 2030s drought events are simulated to be severe especially from 2033 to 2037 (Figure 0.1). This can be explained by the fact that the mean annual precipitation for RCP8.5 (Figure 0.1b) is lower than that for RCP4.5 (Figure 0.1a). Furthermore, the precipitation increases with increase in recharge that indicates a good correlation between both. In general, the recharge is zero or close to zero when the total annual precipitation is less than the mean annual precipitation. These calculated recharges were used into the WEAP model as an input data.
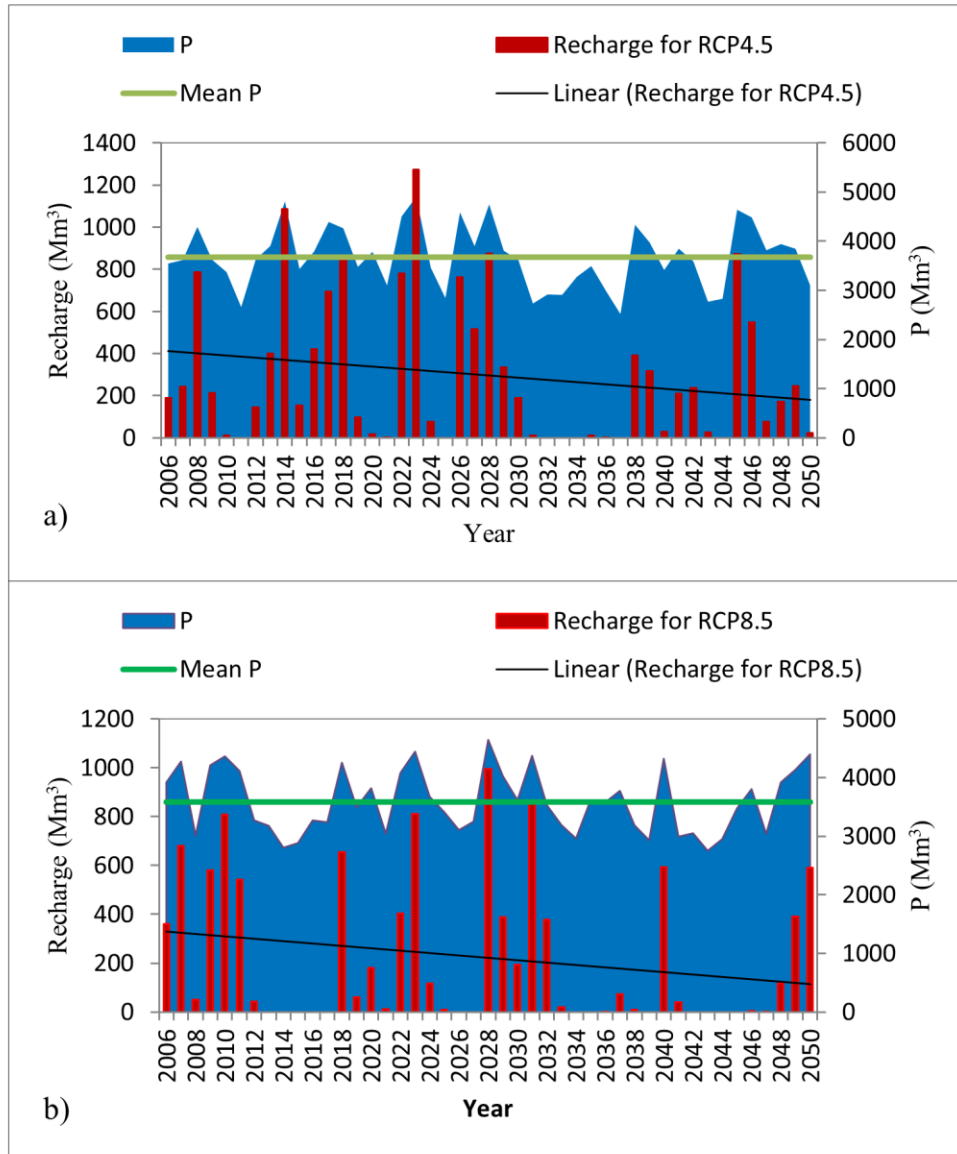
Figure 0.1 Estimated annual recharge (Mm^3) and annual precipitation (Mm^3) for scenarios (a) RCP4.5 and (b) RCP8.5 in the Klela basin from 2006-2050

6.3.   Water demand

The water demand for the Klela basin regarding different human activities was estimated to be about 75 million cubic meters for the current account year, 2013. From this current year, the reference, socio-economic and high population growth scenarios were developed in order to examine the water demand in the future for the inhabitants of the Klela basin.

Water demand was computed considering all scenarios cited above and all sectors of water use (irrigation, domestic, livestock, and industry), which started from the baseline year 2013 up to the end of the year 2050.

As explained in the scenario development, the scenarios were developed based on the growth of economics and population in the study area. In socio-economic scenarios, the irrigation and industry water demands were sufficiently increased, while the domestic water demand was intensified in high population growth scenario in order to cover the eventual future demand.

The annual water demand can be seen in Figure 0.2, where the demand increases considerably over time for all the scenarios. However, scenario E2 requires more water than others, and the annual demand achieves approximately 224 Mm^3 by 2050. The difference between the reference scenario, which is the lower annual water demand about 143 Mm^3, and the others for annual water demand starts to be significant from the beginning, in 2013, until 2050. Scenario E1 and the high population growth scenario are close to each other in terms of water demand because they represent the moderate water demand, but demand is higher in scenario E1 than that in high population growth scenario. The similarity between these two scenarios is due to the fact that they use the same climate data and the socio-economic in scenario E1 is near the high population growth scenario, but different from irrigation (higher in scenario E1) and population growth (higher in scenario population growth).
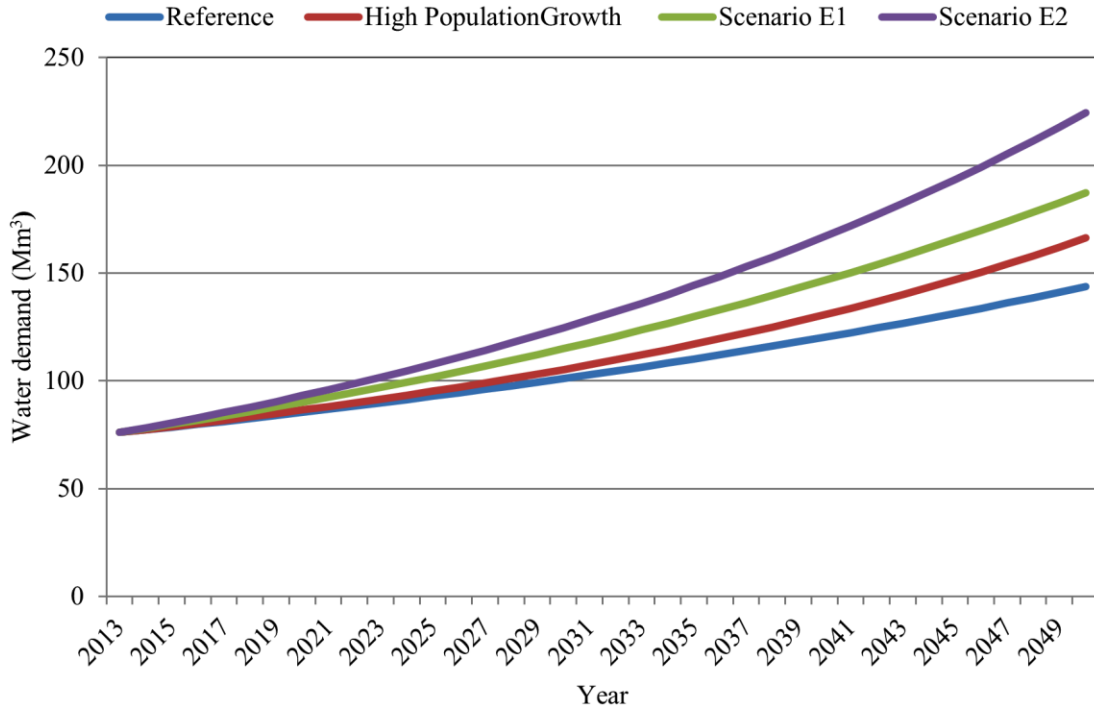
Figure 0.2 Annual water demand in million cubic meters for the scenarios reference, high population and socio-economic from 2013-2050

Furthermore, the model of WEAP was applied to calculate the water demand per sector as shown in Figure 0.3. Irrigation is the sector on which water use is much higher than that for domestic. The annual water demand for irrigation reaches 199 Mm^3 in 2050 in the worst scenario E2. This is normal in an area where most of the activities are agriculture. Water demand for livestock was set as constant over time for all the scenarios because development of industry in an area may reduce the activities of animal husbandry in this zone, which can be compensated by increased water demand due to industrial activities. Water demand for domestic activities are also important, however, it is more significant in urban than in rural areas. This may explain the rapid growth rate of urbanization in the study area. In the high population growth scenario, the domestic water use is more significant, particularly in the future due to the increase in the population growth rate in the study area. Presently, the industry is poorly developed in the study area, but it is expected to increase in the future due to the rapid increase of urbanization and agriculture. Therefore, the water use for the industry in scenario E2 was consequently increased in order to cover the demand in the future.
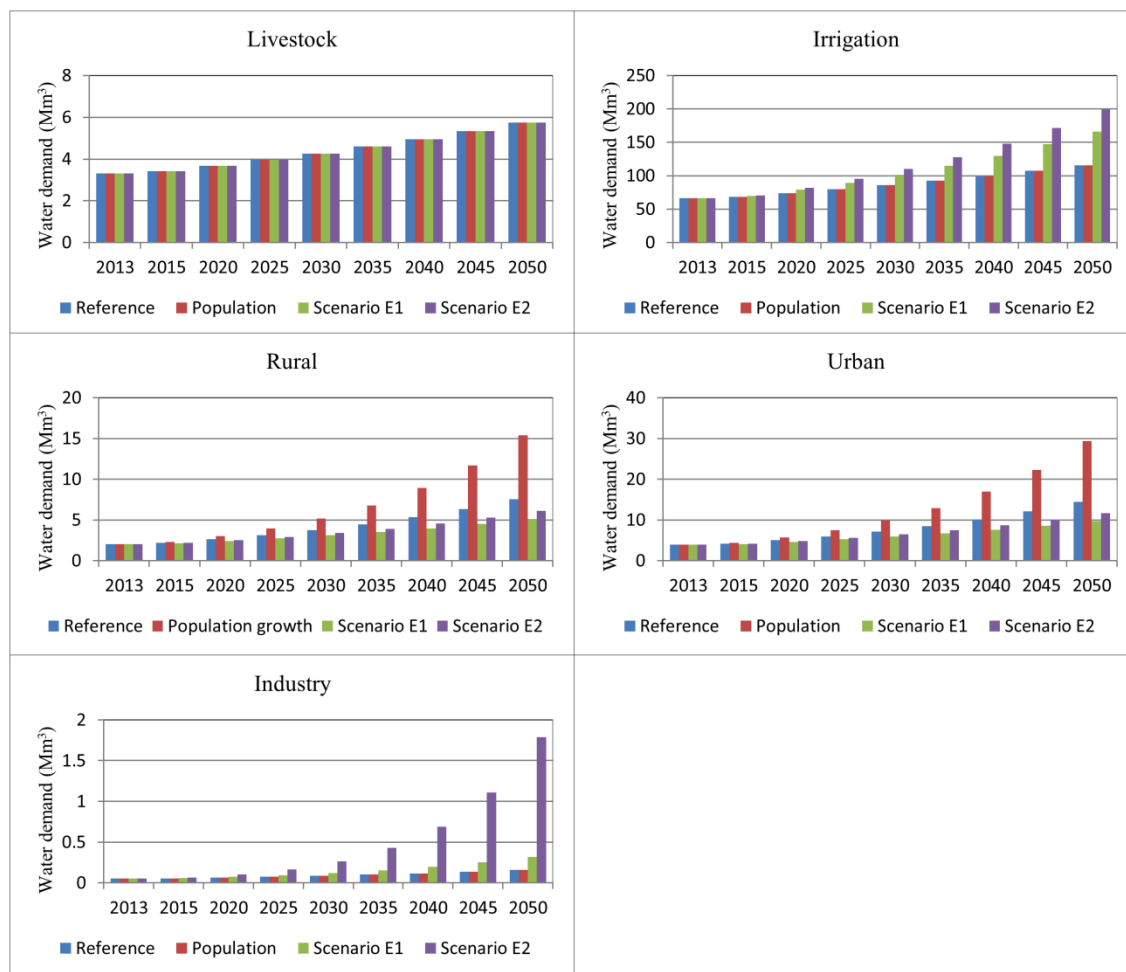
Figure 0.3 Water demand by sector in million cubic meters for three scenarios Reference, scenario E1 medium economic growth, and scenario E2 high economic growth

Monthly water demand graph (Figure 0.4) shows that during the rainy season water demand increases and decreases during the dry season. This is mainly due to the effect of irrigation because irrigation increases during the rainy season from June to October and decreases progressively until March (the hot dry season) where water demand for irrigation is insignificant. Therefore, the hot dry season is the lowest period of water demand during the year, where water is nearly only used for domestic and livestock purpose, which requires less water compared to irrigation. Since irrigation is still mainly based on the use of traditional wells, and during the hot dry season the water availability is low due to the increase of temperature and absence of rainfall; therefore, water used for irrigation can be neglected in the dry period.
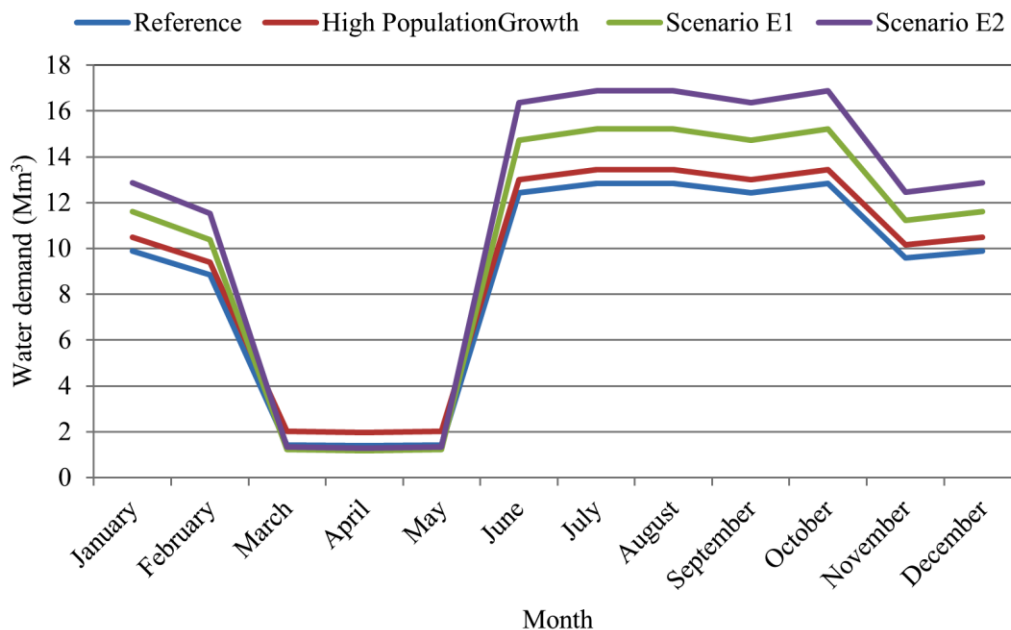
Figure 0.4 Average monthly water demand in million cubic meters for the four scenarios

All demands are constantly satisfied and therefore the coverage is 100% for all sectors

6.4. Hydrology

The WEAP model was able to estimate the components of the hydrologic system, *i.e.,* the inflow and outflow of groundwater (Table 0.1). The hydrological model results show a five year time steps variation between groundwater inflows and outflows in both scenarios. However, the extreme drought events occurred in the RCP4.5 scenario, where groundwater recharge is zero from 2031 to 2035 (Table 0.1).

Table 0.1 Annual precipitation, groundwater recharge and outflows in billion cubic meters for the current account and climate change scenarios RCP4.5 and RCP8.5 for the Klela basin

Climate	Interval of years	Recharge (km^3)	Precipitation (km^3)	GW outflow (km^3)
Current account	2013	0.52	4.65	0.44
Scenario RCP4.5	2013-2015[*]	0.59	4.05	0.45
	2016-2020	0.41	3.94	0.45
	2021-2025	0.43	3.76	0.41
	2026-2030	0.54	4.13	0.41
	2031-2035	0.00	3.06	0.33
	2036-2040	0.15	3.45	0.23
	2041-2045	0.27	3.53	0.18
	2046-2050	0.21	3.84	0.18
Scenario RCP8.5	2013-2015[*]	0.17	2.95	0.43
	2016-2020	0.18	3.61	0.34
	2021-2025	0.27	3.73	0.29
	2026-2030	0.32	3.73	0.25
	2031-2035	0.25	3.53	0.27
	2036-2040	0.14	3.56	0.18
	2041-2045	0.01	3.04	0.13
	2046-2050	0.22	3.86	0.07

[*] The first period for scenarios is different from the others by its length, which is only three years.

Comparison between the precipitation and groundwater dynamic can be seen in Figure 0.5. For both scenarios, the groundwater dynamic has a decreasing trend, but more significant in the climate scenario RCP8.5. This is evident because the precipitation is projected from 2013 to 2050 in climate scenario RCP8.5 to be the lowest due to the increase in greenhouse gas emissions. The important reducing of groundwater dynamic for the scenario RCP4.5 is recorded in the period from 2031 to 2035, with approximately 35% of groundwater dynamic rate of the current account year (Table 0.1 and Figure 0.5). In the scenario RCP8.5, groundwater dynamic from the period 2041 to 2045 is approximately 15% of the amount of current account year.
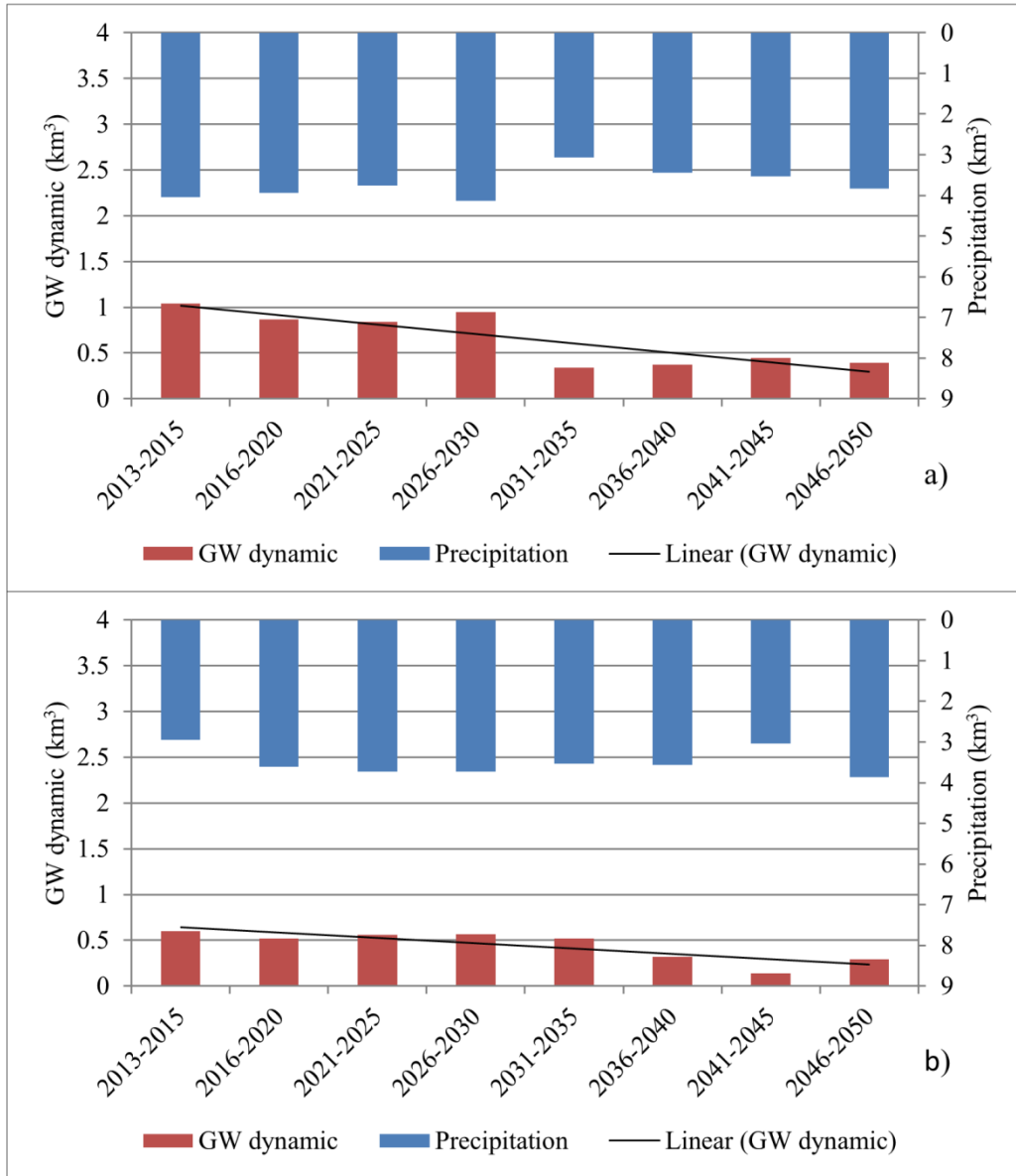
Figure 0.5. Comparison between precipitation and groundwater dynamic (groundwater recharge plus groundwater outflow) in billion cubic meters in the Klela basin for the climate scenarios (a) RCP4.5 and (b) RCP8.5

In order to model long-term groundwater storage, the equation 5.1 was firstly used to calculate the groundwater storage in equilibrium, which was estimated to 4.6 billion cubic meters. The initial groundwater storage was modeled during the modeling process to be about 11 billion cubic meters. The results are shown in Figure 0.6 that revealed that groundwater storage is decreasing over time for all the scenarios

considered. The lowest groundwater storage occurred in July, while the highest is recorded in October for the reference, population growth, socio-economic E1 and E2 scenarios (Figure 0.6a). However, because of the effect of population growth, the storage decreases more rapidly from 2030-2050 compare to reference scenario, whereas the scenario E2 experiencing the worst decrease (Figure 0.6a) due to the increase of domestic water use. Regarding climate change scenarios, RCP4.5 and RCP8.5 (Figure 0.6b), reducing of groundwater storage is more substantial compared to the previous scenarios. This is directly due to the projected change in precipitation for both scenarios; therefore, change in groundwater recharge and storage. Even though the drought events are predicted in both climate scenarios, some wet years can be observed in scenario RCP4.5, especially in 2018 and 2023, where the amount of groundwater storage exceeds that for initial storage. The most important rapid decrease of groundwater storage starts from June 2031 and ends in March 2038 for the RCP4.5 scenario, while in the RCP8.5 scenario it begins from January 2032 and stops in March 2040.

Like groundwater storage, long term annual groundwater outflow to the river decreases over time (Figure 0.7). This decrease is faster in climate change (Figure 0.7b) scenarios than in reference, high population growth, and socio-economic E1 and E2 scenarios (Figure 0.7a). This assumes that the impact of climate change on groundwater resources is more significant than the impact of the change in socio-economic and population growth rate. The lowest groundwater discharge is recorded in scenario RCP8.5 in 2048, which would indicate possible extreme drought events in this year.
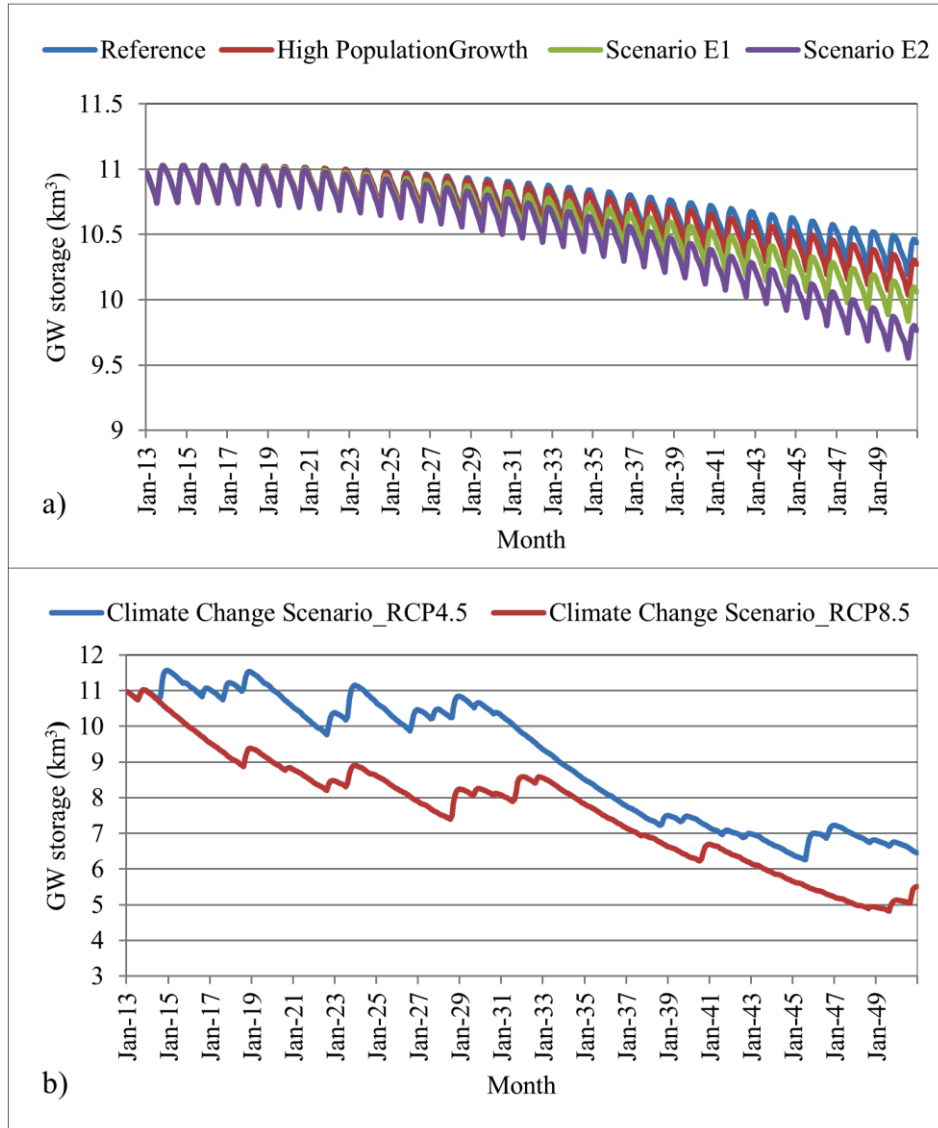
Figure 0.6 Groundwater storage in billion cubic meters for different scenarios (a) reference, population growth, socio-economic E1 and E2 and (b) climate change RCP4.5 and RCP8.5

Moreover, there is a strong correlation between monthly mean groundwater storage and groundwater outflow (Figure 0.8); *i.e.,* over the period, when groundwater storage decreases, groundwater outflow to the river is less important.
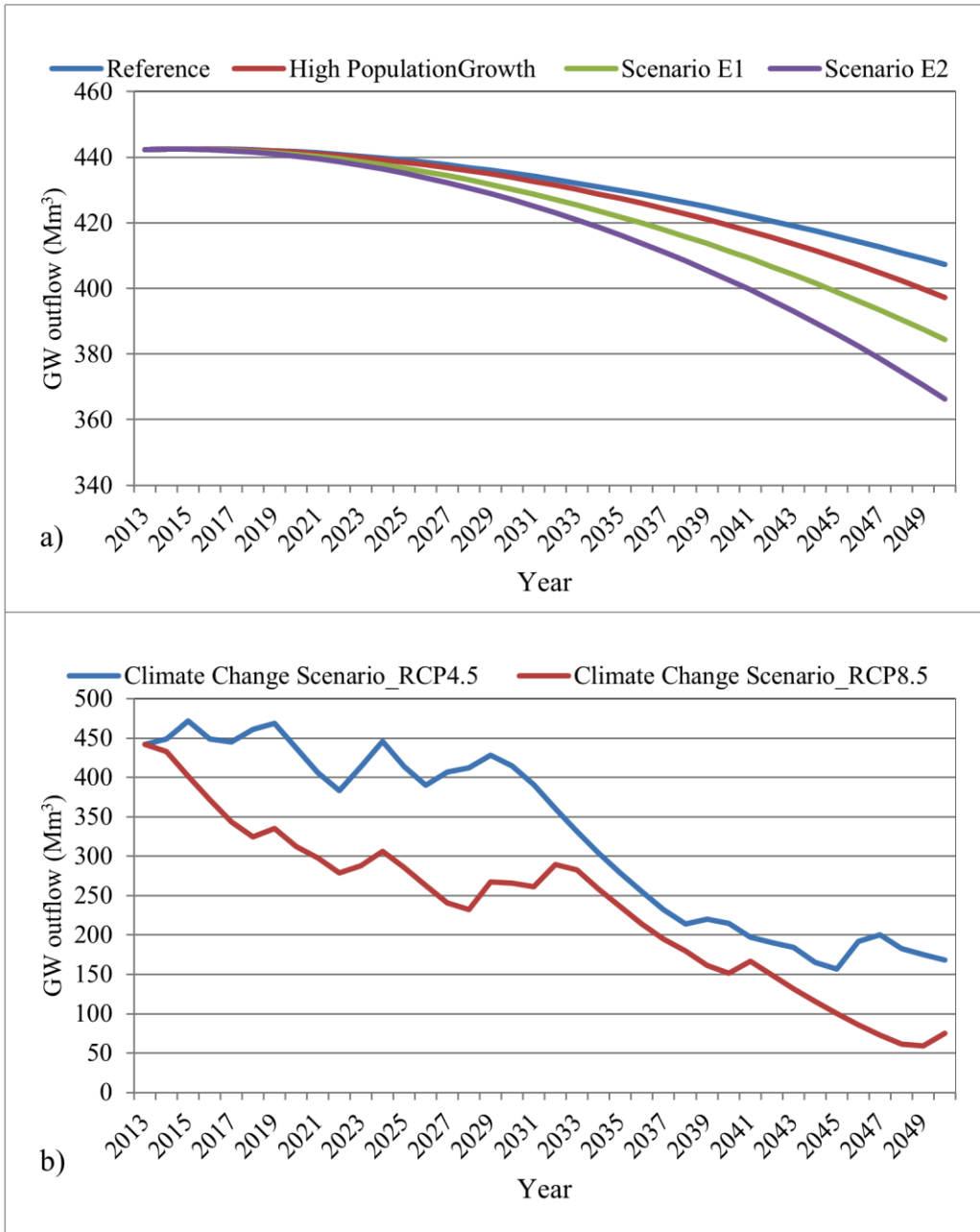
Figure 0.7 Long-term annual groundwater discharge in million cubic meters for all the scenarios: (a) reference, high population growth, socio-economic E1 and E2; and (b) climate change RCP4.5 and RCP8.5
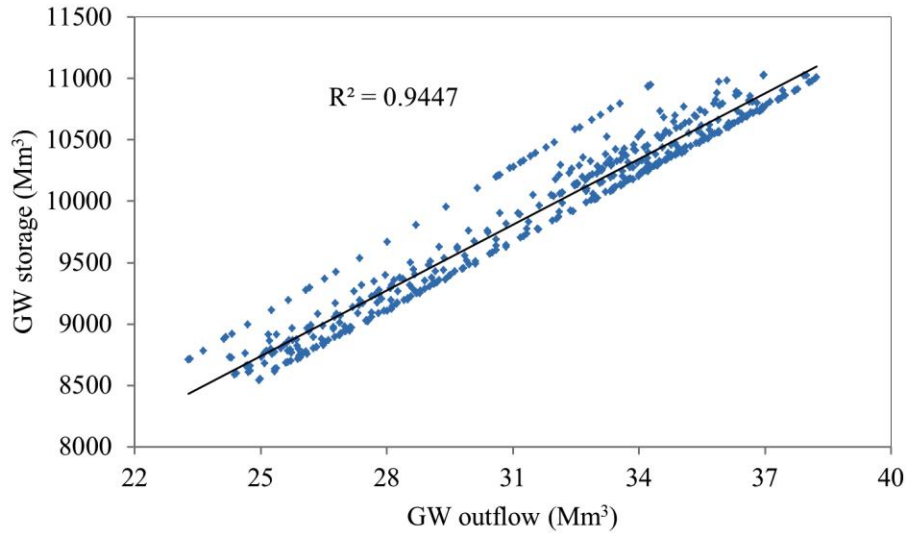
Figure 0.8 Linear comparison between mean monthly groundwater storage and groundwater outflow in million cubic meters from 2013-2050 for the scenarios RCP4.5 and RCP8.5

6.5.   Connection between water demand and supply

The relationship between groundwater depletion and supply resources are mentioned in Figure 0.9. Groundwater depletion is decreasing over time for both climate change scenarios RCP4.5 and RCP8.5. Through the length of both figures (Figure 0.9a - Figure 0.9b), groundwater depletion declines with decreasing of natural groundwater recharge; this is due to the fact that groundwater outflow, an important component of groundwater depletion, depends directly on annual natural recharge amount. In most of the years, groundwater depletion is greater than the natural groundwater recharge that has a direct consequence on groundwater storage by reducing its volume over time (Figure 0.9).
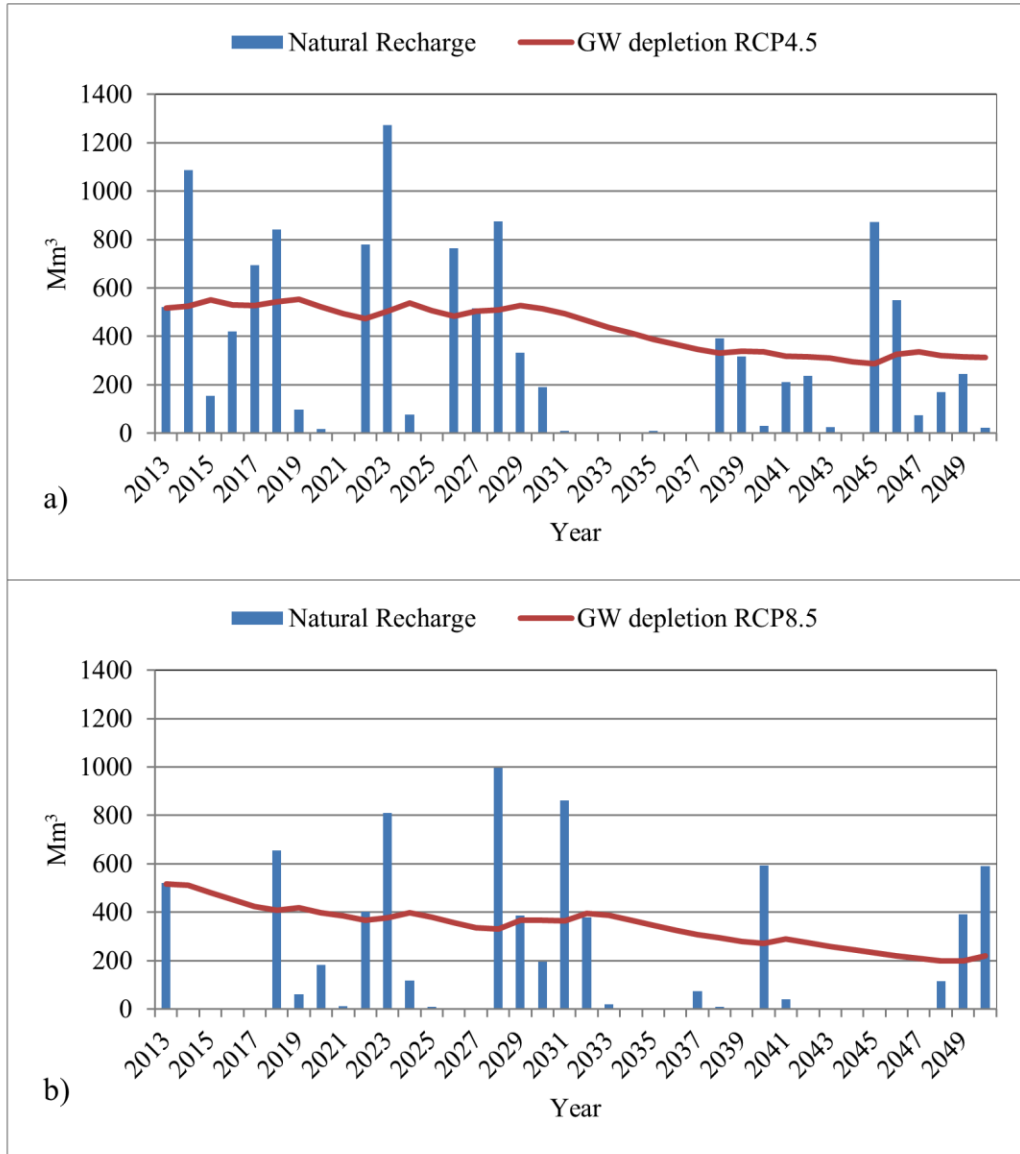
Figure 0.9 Annual natural groundwater recharge and groundwater depletion (water demand + groundwater outflow) in million cubic meters, (a) for RCP4.5 scenario; (b) for RCP8.5 scenario

Figure 0.10 displays the average monthly groundwater inflow and outflow and change in storage. All the figures show that the main inflow to the aquifer is the recharge and that is particularly higher during the rainy season after the first two months of rainfall. This recharge is greater in reference scenario than climate change scenarios.

Change in storage (the difference between the increase in storage and decrease in storage for groundwater) increases during the rainy season.

a)

b)
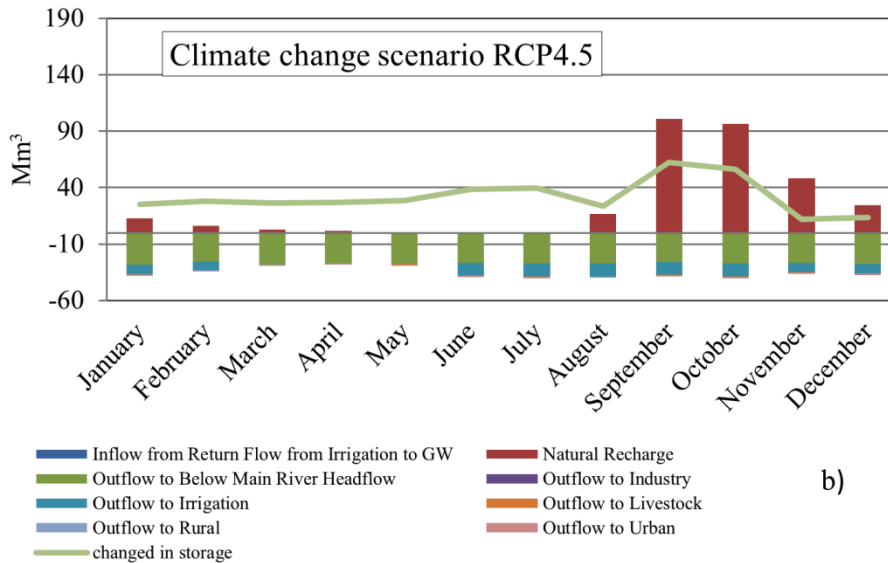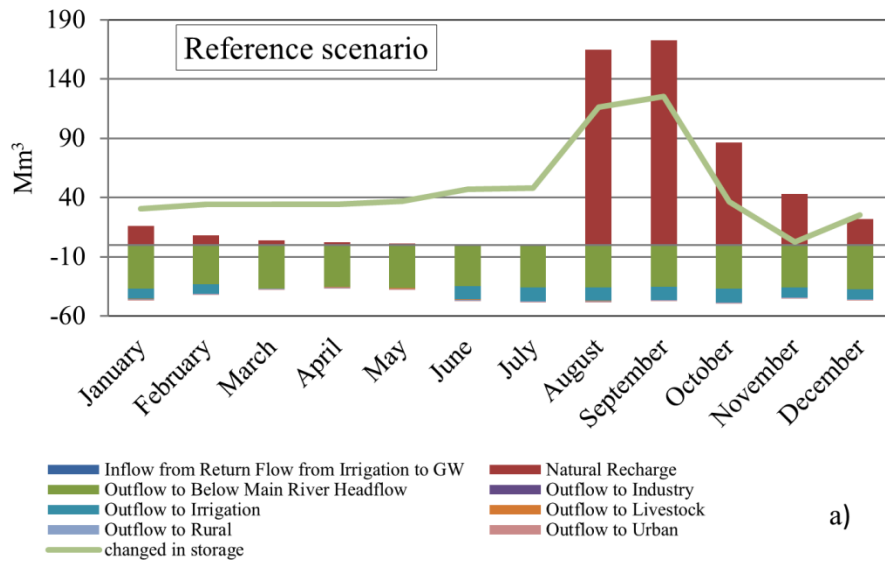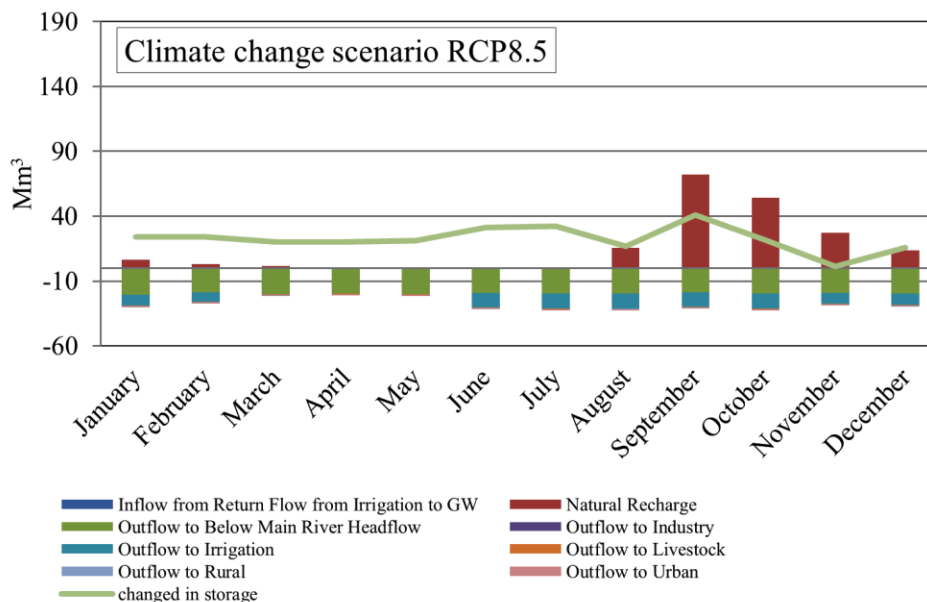
Figure 0.10. Monthly inflow, outflow and changed in storage of groundwater in million cubic meters for the three scenarios, (a) reference scenario; (b) climate change scenario RCP4.5; and (c) climate change scenario RCP8.5

6.6. WEAP model application

The WEAP model is fundamentally based on water balance accounting principle and can be applied to municipal and agricultural systems, single subbasin or complex transboundary river systems (Nayak *et al.,* 2015; SEI, 2015). It may address a wide range of issues; for instance, sectoral demand analyses, water conservation, water rights and allocation priorities, groundwater and streamflow simulations. Commonly, WEAP applications concern several steps (SEI, 2001): (i) the problem of study definition including "time frame, spatial boundary, system components and configuration of the problem, (ii) creating current accounts that provide a snapshot of actual water demand, pollution loads, resources and supplies for the system, (iii) developing future scenario based on policies, costs, technological development and other factors that affect demand, pollution, supply and hydrology" and (iv) assessing the scenarios with regard to water resources availability for supply, costs and benefits and environmental impacts. The WEAP model has been applied by many authors (Raskin *et al.,* 1992; Lévite *et al.,* 2002; Haddad *et al.,* 2007; Hagan, 2007; Mounir *et al.,* 2011; Ghallabi *et al.,* 2011; Schuler and

Margane, 2013) through the world, and they found the model as a satisfactory tool for integrating water resources management and planning. WEAP has been developed for simulating water balances and evaluating the water management strategies, by building a future scenario policy on water resources, in the Aral Sea Region (Raskin *et al.,* 1992). In the upper Est of Ghana, Hagan (2007) modeled within WEAP the impact of small reservoirs. The results reveal that the reservoirs have a low impact on the flow of the White Volta River, and he suggested a construction of large reservoirs that could significantly affect that flow. WEAP has been applied in Jeita spring, Lebanon to establish water balance for the groundwater contribution zone. They have shown that 370 Mm^3 (59.6% of total annual precipitation) are direct groundwater recharge, the rest are due to direct evapotranspiration and runoff respectively 110 Mm^3 (17.7% of total annual precipitation) and 141 Mm^3 (22.7% of total annual precipitation). Mounir *et al.* (2011) also evaluated the future water demands in the Niger River in Niger by applying the WEAP model. However, most of the studies involved surface water; only a few studies applied directly groundwater modeling within the WEAP, may be due to its limitation with fractured rock aquifers (Höllermann *et al.,* 2010).

6.7. Groundwater level prediction with MODFLOW

One of the most important objectives of our groundwater modeling study is to use the scenario data to predict the future behavior of the aquifer system. Thus, the model was used to quantify groundwater levels considering scenario data after model calibration and verification using three different piezometer data sets. Monthly precipitation data from the RCP4.5 and RCP8.5 scenarios were used to calculate the groundwater recharge (see Figure 0.1), which was used as model input to quantify future groundwater levels in the Klela basin from June 2010 to November 2050.

The results of the simulated MODFLOW model reveal a decrease in groundwater level (GWL) over time (Figure 0.11). From June 2010 to November 2050, GWL decreases from 365 mamsl to 348 mamsl, or to approximately 17 m, in piezometer F7, in the RCP4.5 scenario, while groundwater depletion achieves 24 m, in the RCP8.5 scenario. During the same period, in the RCP4.5 scenario, F18 decreases from 356 mamsl to 338 mamsl, or approximately 18 m, whereas GWL is 20 m, in the RCP8.5 scenario. In

the RCP4.5 scenario, GWL decreases approximately to 11 m, in F15 and it is 15 m, RCP4.5 scenario.
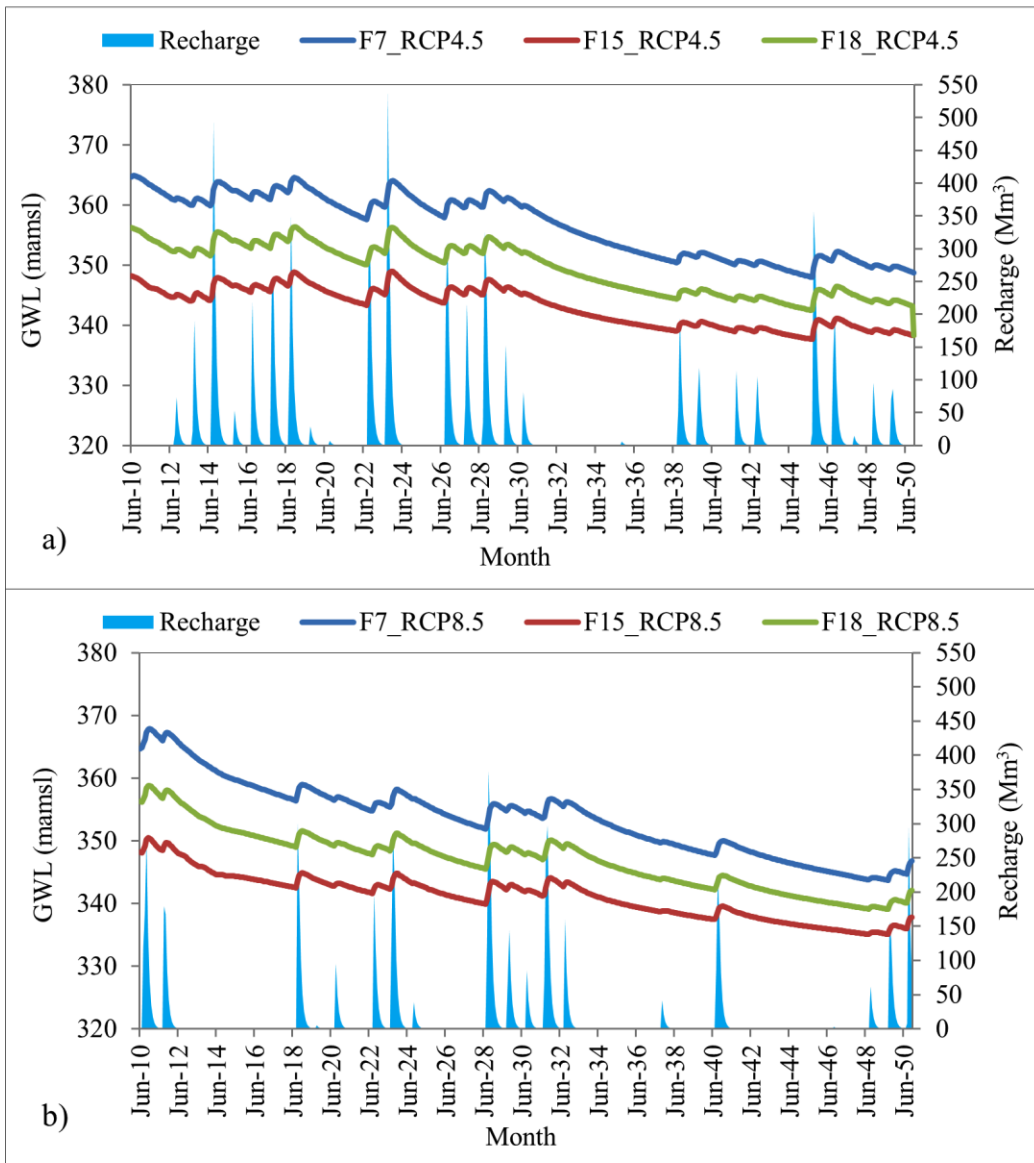
Figure 0.11 Long-term monthly groundwater levels, in meters above mean sea level and monthly groundwater recharge (Mm^3) in the Klela basin, from June 2010 to November 2050 calculated using climate change data (a) RCP4.5, and (b) RCP8.5

The overall mean of all the piezometer drops was approximately 15 m, in RCP4.5 and 20 m, in RCP8.5. It may be concluded that groundwater levels decreased more in RCP8.5 than in RCP4.5. Furthermore, a great decline in groundwater storage in the 2030s

was modeled in all the piezometers and both scenarios considered in this study. Groundwater level reductions may intensify if water extraction increases over time.

6.8.   Conclusion

Hydrological model (WEAP) was applied to evaluate the impact of climate change and population growth on groundwater resources for the Klela basin. The overall results show that groundwater storage is decreasing due mainly to climate change effect and human activities. Groundwater recharge estimated using Thornthwaite model reveals an important decrease in both scenarios RCP4.5 and RCP8.5 especially in the 2030s. This decrease in recharge rate, more highlighted in climate change scenario RCP8.5, is essentially due to climate change. As predicted in recharge estimation, groundwater storage also decreases consequently in the 2030s. Because of population growth and socio-economic development, groundwater storage diminishes over time; but this diminution of groundwater storage is less compared to that provoked by climate change effects.

This study concludes that groundwater resources are consequently affected by climate change and population growth. Therefore, the decision makers should be informed about these results, although the study has been performed with some uncertainties   at   model   level   as   well   as   observed   input   data.

CHAPTER 7: GENERAL CONCLUSION AND RECOMMENDATIONS

7.1.   Introduction

Klela basin one of the subbasins of the Bani's basin (a tributary of the Niger River) is very important for all the Malian population in general, and the inhabitant of Sikasso circle in particular; because it is among the areas where the irrigation product rate is higher. Actually, the amount of groundwater resources, principal permanent water resources, is largely sufficient to cover all the demands. Though, it is important to notice that this quantity of groundwater resources is decreasing from year to year due to many factors including increasing population and urbanization rate, climate variability and change, deforestation for extension of agriculture fields, *etc.* Regarding these challenges, the future climate change is projected to be drier period; then, exploitation of groundwater resources is expected to be higher, which could lead to its depletion, particularly in the Sikasso commune where the socio-economic development is increasing. It is therefore indispensable to adapt a sustainable management of these vital resources for the well-being of the inhabitants of the Basin.

For that, this current study was designed to develop groundwater model and scenario analyses in the study area in order to contribute to the sustainability of groundwater resources management.

Several methods (water table fluctuation method, chloride mass balance method) and models (EARTH model and Thornthwaite model) were applied in this study to estimate the reasonable groundwater recharge, which permitted evaluating groundwater behavior in the present and future, using PMWIN model and WEAP model.

7.2.   Recharge estimation

The recharge rate was estimated using:

-    **Water table fluctuation method**

This technique, widely used in arid and semi-arid regions, was applied in this study to estimate groundwater recharge. The results show a large different between the

minimum value and the maximum value of recharge. For example, for piezometer F7 in 2013, the value of recharge varies from 3 to 16.2% of mean annual rainfall. This variation is mainly due to the specific yield of which the determination of its value is very critical. Therefore, the results of this method should be taken with many precautions. Other uncertainties using this method are from groundwater level fluctuation, which is very subjective. As a conclusion, it is difficult to confirm the reliable groundwater recharge estimated for an area by using only the water table fluctuation method due to uncertainties linked to this technique.

- **Chloride mass balance method**

Like water table fluctuation method, the chloride mass balance method is also widely used in arid and semi-arid regions. This method was used in this study to estimate the recharge rate. The results ranged from 3 to 29% of mean annual rainfall. The results from this method should be considered as overestimated because of lack of data of the dry chloride deposit in the study area. The main uncertainty linked to this method is the difficulty in determination of chloride concentration from rainfall and the unavailability of long-term chloride concentration data from rainwater.

- **EARTH model**

EARTH model was able to estimate the recharge in the study area. This model used daily groundwater level and evapotranspiration as input data to simulate groundwater recharge. The results from this model ranged from 12.9-14.9% (with the average of 13.9%) of mean annual rainfall. The results of this model seem to be more reliable than others because the difference between the minimum and maximum recharge is small; this can explain the precision in this method compared to the previous ones. Furthermore, the EARTH model was evaluated qualitatively (using line graphs) and quantitatively (considering model performance efficiency methods) to be acceptable. Although this result is considered more reliable, there are some uncertainties in the calibration process. Ten parameters from field data should be modified during the calibration process to simulate the recharge. As the real field data was not available, some of the ten parameters could be over- or underestimated.

- **Thornthwaite model**

As a long-term historical and future groundwater level measurement data was not available, the Thornthwaite model was used to simulate groundwater recharge which requires only monthly rainfall and temperature as input data. Even though the uncertainty was high in this modeling due to the absence of hydrogeological data packages into the model, the results were realistic. The annual recharge is close to zero or zero in the year where the annual rainfall is less than the overall average precipitation.

7.3.   Groundwater modeling

The MODFLOW model has been calibrated for the Klela basin from 2010-2014 with three piezometer data. This calibration of groundwater model permitted the estimation of the flow and direction of groundwater movement for the aquifer system and its interaction with the surrounding streams. The recharge, which is considered as the only responsible for annual groundwater replenishment because the boundary of the whole basin was set to no flow boundary, was estimated to be approximately 635 Mm^3/a, representing 13.9% of the total annual precipitation. The established water budget has allowed connecting groundwater to surface water by specifying the amount of water outflowing and inflowing from and to the aquifer, respectively. However, the leakage to the streams representing water from the aquifer dominated with an annual amount of approximately 618 Mm^3/a, or 97% of groundwater recharge. It can, therefore, conclude that the main factor of actual groundwater depletion is water extraction (about 57 Mm^3/a) by population for their numerous and differentiated activities. The increase of the population as predicted by many studies and the rapid socio-economic development in the region will increase the water demand consequently lead to a further decrease in groundwater resources.

The piezometric map generated by the model shows that groundwater level is decreasing from south to north, which indicates that the northern part of the basin is the discharging point as in the topographic map.

The results of this modeling are carried out with many uncertainties including the computation error in the model, model conceptualization, input data, but the important

uncertainty is from the boundary, which is unknown; although, these results are reliable, and the model can be used in water management in the study area.

7.4. Climate change impact on groundwater

The impacts of climate change on groundwater resources have been assessed using RCP4.5 and RCP8.5 scenarios from the GCM ECHAM downscaled to a 0.44° resolution by the Swedish Meteorological Service and provided by the CORDEX initiative. This climate series was found to be suitable for direct use in the WEAP and MODFLOW models to evaluate the impact of climate change on groundwater resources in the Klela basin. The results indicate that groundwater storage is decreasing over time for all the scenarios considered in this study, especially in the 2030s, where the depletion is expected to be highlighted. This can be explained by the fact that the water demand, due to the population growth and socio-economic development, is increasing, while the precipitation, responsible for recharge, is decreasing.

7.5. General conclusion

It could be generally concluded that groundwater resources are negatively affected mainly due to climate change and human activities. Groundwater resources at the moment cover the present water demands, but as these resources are decreasing over time, to cover the future demand would be a problem. It is therefore urgent to adapt an integrated groundwater resource management in order to prevent this vital resource from rapid expected depletion.

7.6. Recommendations

As groundwater is an important permanent water resource in the study area, its protection for sustainable planning is essential for the inhabitants of the basin. Even though the results of this study contribute to the water management of the region, they should be considered with some precaution as the quality and quantity of primary and secondary data used were limited; in the same manner, the spatial and temporal hydrological and hydrogeological data were limited too. The authorities of the basin should, therefore, double the effort in order to facilitate the future studies in the study

area by making a strong database, which will be updated continuously. Some data are very important to be known in groundwater management such that groundwater level fluctuation, specific yield and chloride concentration. These recommendations below could help improve data collection.

The piezometers are poorly distributed spatially in the basin and produce temporally limited data. During the fieldwork, it was noticed that there were many abandoned boreholes throughout the basin. These boreholes could be fit out and used as piezometers because the implementation of piezometers especially for groundwater monitoring could be expensive for the government. Until date, the water level meter is still used for groundwater level measurement which is tiresome for daily time step and the measurement is sometimes subjective. Then, it is recommended to use the automatic data loggers, which are not so expensive and easy to use, and the results are more consistent. A good measurement of groundwater levels on long term period leads to improve the calibration because groundwater models require water level as the most important input data.

Furthermore, the specific yield, which is determined from pumping test data, is essential in groundwater modeling. The pumping test data is deducted from borehole construction. In the study area, the boreholes are implemented by companies including government company, NGO, private societies, individuals. Only the data from the first two companies are more reliable and are communicated to the Regional Hydraulic Direction of Sikasso. They used only the short-term pumping test that cannot help in determining specific yield. The geophysics and other techniques used during the borehole constructions provide poor information. It is therefore recommended to abide by the International standards in borehole implementations by considering long-term pumping test and informing the companies of the importance of these data in groundwater management.

In addition, chloride mass balance method uses chloride concentration to estimate groundwater recharge. The chloride concentration from rainwater should be analyzed continuously to facilitate the next studies regarding this technique.

The future studies should concentrate on estimating groundwater recharge and identify the eventual cause of groundwater level rise that is likely influenced by other

large-scale groundwater flow. The identification of possible lateral groundwater flow to the basin is required for establishing the water budget because the real boundary of the basin is unknown. The hydrogeological investigations are therefore required to know whether surface and subsurface catchment is the same.

References

Ackerman, F., Stanton, E.A., 2011. Climate Economics: The State of the Art. SEI.

Ahern, J.A., 2005. Ground-water capture-zone delineation: method comparison in synthetic case studies and a field example on fort wainwright, Alaska (M.Sc). University of Alaska Fairbanks, United States. Available at: http://issuu.com/universityofalaskafairbanks/docs/jahernthesis3. Accessed 30 Nov. 2015.

Alavian, V., Qaddumi, H. M., Dickson, E., Diez, S., M., Danilenko, A. V., Hirji, R. F., Puz, G., Pizarro, C., Jacobsen, M., Blankespoor, B., 2009. Water and Climate Change: Understanding the Risks and Making Climate-Smart Investment Decisions. The World Bank.

Alexander, D., Palmer, R.N., 2007. Technical Memorandum #8: Impacts of Climate Change on Groundwater Resources: A Literature Review.

Al-Gamal, S.A., Sokona, Y., Dodo, A.-K., 2009. Climatic changes and groundwater resources in Africa. Int. J. Clim. Change Strateg. Manag. 1, 133–145. doi:10.1108/17568690910955603

Allison, G. B., Gee, G. W., Tyler, S. W., (1994) Vadose-zone techniques for estimating groundwater recharge in arid and semi-arid regions. Soil Sci. Soc. Am. J. 58, 6–14.

Anderson, M.P., Woessner, W.W., 1992. Applied groundwater modeling: simulation of flow and advective transport. Academic Press, San Diego.

Arnell, N.W., 2004. Climate change and global water resources: SRES emissions and socio-economic scenarios. Global Environmental Change 14, 31-52. doi:10.1016/j.gloenvcha.2003.10.006

Baalousha, H.M., 2003. Risk assessment and uncertainty analysis in groundwater modelling (PhD). Westfälischen Technischen Hochschule Aachen, Germany. Available at: https://www.deutsche-digitale bibliothek.de/binary/66XM233YFAT4D7CFYX64QMR33DZTZRSG/full/1.pdf. Accessed 29 Feb. 2016.

Baalousha, H., 2009. Fundamentals of Groundwater Modelling, in: König, L.F., Weiss, J.L. (Eds.), Groundwater: Modelling, Management and Contamination. Nova Science Publishers, New York, pp. 149–166.

Banning, R.O.B., 2010. Analysis of the groundwater/surface water interactions in the Arikaree River Basin of Eastern Colorado (M.Sc). University of Colorado State, Colorado. Available at: http://dspace.library.colostate.edu/webclient/DeliveryManager/digitool_items/csu01_storage/2011/01/21/file_1/87893. Accessed 27 Nov. 2015.

Barron, O.V., Crosbie, R.S., Dawes, W.R., Charles, S.P., Pickett, T., Donn, M.J., 2012. Climatic controls on diffuse groundwater recharge across Australia. Hydrol. Earth Syst. Sci. 16, 4557–4570. doi:10.5194/hess-16-4557-2012

Bates, B.C., Kundzewicz, Z., Wu, S., Palutikof, J., Eds., 2008. Climate change and water. Technical Paper of the Intergovernmental Panel on Climate Change, IPCC Secretariat, Geneva,210 pp.

Bazuhair, A.S., Wood, W.W., 1996. Chloride mass-balance method for estimating ground water recharge in arid areas: examples from western Saudi Arabia. J. Hydrol. 186, 153–159.

Belay, E.A., 2009. Growing lake with growing problems: integrated hydrogeological investigation on Lake Beseka, Ethiopia (PhD). University of Bonn, Germany. Available at: http://hss.ulb.uni-bonn.de/2009/1645/1645.pdf. Accessed 13 Jun. 2013

Blaney, H.F., Criddle, W.D., 1962. Determining Consumptive Use and Irrigation Water Requirements. Technical Bulletin No. 1275, Washington.

Bokar, H., Mariko, A., Bamba, F., Diallo, D., Kamagaté, B., Dao, A., Soumare, O., Kassogue, P., 2012. Impact Of Climate Variability on Groundwater Resources in Kolondieba Catchment Basin, Sudanese Climate Zone in Mali. Int. J. Eng. Res. Appl. 2, 1201–1210.

Bonsor, H.C., MacDonald, A.M., 2010. Groundwater and climate change in Africa: review of recharge studies (No. IR/10/075.). British Geological Survey offices.

Brassington, F.C, 2004. Developments in UK hydrogeology since 1974, in: Mather, J.D. (Ed.), 200 Years of British Hydrogeology, Geological Society Special Publication. The Geological Society of London, London, pp. 363–385.

Bredenkamp, D.B., Botha, L.J., Tonder, G.J.V., Rensburg, H.J.V., 1995. Manual on quantitative estimation of groundwater recharge and aquifer storativity : based on practical hydro-logical methods. Pretoria Water Res. Comm. WRC report, no. TT 73/95.

Bredenkamp, D.B., Xu, Y., 2003. Perspectives on recharge estimation in dolomitic aquifers in South Africa, in: Xu, Y., Beekman, H.E. (Eds.), Groundwater Recharge Estimation in Southern Africa. Unesco, Paris.

Bricquet, J.P., Bamba, F., Mahé, G., Toure, M., Olivry, J.C., 1997. Évolution récente des ressources en eau de l'Afrique atlantique. Rev. Sci. Eau 10, 321. doi:10.7202/705282ar

Brouwer, C., Heibloem, M., 1986. Irrigation Water Management: Irrigation Water Needs. FAO, Rome.

Brunner, P., Simmons, C.T., Cook, P.G., Therrien, R., 2010. Modeling Surface Water-Groundwater Interaction with MODFLOW: Some Considerations. Ground Water 48, 174–180. doi:10.1111/j.1745-6584.2009.00644.x

Bundschuh, J., Arriaga, M.C.S. (Eds.), 2010. Multiphysics Modeling. CRC/Balkema, Taylor & Francis Group.

Calow, R., Bonsor, H., Jones, L., O'Meally, S., MacDonald, A., Kaur, N., 2011. Climate change, water resources and WASH: A scoping study. Overseas Development Institute, London.

Calow, R., MacDonald, A., 2009. What will climate change mean for groundwater supply in Africa? Overseas Development Institute, London.

Candela, L., von Igel, W., Elorza F.J., Aronica, G., 2009. Impact assessment of combined climate and management scenarios on groundwater resources and associated wetland (Majorca, Spain). J. Hydrol. 376, 510–527. doi:10.1016/j.jhydrol.2009.07.057

Carter, R.C., Parker, A., 2009. Climate change, population trends and groundwater in Africa. Hydrol. Sci. J. 54, 676–689. doi:10.1623/hysj.54.4.676

Cavé, L., Beekman, H.E., Weaver, J., 2003. Impact of Climate Change on Groundwater Recharge Estimation, in: Xu, Y., Beekman, H.E. (Eds.), Groundwater Recharge Estimation in Southern Africa, No. 64. Unesco, Paris.

Chiang, W.-H., Kinzelbach, W., 2005. 3D-groundwater modeling with PMWIN, Second Edition. ed. Springer, Berlin-Heidelberg ; New York. 397 pp.

Chiang, W.-H., Kinzelbach, W., 2001. 3D-groundwater modeling with PMWIN, First Edition. ed. Springer, Berlin-Heidelberg ; New York. ISBN 3-540 67744-5, 346 pp.

Chiang, W.-H., Kinzelbach, W., 1998. Processing Modflow A Simulation System for Modeling Groundwater Flow and Pollution.

Clifton, C., Evans, R., Hayes, S., Hirji, R., Puz, G., Pizarro, C., 2010. Water and Climate Change: Impacts on groundwater resources and adaptation options (No. 25). Water Working Notes.

Cook, P.G., 2003. A guide to regional groundwater flow in fractured rock aquifers. CSIRO, Glen Osmond, Aust.

Cooley, R.L., 1992. A MODular Finite-Element model (MODFE) for areal and axisymmetric ground-water-flow problems, part 2: derivation of finite-element equations and comparisons with analytical solutions. U.S. Geological Survey Techniques of Water-Resources Investigations Book 6, Chapter A4, 153 p.

Cooper, H.H., Jacob, C.E., 1946. A generalized graphical method of evaluating formation constants and summarizing well-field history. Am Geophys Union Trans Vol. 27, pp. 526–534.

Council, G.W., 1999. A Lake Package for MODFLOW (LAK2).

Crosbie, R.S., Binning, P., Kalma, J.D., 2005. A time series approach to inferring groundwater recharge using the water table fluctuation method: Inferring groundwater recharge. Water Resour. Res. 41. doi:10.1029/2004WR003077

Crosbie, R.S., McCallum, J.L., Walker, G.R., Chiew, F.H., 2012. Episodic recharge and climate change in the Murray-Darling Basin, Australia. Hydrogeol. J. 20, 245–261.

Csaba, P., Csaba, J., 2011. Hydrology, Digital textbook library. Available online at: http://www.tankonyvtar.hu/en/tartalom/tamop425/0032_hidrologia/ch04.html. Accessed 10 March 2017.

Dao, A., 2013. Caractérisation des composantes du cycle de l'eau et processus de production de l'écoulement : cas du bassin versant transfrontalier de Kolondieba au sud du Mali en milieu tropical de socle. Doctorat. Université Nangui Abrogoua, Abidjan.

Delin, G.N., Healy, R.W., Lorenz, D.L., Nimmo, J.R., 2007. Comparison of local- to regional-scale estimates of ground-water recharge in Minnesota, USA. J. Hydrol. 334, 231–249. doi:10.1016/j.jhydrol.2006.10.010

de Vries, J., Simmers, I., 2002. Groundwater recharge: an overview of processes and challenges. Hydrogeol. J. 10, 5–17. doi:10.1007/s10040-001-0171-7

Diakité, L., Zida., M., 2003. Étude diagnostique de la filière pomme de terre dans trois pays de l'Afrique de l'ouest: cas du Mali. Institut du Sahel

Diall, O., 2001. Programme Against African Trypanosomosis Options For Tsetse Fly Eradication in the Moist Savannah Zone of West Africa: Technical and Economic Feasibility Study, Phase 1 (Mali).

Diallo, I., Sylla, M.B., Giorgi, F., Gaye, A.T., Camara, M., 2012. Multimodel GCM-RCM Ensemble-Based Projections of Temperature and Precipitation over West Africa for the Early 21st Century. Int. J. Geophys. 2012, 1–19. doi:10.1155/2012/972896

Diouf, O.C., Faye, S.C., Diedhiou, M., Kaba, M., Faye, S., Gaye, C.B., Faye, A., Englert, A., Wohnlich, S., 2012. Combined uses of water-table fluctuation (WTF), chloride mass balance (CMB) and environmental isotopes methods to investigate groundwater recharge in the Thiaroye sandy aquifer (Dakar, Senegal). Afr. J. Environ. Sci. Technol. 6, 425–437. doi:10.5897/AJEST12.100

Döll, P., Fiedler, K., 2008. Global-scale modeling of groundwater recharge. Hydrol. Earth Syst. Sci. 12, 863–885.

Duan, Q., Gupta, H.V., Sorooshian, S., Rousseau, A.N., Turcotte, R., (Ed.), 2003. Calibration of watershed models, Water science and application. American Geophysical Union, Washington, D.C.

Edmunds, W.M., 2010. Conceptual models for recharge sequences in arid and semi-arid regions using isotopic and geochemical methods, in: Wheater, H., Mathias, S.A., Li, X. (Eds.), Groundwater Modelling in Arid and Semi-Arid Areas, International Hydrology Series. Cambridge University Press, New York, pp. 21–37.

Essink, G.H.P.O., 2001. Density Dependent Groundwater Flow Salt Water Intrusion and Heat Transport.

Essink, G.H.P.O., 2000. Groundwater Modelling. University of Utrecht.

Evans, J.P., 2011. CORDEX – An international climate downscaling initiative. Presented at the 19th International Congress on Modelling and Simulation, Perth, Australia, pp. 2705–2711.

Falkenmark, M., Rockström, J., 2004. Balancing water for humans and nature: the new approach in ecohydrology. Earthscan, London ; Sterling, VA.

FAO (1995) 'Land and water integration and river basin management'. Proceedings of an informal workshop 31 Jan-2 Feb, 1993. Land and Water Bulletin. Food and Agricultural Organization, Rome.

FAO (1997) 'Food production: the critical role of water'. World Food Summit. Technical Background Document 7. Food and Agricultural Organization, Rome.

FAO-UNESCO, 1974. Soil map of the world, Volume I Legend. ed. Unesco - Paris.

Fetter, C.W, 2001. Applied Hydrogeology, 4th Ed. Prentice Hall, Englewood Cliffs, NJ, 598 p.

Funk, C., Rowland, J., Adoum, A., Eilerts, G., White, L., 2012. A Climate Trend Analysis of Mali (Famine Early Warning Systems Network—Informing Climate Change Adaptation Series). U.S. Geological Survey.

Gebreyohannes, H.G., 2008. Groundwater recharge modelling: A case study in the central Veluwe, the Netherlands (M.Sc). International institute for geo-information science and Earth observation Enschede, The Netherlands. Available at: https://www.itc.nl/library/papers_2008/./hiwot.pdf. Accessed 5 May 2016.

Genetti, A.J., 1999. Engineering and design groundwater hydrology. Department of the Army U.S. Army Corps of Engineers Washington.

Ghallabi, L.B., Messouli, M., Yacoubi, M., 2011. Integrated Approaches to the Assessment of the Impacts of Climate and Socio-economic Change on Groundwater Resources in the Tensift Basin, Morocco. Int. J. Water Resour. Arid Environ. 1 (3), 219–225.

Giorgi, F., Diffenbaugh, N.S., Gao, X.J., Coppola, E., Dash, S.K., Frumento, O., Rauscher, S.A., Remedio, A., Seidou Sanda, I., Steiner, A., Sylla, B., Zakey, A.S., 2008. The Regional Climate Change Hyper-Matrix Framework. Eos 89, 445–456.

Giorgi, F., Jones, C., Asrar, G.R., 2009. Addressing climate information needs at the regional level: the CORDEX framework. WMO Bull. 58 (3), 175–183.

Goulden, M., Conway, D., Persechino, A., 2009. Adaptation to climate change in international river basins in Africa: a review / Adaptation au changement climatique dans les bassins fluviaux internationaux en Afrique: une revue. Hydrol. Sci. J. 54, 805–828. doi:10.1623/hysj.54.5.805

Green, T.R., Taniguchi, M., Kooi, H., Gurdak, J.J., Allen, D.M., Hiscock, K.M., Treidel, H., Aureli, A., 2011. Beneath the surface of global change: Impacts of climate change on groundwater. J. Hydrol. 405, 532–560. doi:10.1016/j.jhydrol.2011.05.002

Guan, H., Love, A.J., Simmons, C.T., Kayaalp, A.S., Makhnin, O., 2009. Factors influencing chloride deposition in a coastal hilly area and application to 1 chloride deposition mapping. Hess_2009_180 29.

Gurdak, J.J., Hanson, R.T., Green, T.R., 2009. Effects of Climate Variability and Change on Groundwater Resources of the United States. U.G. Geological Survey. Fact Sheet 2009-3074. Available at: http://www.usgs.gov/global_change.

Haddad, M., Jayousi, A., Hantash, S.A., 2007. Applicability of WEAP as water management decision support system tool on localized area of watershed scales: Tulkarem District In Palestine as case study. Presented at the Eleventh International Water Technology Conference, IWTC11 2007, Sharm El-Sheikh, Egypt.

Hagan, I., 2007. Modelling the impact of small reservoirs in the Upper East Region of Ghana (M.Sc). University of Lund, Sweden. Available at: http://www.weap21.org/downloads/smallresghana.pdf. Accessed 29 Mar. 2016.

Harbaugh, A.W., 2005. MODFLOW-2005, The U.S. Geological Survey Modular Ground-Water Model—the Ground-Water Flow Process. U.S. Geological Survey Techniques and Methods 6-A16, variously paginated.

Harbaugh, A.W., Banta, E.R., Hill, M.C., McDonald, M.G., 2000. MODFLOW-2000, the U.S. Geological Survey Modular Ground-Water Model—User Guide to Modularization Concepts and the Ground-Water Flow Process. U.S. Geological Survey Open-File Report 00-92.

Healy, R., Cook, P., 2002. Using groundwater levels to estimate recharge. Hydrogeol. J. 10, 91–109. doi:10.1007/s10040-001-0178-0

Healy, R.W., Scanlon, B.R., 2010. Estimating groundwater recharge. Cambridge University Press, New York.

Hendrickx, J.M., Philips, F.M., Harrison, B.J., 2003. Water flow processes in arid and semi-arid vadose zones, in: Simmers, I. (Ed.), Understanding Water in a Dry Environment: Hydrological Processes in Arid and Semi-Arid Zones, International Contributions to Hydrogeology. A. A. Balkema, Lisse ; Exton, Pa, pp. 151–210.

Henry, C.M., 2011. An integrated approach to estimating groundwater recharge and storage variability in southern Mali, Africa (M.Sc.). University of Simon Fraser, Canada. Available at: http://summit.sfu.ca/system/files/iritems1/11759/etd6705_CMHenry.pdf. Accessed 29 Feb. 2016.

Herrera-Pantoja, M., Hiscock, K.M., 2008. The effects of climate change on potential groundwater recharge in Great Britain. Hydrol. Process. 22, 73–86. doi:10.1002/hyp.6620

Hill, M.C., 1998. Methods and guidelines for effective model calibration (No. 98-4005). U.S. Geological Survey.

Hill, M.C., Tiedeman, C.R., 2007. Effective groundwater model calibration: with analysis of data, sensitivities, predictions, and uncertainty. John Wiley & Sons, Inc, Hoboken, N.J.

Hiscock, K., Sparkes, R., Hodgson, A., Martin, J.L., Taniguchi, M., 2008. Evaluation of future climate change impacts in Europe on potential groundwater recharge. Geophys. Res. Abstr. 10.

Hoff, H., Bonzi, C., Joyce, B., Tielbörger, K., 2011. A Water Resources Planning Tool for the Jordan River Basin. Water 3, 718–736. doi:10.3390/w3030718

Höllermann, B., Giertz, S., Diekkrüger, B., 2010. Benin 2025—Balancing Future Water Availability and Demand Using the WEAP "Water Evaluation and Planning" System. Water Resour. Manag. 24, 3591–3613. doi:10.1007/s11269-010-9622-z

Holman, I.P., 2006. Climate change impacts on groundwater recharge- uncertainty, shortcomings, and the way forward? Hydrogeol. J. 14, 637–647. doi:10.1007/s10040-005-0467-0

IPCC 2001: the scientific basis: contribution of Working Group I to the third assessment report of the Intergovernmental Panel on Climate Change, 2001. Cambridge University Press, Cambridge, United Kingdom and New York, NY, USA, 881 pp.

IPCC 2007: impacts, adaptation and vulnerability: contribution of Working Group II to the fourth assessment report of the Intergovernmental Panel on Climate Change, 2007. Cambridge University Press, Cambridge, U.K. ; New York.

IUSS Working Group WRB, 2015. World reference base for soil resources 2014, update 2015 International soil classification system for naming soils and creating legends for soil maps, World Soil Resources Reports No. 106. ed. FAO, Rome.

Jackson, J.M., 2007. Hydrogeology and groundwater flow model, central catchment of Bribie Island, southeast Queensland (M.Sc). Queensland University of Technology, Australia. Available at:

http://eprints.qut.edu.au/18347/1/Joanne_M._Jackson_Thesis.pdf. Accessed 27 Nov. 2015.

Jassas, H., Merkel, B., 2014. Estimating Groundwater Recharge in the Semiarid Al-Khazir Gomal Basin, North Iraq. Water 6, 2467–2481. doi:10.3390/w6082467

Johnson, A.I., 1967. Specific Yield: Compilation of Specific Yields for Various Materials (No. 1662), Water Supply Paper. U.S. Government Printing Office, Washington, D.C.

Juo, A.S.R., Franzluebbers, K., 2003. Tropical soils: properties and management for sustainable agriculture. Oxford University Press, Inc, New York, N.Y.

Jyrkama, M.I., Sykes, J.F., 2007. The Impact of Climate Change on Groundwater, in: Delleur, J.W. (Ed.), The Handbook of Groundwater Engineering: Second Edition. CRC Press-Taylor & Francis Group, Boca Raton, London, New York.

Kabir, M., 2010. Long-Term impact study for climate change in the shallow unconfined groundwater recharge in Ranger Uranium Mine Mobashwera (PhD). University of Monash, Australia. Available at: users.monash.edu.au/~gmudd/files/Kabir-PhD.pdf. Accessed 5 May 2016.

Keïta, S., Konaté, F.O., 2003. Le Mali et sa population, in: Hertrich, V., Keïta, S. (Eds.), Questions de Population Au Mali. UNFPA, 11-64.

Kim, N.W., Chung, I.M., Won, Y.S., Arnold, J.G., 2008. Development and application of the integrated SWAT–MODFLOW model. J. Hydrol. 356, 1–16. doi:10.1016/j.jhydrol.2008.02.024

Kinzelbach, W., 1986. Groundwater modelling: an introduction with sample programs in BASIC, Developments in water science. Elsevier; Distributors for the United States and Canada, Elsevier Science Pub, New York.

Konikow, L.F., Reilly, T., 1998. Use of numerical models to simulate groundwater flow and transport.

Kouli, M., Lydakis-Simantiris, N., Soupios, P., 2009. GIS-Based Aquifer Modeling And Planning Using Integrated Geoenvironmental And Chemical Approaches, in: König, L.F., Weiss, J.L. (Eds.), Groundwater: Modelling, Management and Contamination. Nova Science Publishers, New York.

Krautstrunk, M. L., 2012. An Estimate of Groundwater Recharge in the Nabogo River Basin, Ghana Using Water Table Fluctuation Method and Chloride Mass Balance (M.Sc). University of Nevada, Las Vegas. Available at: http://digitalscholarship.unlv.edu/cgi/viewcontent.cgi?article=2746&context=thesesdissertations. Accessed 5 May 2016.

Kumar, C.P., 2012. Climate Change and Its Impact on Groundwater Resources. Int. J. Eng. Sci. 1, 43–60.

Lamarque, J.-F., Kyle, G.P., Meinshausen, M., Riahi, K., Smith, S.J., van Vuuren, D.P., Conley, A.J., Vitt, F., 2011. Global and regional evolution of short-lived radiatively-active gases and aerosols in the Representative Concentration Pathways. Clim. Change 109, 191–212. doi:10.1007/s10584-011-0155-0

Lee, J.-Y., Lim, H., Yoon, H., Park, Y., 2013. Stream Water and Groundwater Interaction Revealed by Temperature Monitoring in Agricultural Areas. Water 5, 1677–1698. doi:10.3390/w5041677

Lee, K.K., Risley, J.C., 2002. Estimates of Ground-Water Recharge, Base Flow, and Stream Reach Gains and Losses in the Willamette River Basin, Oregon. U.S. Geological Survey Water-Resources Investigations, Report 01–4215, 52 p.

Lehner, B., 2013. HydroSHEDS: Technical Documentation version 1.2.

Lerner, D.N., Issar, A.S., Simmers, I., 1990. Groundwater Recharge: A Guide to Understanding and Estimating Natural Recharge, International Contributions to Hydrogeology. ed.

Lévite, H., Sally, H., Cour, J., 2002. Water demand management scenarios in a water-stressed basin in South Africa. Presented at the Proceedings of 3rd WARSFA/ Waternet Symposium, Arusha, Tanzania.

Lin, Y.-F., Walter, D., Meyer, S., 2003. Groundwater Flow Models of Northeastern Illinois a case study for building MODFLOW models with GIS.

Loaiciga, H.A., Valdes, J.B., Vogel, R., Garvey, J., Schwarz, H., 1996. Global warming and the hydrologic cycle. J. Hydrol. 174, 83–127.

Lubczynski, W.M., Gurwin, J., 2005. Integration of various data sources for transient groundwater modeling with spatio-temporally variable fluxes—Sardon study case, Spain. J. Hydrol. 306, 71–96. doi:10.1016/j.jhydrol.2004.08.038

Lutz, A., Minyila, S., Saga, B., Diarra, S., Apambire, B., Thomas, J., 2014. Fluctuation of Groundwater Levels and Recharge Patterns in Northern Ghana. Climate 3, 1–15. doi:10.3390/cli3010001

Lu, X., Zhou, Z., 2011. Analysis on interactions among atmosphere, surface and ground water using EARTH model in the unsaturated zone. 2nd Int. Conf. Environ. Sci. Technol.

Lu, X., Zhou, Z., Wang, J., 2011. Analysis on Interactions Among Atmosphere, Surface and Ground Water using EARTH Model in the Unsaturated Zone. Procedia Environ. Sci. 8, 134–139. doi:10.1016/j.proenv.2011.10.022

Mahé, G., 2009. Surface/groundwater interactions in the Bani and Nakambe rivers, tributaries of the Niger and Volta basins, West Africa. Hydrol. Sci. J. 54, 704–712. doi:10.1623/hysj.54.4.704

Mahé, G., Olivry, J.C., Dessouassi, R., Orange, D., Bamba, F., Servat, E., 2000. Relations eaux de surface-eaux souterraines d'une rivière tropicale au Mali. Sci. Terre Planetes 330, 689–692.

Maiga, A., 2004. Etude sur les référentiels technico Economiques : Diffusion des technologies d'irrigation et de Production (DTIP- PCDA). Programme Competitivite et Diversification Agricole, PCDA, Mali.

Mandle, R.J., 2002. Groundwater Modeling Guidance (Groundwater Modeling Program). Michigan Department of Environmental Quality.

Maréchal, J.C., Dewandel, B., Ahmed, S., Galeazzi, L., Zaidi, F.K., 2006. Combined estimation of specific yield and natural recharge in a semi-arid groundwater basin with irrigated agriculture. J. Hydrol. 329, 281–293. doi:10.1016/j.jhydrol.2006.02.022

Marei, A., Khayat, S., Weise, S., Ghannam, S., Sbaih, M., Geyer, S., 2010. Estimating groundwater recharge using the chloride mass-balance method in the West Bank, Palestine. Hydrol. Sci. J. 55, 780–791. doi:10.1080/02626667.2010.491987

Mariko, A., 2003. Caractérisation et suivi de la dynamique de l'inondation et du couvert végétal dans le Delta intérieur du Niger (Mali) par télédétection. Universite Montpellier II.

Martin, N., 2005. Development of a water balance for the Atankwidi catchment, West Africa – A case study of groundwater recharge in a semi-arid climate (PhD). Cuvillier Verlag Göttingen, Germany. Available at: www.zef.de/fileadmin/template/Glowa/Downloads/thesis_martin.pdf. Accessed 30 Mar. 2016.

Maurer, D.K., Berger, D.L., Prudic, D.E., 1996. Subsurface Flow to Eagle Valley from Vicee, Ash, and Kings Canyons, Carson City, Nevada, Estimated from Darcy's Law and the Chloride-Balance Method. U.S. Geological Survey Water-Resources Investigations, Carson City, Nevada.

Mazor, E., 2004. Chemical and isotopic groundwater hydrology, 3rd ed. ed, Books in soils, plants, and the environment. M. Dekker, New York.

McCabe, G.J., Markstrom, S.L., 2007. A monthly water-balance model driven by a graphical user interface. U.S. Geological Survey, Open-File Report 2007-1088, 6p.

McCartney, M.P., Arranz, R., 2007. Evaluation of Historic, Current and Future Water Demand in the Olifants River Catchment, South Africa. International Water Management Institute, Colombo, Sri Lanka.

McDonald, M.G., Harbaugh, A.W., 1988. A modular three-dimensional finite-difference groundwater flow model. U.S. Geological Survey Techniques of Water-Resources Investigations, Book 6, Chp A1, 586 p.

McKee, T.B., Doesken, N.J., Kleist, J., 1993. The relationship of drought frequency and duration to time scales. Presented at the Proceedings of the Eighth Conference on Applied Climatology, Anaheim, California.

McMahon, P.B., Dennehy, K.F., Bruce, B.W., Böhlke, J.K., Michel, R.L., Gurdak, J.J., Hurlbut, D.B., 2006. Storage and transit time of chemicals in thick unsaturated zones under rangeland and irrigated cropland, High Plains, United States. Water Resour. Res. 42, n/a–n/a. doi:10.1029/2005WR004417

Mearns, L.O., Giorgi, F., Whetton, P., Pabon, D., Hulme, M., Lal, M., 2003. Guidelines for Use of Climate Scenarios Developed from Regional Climate Model Experiments.

Meinshausen, M., Smith, S.J., Calvin, K., Daniel, J.S., Kainuma, M.L.T., Lamarque, J.-F., Matsumoto, K., Montzka, S.A., Raper, S.C.B., Riahi, K., Thomson, A., Velders, G.J.M., van Vuuren, D.P.P., 2011. The RCP greenhouse gas concentrations and their extensions from 1765 to 2300. Clim. Change 109, 213–241. doi:10.1007/s10584-011-0156-z

Meinzer, O.E., 1923. The Occurrence of Ground Water in the United States With a Discussion of Principles. U.S. Geological Survey Water-Supply Paper 489, Washington.

Middlemis, H., 2004. Benchmarking best practice for groundwater flow modelling. Principal Water Resources Engineer, Aquaterra, PO Box 2043, Kent Town, 5071, South Australia.

Middlemis, H., 2001. Groundwater flow Modeling Guideline (No. 125). Aquaterra Consulting Pty Ltd, Australia.

Milly, P.C.D., Dunne, K.A., Vecchia, A.V., 2005. Global pattern of trends in streamflow and water availability in a changing climate. Nature 438, 347–350. doi:10.1038/nature04312

Moore, J.E., 2002. Field hydrogeology: a guide for site investigations and report preparation. Lewis Publishers, Boca Raton.

Moss, R., Babiker, M., Brinkman, S., Calvo, E., Carter, T., Edmonds, J., Elgizouli, I., Emori, S., Erda, L., Hibbard, K., Jones, R., Kainuma, M., Kelleher, J., Lamarque, J.F., Manning, M., Matthews, B., Meehl, J., Meyer, L., Mitchell, J., Nakicenovic, N., O'Neill, B., Pichs, R., Riahi, K., Rose, S., Runci, P., Stouffer, R., Vuuren, D. van, Weyant, J., Wilbanks, T., Ypersele, J.P. van, Zurek, M., 2008. Towards new scenarios for analysis of emissions, climate change, impacts, and response strategies, Intergovernmental Panel on Climate Change. ed. Geneva, 132 pp.

Mounir, Z.M., Ma, C.M., Amadou, I., 2011. Application of Water Evaluation and Planning (WEAP): A Model to Assess Future Water Demands in the Niger River (In Niger Republic). Mod. Appl. Sci. 5, 38–49.

Nakićenović, N., Intergovernmental Panel on Climate Change, 2000. Special report on emissions scenarios: a special report of Working Group III of the Intergovernmental Panel on Climate Change. Cambridge University Press, Cambridge; New York, 559 pp.

Nash, J., Sutcliffe, J., 1970. River flow forecasting through conceptual models, Part I - A discussion of principles. J Hydrol 10, 282–290.

Nayak, P.C., Wardlaw, R., Kharya, A.K., 2015. Water balance approach to study the effect of climate change on groundwater storage for Sirhind command area in India. Int. J. River Basin Manag. 13, 243–261. doi:10.1080/15715124.2015.1012206

N'Djim, H., Doumbia, B., 1998. Population and Water Issues: case study Mali.

Nicholson, S.E., 2009. A revised picture of the structure of the "monsoon" and land ITCZ over West Africa. Clim Dynam 32.

Nyagwambo, N.L., 2006. Groundwater recharge estimation and water resources assessment in a tropical crystalline basement aquifer (PhD). University of Delft, The Netherlands. Available at: repository.tudelft.nl/assets/uuid./ceg_nyagwambo_20060629.pdf. Accessed 5 May 2016.

Nyende, J., 2013. Application of Isotopes and Recharge Analysis in Investigating Surface Water and Groundwater in Fractured Aquifer under Influence of Climate Variability. J. Earth Sci. Clim. Change 04, 1–14. doi:10.4172/2157-7617.1000148

Nyenje, P.M., Batelaan, O., 2009. Estimating the effects of climate change on groundwater recharge and baseflow in the upper Ssezibwa catchment, Uganda. Hydrol. Sci. Sci. Hydrol. 54, 713–727.

Obuobie, E., 2008. Estimation of groundwater recharge in the context of future climate change in the White Volta River Basin, West Africa (PhD). University of Bonn,

Germany. Available at: hss.ulb.uni-bonn.de/2008/1616/1616.pdf. Accessed 5 Jul. 2013.

Odada, E.O., 2013. Our Freshwater Under Threat – Vulnerability of Water Resources to Environmental Change in Africa. AfricanNESS Secretariat, Nairobi, Kenya.

Olivry, J.C., Jarosewich-Holder, M., Dione, O., Andersen, I., 2005. The Niger River Basin: A Vision for Sustainable Manage. The World Bank, Washington.

Ordens, C.M., Werner, A.D., Post, V.E.A., Hutson, J.L., Simmons, C.T., Irvine, B.M., 2011. Groundwater recharge to a sedimentary aquifer in the topographically closed Uley South Basin, South Australia. Hydrogeol. J. 20, 61–72. doi:10.1007/s10040-011-0794-2

Osman, K.T., 2013. Soils Principles, Properties and Management. Springer Netherlands, Dordrecht.

Owais, S., Atal, S., Sreedevi, P., 2008. Governing Equations of Groundwater Flow and Aquifer Modelling Using Finite Difference Method, in: Ahmed, S., Jayakumar, R., Salih, A. (Eds.), Groundwater Dynamics in Hard Rock Aquifers. Springer, Dordrecht, pp. 201–218.

Ozturk, T., Altinsoy, H., Türkeş, M., Kurnaz, M., 2012. Simulation of temperature and precipitation climatology for the Central Asia CORDEX domain using RegCM 4.0. Clim. Res. 52, 63–76. doi:10.3354/cr01082

Paralta, E., Oliveira, M., 2005. Assessing and modelling hard rock aquifer recharge based on complementary methodologies - A case study in the " Gabbros of Beja" aquifer system (South Portugal). Presented at the Proceedings of the 2nd Workshop of the Iberian Regional working group on hardrock hydrogeology, Evora, Portugal, p. 15 pp.

Prudic, D.E., 1989. Documentation of a computer program to simulate Stream-aquifer relations using a modular, finite difference, Ground-water flow model (No. Open-File Report 88-729). U.S. Geological Survey.

Prudic, D.E., Konikow, L.F., Banta, E.R., 2004. A new Streamflow-Routing (SFR1) package to simulate stream-aquifer interaction with MODFLOW-2000 (No. Open-File Report 2004-1042, 95 p). U.S. Geological Survey.

Prych, E.A., 1998. Using Chloride and Chlorine-36 as Soil-Water Tracers to Estimate Deep Percolation at Selected Locations on the U.S. Department of Energy Hanford Site, Washington. US Geol. Surv. Water-Supply 1–67.

Ramsahoye, L.E., Lang, S.M., 1961. A Simple Method for Determining Specific Yield from Pumping Tests. UG Geol. Surv. 42–46.

Rapport 2005 sur le développement humain au Mali, 2005. Gestion de l'Environnement pour un développement humain durable. UNDP-ODHD, Mali.

Raskin, P., Hansen, E., Zhu, Z., Iwra, M.,1992. Simulation of Water Supply and Demand in the Aral Sea Region. Water Int. 17, 55–67.

Reichelt, R., 1971. Étude géologique résumée du gourma (Afrique occidentale) Un "'seuil'" et un bassin du Précambrien supérieur. Universite de Clermont-Ferrand.

RGPH, 2009. Population du Mali par région, cercle et commune.

Riahi, K., Rao, S., Krey, V., Cho, C., Chirkov, V., Fischer, G., Kindermann, G., Nakicenovic, N., Rafaj, P., 2011. RCP 8.5—A scenario of comparatively high greenhouse gas emissions. Clim. Change 109, 33–57. doi:10.1007/s10584-011-0149-y

Risser, D.W., Gburek, W.J., Folmar, G.J., 2005. Comparison of Methods for Estimating Ground-Water Recharge and Base Flow at a Small Watershed Underlain by Fractured Bedrock in the Eastern United States. U.S. Geological Survey Scientific Investigations Report 2005-5038, 31 p.

Rosenberg NJ, Epstein DJ, Wang D, Vail L, Srinivasan R, Arnold JG 1999. Possible impacts of global warming on the hydrology of the Ogallala Aquifer region. Climate Change 42:677–692

Rosenzweig, C., Strzepek, K.M., Major, D.C., Iglesias, A., Yates, D.N., McCluskey, A., Hillel, D., 2004. Water resources for agriculture in a changing climate: international case studies. Glob. Environ. Change 14, 345–360. doi:10.1016/j.gloenvcha.2004.09.003

Roudier, P., Mahé, G., 2010. Study of water stress and droughts with indicators using daily data on the Bani river (Niger basin, Mali). Int. J. Climatol. 30, 1689–1705. doi:10.1002/joc.2013

Saatsaz, M., Chitsazan, M., Eslamian, S., Sulaiman, W.N.A., 2011. The application of groundwater modelling to simulate the behaviour of groundwater resources in the Ramhormooz Aquifer, Iran. Int J Water Vol. 6, pp.29–42.

Sandstorm K (1995) Modeling the effects of rainfall variability on groundwater recharge in semi-arid Tanzania. Nordic Hydrol 26:313–330

Scanlon, B., Healy, R., Cook, P., 2002. Choosing appropriate techniques for quantifying groundwater recharge. Hydrogeol. J. 10, 18–39. doi:10.1007/s10040-001-0176-2

Schmidli, J., Frei, C., Vidale, P.L., 2006. Downscaling from GCM precipitation: a benchmark for dynamical and statistical downscaling methods. Int. J. Climatol. 26, 679–689. doi:10.1002/joc.1287

Schuler, P., Margane, A., 2013. Water Balance for the Groundwater Contribution Zone of Jeita Spring using WEAP Including Water Resources Management Options & Scenarios (Technical Report No. No. 6). BGR, Lebanon.

Schwanghart, W., Schütt, B., 2008. Meteorological causes of Harmattan dust in West Africa. Geomorphology 95, 412–428. doi:10.1016/j.geomorph.2007.07.002

SDRFPTE, 2010. Schéma Directeur Régional de la Formation Professionnelle et Technique pour l'Emploi (SDRFPTE). Assemblee Regionale de Sikasso, Mali.

Sehatzadeh, M., 2011. Groundwater Modelling in the Chikwawa district, lower Shire area of southern Malawi (M.Sc). University of Oslo, Norway. Available at: https://www.duo.uio.no/bitstream/handle/10852/12531/MASTERxTHESIS.pdf?sequence=1&isAllowed=y. Accessed 27 Nov. 2015.

SEI, 2015. WEAP tutorial: A collection of stand-alone modules to aid in learning the WEAP software.

SEI, 2005. WEAP: Water Evaluation And Planning System Tutorial: A collection of stand-alone modules to aid in learning the WEAP software. Stockholm Environment Institute, Boston MA, U.S.A.

SEI, 2001. WEAP: Water Evaluation And Planning System, User Guide for WEAP21. Stockholm Environment Institute, Boston MA, U.S.A.

Seneviratne, A.A.A.K.K., 2007. Development of Steady State Groundwater Flow Model in Lower Walawa Basin-Sri Lanka (Integrating GIS, Remote Sensing and Numerical Groundwater Modelling) (M.Sc). International institute for geo-information science and Earth observation EnschedeX, The Netherlands. Available at: https://www.itc.nl/library/papers./amarasinghe.pdf. Accessed 29 Mar. 2016.

Serrat-Capdevila, A., Valdés, J.B., Pérez, J.G., Baird, K., Mata, L.J., Maddock, T., 2007. Modeling climate change impacts – and uncertainty – on the hydrology of a riparian system: The San Pedro Basin (Arizona/Sonora). J. Hydrol. 347, 48–66. doi:10.1016/j.jhydrol.2007.08.028

Shelton, C.W., 2011. An analytical and numerical investigation of stream/aquifer interaction methodologies (M.Sc). University of Washington State, Washington. Available at: http://www.dissertations.wsu.edu/Thesis/Fall2011/c_shelton_110111.pdf. Accessed 29 Mar. 2016.

Sherif, M.M., Singh, V.P., 1999. Effect of climate change on sea water intrusion in coastal aquifers. Hydrol. Process. 13, 1277–1287.

Sibanda, T., Nonner, J.C., Uhlenbrook, S., 2009. Comparison of groundwater recharge estimation methods for the semi-arid Nyamandhlovu area, Zimbabwe. Hydrogeol. J. 17, 1427–1441. doi:10.1007/s10040-009-0445-z

Simmons, C.T., Bauer-Gottwein, P., Graf, T., Kinzelbach, W., Kooi, H., Li, L., Post, V., Prommer, H., Therrien, R., Voss, C., Ward, J., Werner, A., 2010. Variable density groundwater flow: from modelling to applications, in: Wheater, H.S., Mathias, S.A., Li, X. (Eds.), Groundwater Modelling in Arid and Semi-Arid Areas. Cambridge University Press, New York, pp. 87–117.

Singhal, B.B.S., Gupta, R.P., 2010. Applied hydrogeology of fractured rocks, 2nd ed. ed. Springer Science+Business Media, Dordrecht ; New York.

Sophocleous, M., 2002. Interactions between groundwater and surface water: the state of the science. Hydrogeol. J. 10, 52–67. doi:10.1007/s10040-001-0170-8

Sophocleous, M., 1985. The role of specific yield in ground-water recharge estimations: A numerical study. Ground Water 23, 52–58.

Sumioka, S.S., Bauer, H.H., 2004. Estimating Ground-Water Recharge from Precipitation on Whidbey and Camano Islands, Island County, Washington, Water Years 1998 and 1999. U.S. Geological Survey Water-Resources Investigations Report 03-4101, Tacoma, Washington.

Synthèse hydrogéologique du Mali, 1990. Systemes aquiferes: Chapitre 3.

Taft, B., Speck, S.W., Morris, J.R., 1997. Surface Water and Ground Water Interaction. Ohio Department of Natural Resources Division of Water Fact Sheet 97-43.

Taylor, C.M., Lambin, E.F., Stephenne, N., Harding, R.J., Essery, R.L.H., 2002. The Influence of Land Use Change on Climate in the Sahel. J. Clim. 15, 3615–3629. doi:10.1175/1520-0442(2002)015<3615:TIOLUC>2.0.CO;2

Taylor, R.G., Koussis, A.D., Tindimugaya, C., 2009. Groundwater and climate in Africa—a review. Hydrol. Sci. J. 54, 655–664. doi:10.1623/hysj.54.4.655

Tebaldi, C., Knutti, R., 2007. The use of the multi-model ensemble in probabilistic climate projections. Philos. Trans. R. Soc. Math. Phys. Eng. Sci. 365, 2053–2075. doi:10.1098/rsta.2007.2076

Thomas, B., Behrangi, A., Famiglietti, J., 2016. Precipitation Intensity Effects on Groundwater Recharge in the Southwestern United States. Water 8, 90. doi:10.3390/w8030090

Thomson, A.M., Calvin, K.V., Smith, S.J., Kyle, G.P., Volke, A., Patel, P., Delgado-Arias, S., Bond-Lamberty, B., Wise, M.A., Clarke, L.E., Edmonds, J.A., 2011. RCP4.5: a pathway for stabilization of radiative forcing by 2100. Clim. Change 109, 77–94. doi:10.1007/s10584-011-0151-4

Ting, C.-S., Kerh, T., Liao, C.-J., 1998. Estimation of groundwater recharge using the chloride mass-balance method, Pingtung Plain, Taiwan. Hydrogeol. J. 6, 282–292.

Torak, L.J., 1992. A Modular Finite-Element Model (MODFE) for areal and axisymmetric ground-water-flow problems, part I: model description and user's manual. U.S. Geological Survey Open-File Report, 90-194.

Toure, A., Diekkrüger, B., Mariko, A., 2016. Impact of Climate Change on Groundwater Resources in the Klela Basin, Southern Mali. Hydrology 3, 17. doi:10.3390/hydrology3020017

Toure, A., Mariko, A., Diekkrüger, B., Boukari, M., 2014. Estimating Groundwater Recharge under Climatic Variability in the Klela Basin in Mali (West Africa) Using Physically Based Methods, in: Proceedings of the 3éme Colloque International Eau–Climat'2014: Regards Croises Nord-Sud. Presented at the 3éme Colloque International Eau–Climat'2014, Hammamet, Tunisia, p. 16.

Traore, M., Sissoko, Y., 2010. Les institutions du marché du travail face aux défis du développement le cas du Mali. BIT, Genève.

Traore, S.M., Doumbia, A.G., Traore, V., Tolno, D.F., 2011. 4ème recensement general de la population et de l'habitat du mali (rgph-2009): Etat et structure de la population. INSTAT.

UN, 2013. World population projected to reach 9.6 billion by 2050.

UN, 2007. Coping with water scarcity challenge of the twenty-first century. UN-Water.

UNEP, 2002. The State of the environment: Past, Present, Future?

UNFCCC, 1992. Definitions.

USAID, 2006. Plan de securite alimentaire commune rurale de Klela. Commune rurale de Kléla.

US Army Corps of Engineers (USACE), 2007. Hydrologic Engineering Center HEC-ResSim, Reservoir System Simulation User's Manual Version 2.0. CPD-82. USACE, Davis, CA, USA.

USGS Fact Sheet, 1997. Modeling Ground-Water Flow with MODFLOW and Related Programs. US Geol. Surv. 1–4.

Usher, B.H., Pretorius, J.A., van Tonder, G.J., 2006. Management of a Karoo fractured-rock aquifer system – Kalkveld Water User Association (WUA). Water SA Httpwwwwrcorgza 32, 9–19.

Valerio, A.M., 2008. Modeling groundwater-surface water interactions in an operational setting by linking riverware with MODFLOW (M.Sc). University of Colorado.

Van der Lee, J., Gehrels, J., 1990. Modeling aquifer recharge, introduction to lumped parameter model EARTH (Hydrological report). Free University of Amsterdam.

van Vuuren, D.P., Edmonds, J., Kainuma, M., Riahi, K., Thomson, A., Hibbard, K., Hurtt, G.C., Kram, T., Krey, V., Lamarque, J.-F., Masui, T., Meinshausen, M., Nakicenovic, N., Smith, S.J., Rose, S.K., 2011. The representative concentration pathways: an overview. Clim. Change 109, 5–31. doi:10.1007/s10584-011-0148-z

Vasiliades, L., Loukas, A., Patsonas, G., 2009. Evaluation of a statistical downscaling procedure for the estimation of climate change impacts on droughts. Nat Hazards Earth Syst Sci 9, 879–894.

Wang, B., Jin, M., Liang, X., 2015. Using EARTH model to estimate groundwater recharge at five representative zones in the Hebei Plain, China. J. Earth Sci. 26, 425–434. doi:10.1007/s12583-014-0487-6

Wayne, G.P., 2013. The Beginner's Guide to Representative Concentration Pathways.

Weiss, M., Gvirtzman, H., 2007. Estimating Ground Water Recharge using Flow Models of Perched Karstic Aquifers. Ground Water 45, 761–773. doi:10.1111/j.1745-6584.2007.00360.x

Wheater, H.S., 2010. Hydrological processes, groundwater recharge and surface water/groundwater interactions in arid and semi-arid areas, in: Wheater, H.S., Mathias, S.A., Li, X. (Eds.), Groundwater Modelling in Arid and Semi-Arid Areas, International Hydrology Series. Cambridge University Press, New York, pp. 5–20.

WHO (Ed.), 2003. The right to water, Health and human rights publication series. Geneva.

Wilby, R., Charges, S., Zorita, E., Timbal, B., Whetton, P., Mearns, L., 2004. Guidelines for Use of Climate Scenarios Developed from Statistical Downscaling Methods.

Winter, T.C., Harvey, J.W., Franke, O.L., Alley, W.M., 1998. Ground water and surface water: a single resource, U.S. Geological Survey circular. U.S. Geological Survey, Denver, Colorado.

Woldeamlak, S.T., Batelaan, O., De Smedt, F., 2007. Effects of climate change on the groundwater system in the Grote-Nete catchment, Belgium. Hydrogeol. J. 15, 891–901. doi:10.1007/s10040-006-0145-x

World Meteorological Organization, 2012. Standardized Precipitation Index User Guide. (M. Svoboda, M. Hayes and D. Wood).(WMO-No. 1090), Geneva.

Wroblicky, G.J., Campana, M.E., Valett, H.M., Dahm, C.N., 1998. Seasonal variation in surface-subsurface water exchange and lateral hyporheic area of two stream-aquifer systems. Water Resour. Res. 34, 317–328.

WWAP, 2006. Rapport national sur la mise en valeur des ressources en eau : Mali (No. 2ème Rapport mondial des Nations Unies sur la mise en valeur des ressources en eau).

Xu, Y., Beekman, H.E., 2003. Groundwater recharge estimation in Southern Africa. Unesco, Paris.

Yates, D., Sieber, J., Purkey, D., Huber-Lee, A., 2005. WEAP21 – A Demand-, Priority-, and Preference-Driven Water Planning Model. Int. Water Resour. Assoc. 30, 487–500.

Candidate biography

Mr. Adama TOURE is PhD candidate in the GRP/ Climate Change and Water Resources Program at University of Abomey-Calavi, Benin in the framework of the WASCAL project. He is also Assistant Teacher in Environmental, and IWRM and climate change lectures at National School Engineers (ENI-ABT) of Bamako, Mali. Mr. TOURE is Master holder in Water and Environmental Chemistry. He is Author of an article on "*Hydrology Journal*" and participated to some International Conferences.

Abstract

Due to the effects of climate change and population growth, global water resources are threatened in terms of quantity and quality. As groundwater is more resilient to climate variability, to date, many studies are addressing the simulation of groundwater dynamics for adaptation purpose.

Groundwater on the Klela basin in Mali, a subbasin of the Bani's basin (one of the main tributaries of the Niger River), is very important for the population because it is required for domestic use, irrigation and livestock. Surface water is limited to seasonal rainfall and run dry a few months after rainy season. Therefore, investigations of groundwater resources to understand aquifer system behavior are vital to the inhabitants of the Klela basin. Actually, groundwater resources are sufficiently enough and available to cover the current water demand, but in the face of climate variability and change, growing population and high urbanization rates, this vital resource is being threatened. Therefore, water assessment tools were used to understand the aquifer behavior of the basin. The focus of this study is on estimating the amount of rainwater that replenishes the aquifer, understanding the hydraulic interactions between surface-water and groundwater, and quantifying and evaluating groundwater dynamics in the context of climate change and population growth, using different scenarios. Different approaches such as the water table fluctuation (WTF), chloride mass balance (CMB), simulations using the EARTH model and the Thornthwaite model for recharge estimation, MODFLOW for groundwater modeling, and the WEAP model for evaluating groundwater resources are applied to achieve the study objectives. Climatological, hydrological, geological, hydrogeological, hydraulic and demographic data are collected and used as models input data. The sandstone aquifer in the study area was simulated under steady and transient conditions, and the groundwater budget was computed. Recharge was estimated to be approximatively 635 Mm^3/a, or 13.9% of the mean annual rainfall for the period 2012-2013. The amount of water discharging the aquifer into the streams was estimated to be approximatively 618 Mm^3/a, representing 97% of recharge amount. Currently, the reduction of groundwater storage of about 39 Mm^3/a (10.6 mm/a) is mainly due to groundwater extraction by population. Scenarios of climate change, population growth and socio-economic development were developed to assess future groundwater resources. The results reveal that the impacts of climate change on groundwater are greater than that of the socio-economic development. However, the climate scenario RCP8.5 appeared to be the worst for groundwater availability. The overall conclusion of this study is that groundwater recharge, groundwater level and storage are decreasing over time, especially in the 2030s, where the simulated drought events are expected. The greatest impacts on groundwater resources are due to climate change and population growth.

Key words: Klela basin, groundwater resources, climate change, modeling, Mali

PhD

Adama Toure

Impacts of climate change and population growth on groundwater resources: case of the Klela basin in Mali, West Africa

GRP/CCWR/INE/WASCAL – UAC March, 2017